Technical Note

1967-44

R. M. Sheppard, Jr.

Values of LASA Time Station Residuals, Velocity and Azimuth Errors

8 September 1967

Prepared for the Advanced Research Projects Agency
under Electronic Systems Division Contract AF 19(628)-5167 by

Lincoln Laboratory

MASSACHUSETTS INSTITUTE OF TECHNOLOGY

Lexington, Massachusetts

The work reported in this document was performed at Lincoln Laboratory, a center for research operated by Massachusetts Institute of Technology. This research is a part of Project Vela Uniform, which is sponsored by the U.S. Advanced Research Projects Agency of the Department of Defense; it is supported by ARPA under Air Force Contract AF 19(628)-5167 (ARPA Order 512).

MASSACHUSETTS INSTITUTE OF TECHNOLOGY

LINCOLN LABORATORY

VALUES OF LASA TIME STATION RESIDUALS, VELOCITY AND AZIMUTH ERRORS

R. M. SHEPPARD, JR.

Group 64

TECHNICAL NOTE 1967-44

8 SEPTEMBER 1967

LEXINGTON MASSACHUSETTS

ABSTRACT

The operation of the Large Aperture Seismic Array (LASA) has provided vast amounts of seismic data. In the study described here arrival time data was first used to obtain values of station residuals to Jeffreys-Bullen P-wave arrival times. Having found that the apparently unrelated residuals and their scatter were large, the residuals were recomputed relative to the P-wave moveouts from site AØ. It was found that the residuals are a strong function of azimuth and distance to the epicenter. In an attempt to see if a plane wave approximation would reduce the residuals to a simple speed and azimuth correction, the data was replotted relative to the plane wave moveouts. In this representation the data still exhibited strong azimuth and distance dependence indicating that the residuals were not small enough to allow only a speed and azimuth correction. When the average values of the station corrections were plotted, they indicated that the anomaly causing the residuals may be in the shape of a syncline with its axis trending northeasterly and passing nearly through the center of LASA.

The aperture of LASA provides the ability of measuring the actual values of $dT/d\Delta$, the slope of the travel time curves. The results of many such measurements were plotted and revealed a distinct separation of the data into two groups of separate velocity curves. Data from the northwest gave one curve while data from the southeast defined another curve. Further investigation revealed that as the LASA aperture was reduced the separation became more severe. The corresponding errors made in determining the azimuth were large and increased as the LASA aperture was reduced. The data on velocity measurements and azimuth errors seem to conform to the picture of the anomaly under LASA that was obtained from individual station correction data.

To examine the anomaly in further detail, a collection of stations that lie entirely on each limb of the anomaly were used. The group of stations on the southeastern limb produced speed and azimuth errors that were completely consistent with the general picture of the anomaly beneath these stations. The group of stations on the northwestern limb produced azimuth and speed errors similar to the other collection and in general agreement with the picture of the anomaly beneath these stations.

Accepted for the Air Force
Franklin C. Hudson
Chief, Lincoln Laboratory Office

I. INTRODUCTION

The purpose of this paper is to present some of the results of work in the area of station time corrections and P-wave velocity measurements at the Montana LASA. The value of the station correction in epicenter determination and beamforming will be shown to be a significant factor in reducing gross errors in epicenters and thereby yielding a more accurate measurement of source and signal characteristics.[1,2] Factors in the crust and mantle that contribute to the station errors will be discussed and some inferences will be drawn from the data,[3] although an earth and crustal model will not be presented in detail.

II. MONTANA LASA

A. The Montana LASA

The Large Aperture Seismic Array, or LASA, is located in east central Montana and is the first large seismic array to be built anywhere in the world. The array contains 525 short-period vertical seismometers, two short-period horizontal seismometers and a total of 63 long-period seismometers. The short-period vertical seismometers are grouped in clusters of 25, called subarrays. In addition to 25 verticals, each subarray has a three-component long-period system installed at its center. The short-period verticals are located at the bottom of boreholes 200 feet deep with the exception of the center hole which is 500 feet deep. The subarray geometry is identical for each of the 21 subarrays except for some rotation about the center point. Figure 1 shows the internal geometry of the subarrays along with the arrangement of the 21 subarrays which form the Montana large aperture array.

The data from the array far exceeds in volume data from any previously existing array. It is therefore necessary that data from all the array seismometers be handled in the most orderly and efficient way possible. The outputs of well over 600 seismometers are digitized and multiplexed in the field then telemetered from various points in the array to the LASA Data Center in Billings, Montana. Here the data are fed into a Digital Equipment Corporation PDP-7 computer and simultaneously recorded on 16 mm microfilm. The PDP-7 computer records the data on standard

computer magnetic tape in two possible formats, high rate or low rate. In the high rate recording format, all array seismometer outputs plus weather and time data are written on tapes. In this recording format a single magnetic tape is completely recorded every eight minutes for a total of 180 tapes per day. It was because of this enormous amount of output that the low rate recording format was introduced. Selected short-period outputs and all long-period outputs are recorded in the low rate format. In this mode of recording a tape is completely recorded in 80 minutes. At the rate of accumulation of 18 low rate tapes per day, the problem of storage and supply now becomes reasonable.

The data recorded on magnetic tape is saved for periods of three weeks to three months for high rate and low rate respectively. At the end of this time selected data tapes are retained in a data library while the others are recycled back into the recording system. The data recorded on microfilm are saved indefinitely. Selected portions of the recorded data are sent to Lincoln Laboratory to support studies in array processing and to aid in the evaluation of new programs and processing techniques. Microfilm data are also sent to Earth Sciences, a Teledyne Company, where P-wave arrival times are read at the 21 LASA sites and recorded on punched cards along with signal amplitudes and periods. This company, under Lincoln Laboratory contract, supplied all data used in this analysis.

B. Use of LASA for Epicenter Determinations

Beamforming is a term used to describe a method in which the outputs of the seismometers are added together with a steering delay. With this method we can obtain a single output signal where the noise is reduced and seismic signal is enhanced. The use of many beams for epicenter location is called beamsplitting and is quite similar to locating a target with a sweeping radar antenna. In the radar antenna case, the output power of the received signal is plotted as a function of the sweep angle or radar position. The point of maximum output is then taken as the maximum reflection from the target. Since the sweeping effect of a LASA is not possible, the idea of a sweeping beam can be approximated by the use of a grid of beams, each directed at some point near the true earthquake epicenter. The output power of the beams can be measured and the epicenter can be located in the area of high signal power.

Another method of epicenter location using a LASA has been described by Kelly.[4] This method involves measuring the speed of the earthquake wavefront as it passed the array and measuring the direction of arrival of the wavefront. Since the speed of the wavefront is actually the first derivative of the travel time curve, $dT/d\Delta$, then it is a measure of the distance to the epicenter. The distance to the epicenter together with the measured direction of arrival of the wavefront will give the position of the epicenter. It is this method that is presently being used to locate all earthquakes recorded across the Montana LASA.

Both the beamsplitting method of epicenter location and the plane wave method rely on a good set of travel time tables and on the knowledge of the station corrections. The station time correction can be a large and significant factor in beamforming and in epicenter location by the best fitting plane wave method.

III. THE CONCEPT OF A STATION CORRECTION

The concept of a station correction to the travel time tables or any other set of tables is not really a new idea but has existed since the first days of seismology. The station correction term can be seen in many equations related to travel time tables or magnitude calculations. In most cases the station correction term was thought to be a single number which would be added into the travel time or the magnitude calculations and would have the effect of bringing that station's P-wave arrival or magnitude into agreement with the mean readings obtained from worldwide data. In most cases the station correction was expressed as a single number which was said to be a representation of only that station. For some stations, the value of the correction to the travel time tables might be as high as 10 seconds while the correction to the magnitude calculation may be as much as one magnitude unit.

With the installation of the Montana LASA, the concept of station corrections became a subject of great interest and concern. It was necessary to obtain some knowledge of the size of station corrections and to determine just how necessary it would be to employ them in beamforming and epicenter location. Some idea of the effect of errors in the plane wave epicenter location method was given by Kelly.[4] In an example he showed that a timing error of 0.3 seconds would move the epicenter about 115 km, the largest component of the error being along the azimuth. Some early values for the station correction gave numbers as large as four or five seconds

relative to the J-B travel time tables and up to one second relative to the AØ subarray readings. It became immediately apparent that station corrections had to be used and that we must base station corrections to some reference other than the travel time tables.

A rather simple way to demonstrate the need for station corrections is to consider a beam formed from hand-picked delays and a beam formed from the delays given from J-B tables. The beam formed from the hand-picked delays is shown in Fig. 2. From the proper alignment of the 21 subarrays one can obtain a beam that will yield a greater degree of information about the seismic signal than one could obtain from a single sensor. This procedure is a great aid in identifying first motion and detecting any surface reflected phases such as pP or sP.[5,6] Figure 3 shows the same event as in Fig. 2, but the beam was formed using the computed delays from the J-B tables. It is quite easy to see that for the beam formed with the theoretical delays there is not a proper phasing of all the 21 subarrays. This is interpreted to mean that a station correction term must be added to insure proper alignment of all 21 signals.

IV. TRAVEL TIME TABLES

A. Jeffreys-Bullen Travel Time Tables

Because the basis for the station correction is the Jeffreys-Bullen travel time tables,[7] it is necessary to examine these tables in some detail. The J-B travel time curve for a depth of 33 km is shown in Fig. 4. This data is generally presented in table form, but for the purpose of this paper it is more revealing to present the data in the form of a curve.

Because LASA is able to give accurate measurements of $dT/d\Delta$ it is important to examine the first derivative of the travel time curves. A plot of $dT/d\Delta$ for the 33 km depth curve is shown in Fig. 5. It is now easy to see that this is not really a smooth function. There are some regions of the curve where one value of velocity will yield two or three values of distance. Figure 6 is a plot of the second derivative of the travel time curve, it is here that the unsmoothness of the $dT/d\Delta$ curve can be seen. Although Fig. 6 seems to show the second derivative is a constant with some noise added, there are four regions where the first derivative curve makes some rather large jumps. The region around 20, 50, 70, and 100 degrees are the areas where the $dT/d\Delta$ curve needs to be smoothed.

B. Smoothing Operation

Because of the roughness of the velocity curve it was necessary to perform a smoothing operation on the travel time curves. This smoothing was achieved by least

square fitting seven points on the travel time curve to a second order polynomial and taking the value at the mid-point as the smoothed value for its corresponding distance. The entire process was repeated after sliding the fit up by one point. In this process the first three and the last three points of the travel time curve are lost. The actual travel time table has not been changed by more than a few tenths of a second, but the resulting velocity curve has now become a smooth function of distance. The entire smoothing operation was performed a second time using the first smoothed tables as the function to be smoothed. The resulting travel time curve is shown in Fig. 7 and its first derivative in Fig. 8. The actual change made in the travel time curve by the second smoothing operation is not significant and in fact is not easily seen in the plots. The travel time tables and corresponding velocity tables that were produced from the second smoothing operation are the tables used throughout the analysis of station corrections and velocity measurements.

V. STATION CORRECTIONS

A. Relative to J-B Tables

The classical meaning of a travel time station correction is considered to be the error term that a station has when it records a P-wave arrival time earlier or later than would have been predicted by some set of travel time tables. Using the J-B tables as a reference, the author collected data on P-wave arrivals and its associated error term for three seismic stations. The plots of the station residuals to the J-B curve for subarray AØ, F1 and for the Tonto Forest Seismological Observatory are shown in Figs. 9, 10, and 11. For this representation, the residuals are defined as observed arrival time minus J-B predicted arrival time. One can easily see that there is a large amount of scatter and that the values of the residuals are rather large. The large scatter is the result of errors in origin time, errors in epicenter location and errors in reading P-wave arrivals. The residuals have been plotted versus azimuth to the epicenter in an attempt to see if there is any dependence of the residual on the direction of approach of the P-wave to the station. Also, four different symbols were used, each denoting a distance range, to see if there would be any effect with distance. The actual values of the range of distances will be given in a later section. There appears to be some azimuth effect, but there seems to be no distance effect, although the scatter of the data may be too large to show any effect. Because of the value of these residuals and because of the large amount of scatter, it is clear that the station

correction presented in this manner would not be of any great aid in beamforming or in improving epicenter determinations.

B. Relative to Subarray AØ

From the scatter of the data in Figs. 9, 10, and 11 it would seem that the station corrections need to be defined relative to a reference that will indicate any consistency of the errors within LASA. By basing the residuals on some reference within the array rather than on the J-B tables, it should be possible to obtain a reduction in the value of the residual, a reduction in the scatter and an idea of how consistent the residuals may be. Subarray AØ was picked as the reference subarray and the residuals were recomputed relative to the arrival time at AØ. For this situation, the residuals are now defined as

$$R = (t_n - t_o) - (t'_n - t'_o)$$

where t_o is the measured time at subarray AØ and t_n is the measured arrival time at some other subarray. The J-B computed arrival times are denoted by t'_n and t'_o. By subtracting out the J-B computed times the author hoped to remove any errors in the J-B tables due to variations in crustal and mantle velocities. Since the most distant station from AØ is only 109 km away, or about one degree in distance, this redefinition of the station correction should remove most of the absolute time errors inherent in the J-B tables. The origin time now has no effect on the residual. While errors in epicenter location will still exist, their effect is considerably lessened. Also, since

the residuals are relative to AØ rather than travel time tables, they should have small values.

The residuals relative to subarray AØ were computed and plotted versus the azimuth to the event. The first plots showed a strong dependence of the residual on azimuth but still exhibited a substantial amount of scatter. The actual value of the residual was considerably reduced from the initial J-B residuals. Because of the scatter at azimuths of 140 and 320 degrees, the author replotted the data using four different symbols to represent four different distance groups. The two azimuths of 140 and 320 degrees, South America and the Aleutians-Kuriles-Japan regions, are the only areas where LASA has a large number of events that offer a good sampling of distances within a narrow azimuth. The large scatter of the residuals that occurred in these azimuths now show a definite grouping of symbols indicating a dependence on distance range as well as azimuth. It is therefore apparent that the residuals are functions of both the azimuth to the event and on the distance of the event from the station. The values of the station corrections obtained in this manner are now suitable for use in epicenter determination programs and are suitable for beamforming.

The residuals for eight typical subarrays have been plotted versus azimuth and are shown in Figs. 12 through 19. In these plots four different symbols were used to represent four separate distance ranges. The same residuals for the eight subarrays were plotted versus distance to the epicenter and are shown in Figs. 20 through 27. In this case the four symbols were used to denote azimuth segments. The values of the symbols are defined as follows:

		Residual vs Azimuth Plot	Residual vs Distance Plot
□	=	0 – 3900 km	115 – 200 degrees
×	=	3900 – 6100 km	280 – 340 degrees
+	=	6100 – 9500 km	200 – 280 degrees
*	=	9500 – 11,500 km	340 – 115 degrees

The general clustering of the data about three azimuths is due to the natural seismicity of the earth. The regions of Europe are at an azimuth of about 40 degrees, Central and South America at 120 to 180 degrees, Fiji-Tonga-Kermadec at 240 degrees and the Aleutians-Kuriles-Japan area is at 300 to 320 degrees. The azimuth range from 340 to 40 degrees corresponds to regions in the U.S.S.R., China and Pakistan.

Although some subarrays exhibit a large amount of scatter in the residuals when they are plotted against azimuth (Figs. 13, 15, 17 and 19, for example), it is the corresponding plot of the residual against epicentral distance that reveals the reason for this large scatter (Figs. 21, 23, 25, and 27). There seems to be an unusual relationship of the residual to azimuth and epicentral distance.

C. Relative to a Plane Wave

For the purpose of beamforming it is necessary to know the value of the station correction well enough so that one can always predict the arrival time at any station within the array to within one-tenth of a second. The reason for this rather strict limitation is due to the frequencies of the seismic signal and the rate of digitization of the signal. The dominant period of seismic signal from events of teleseismic distances

is about 1 Hz while the LASA digitization rate is at 20 samples per second. Therefore, it is necessary that the station correction be accurate to within two samples of data, or 0. 10 seconds.

In an attempt to learn more about the behavior of individual stations, the residuals to a plane wave approximation of the wavefront were computed and plotted in the same manner as the residuals relative to subarray AØ. These residuals, together with a knowledge of the azimuth error and the speed error made in approximating the wavefront by a plane wave, can be used for epicenter location corrections and beamforming corrections. As one would expect, the absolute value of the residuals is now quite small but the problem of scatter has not been solved. From plots of these station corrections one can still see that the azimuth and distance dependence of the residuals is still quite evident. The residuals to a plane wave for the same eight subarrays used earlier have been plotted versus azimuth and epicentral distance and are shown in Figs. 28 through 35 and Figs. 36 through 43. The symbol designation that was described earlier also applies to these figures. Here too the large scatter of the residual can be explained by the unusual relationship of residual to azimuth and epicentral distance

D. Approximating the Station Residuals

In order to facilitate the handling of the station residuals in computer programs, it was necessary to make an approximation to the residuals. A least square fit of a two-term Fourier series was found to be the best means of approximating the data.

The curve, expressed in the form

$$R = A + B \sin(\beta - C) + D \sin(2\beta - E)$$

gave quite satisfactory results and can generally predict the station correction to within 0.10 seconds. There are, however, some regions where the scatter is sufficient to render the curve approximation useless. Figures 12 through 19 and 28 through 35 are shown with the least square fit two-term Fourier series superimposed on the data. The five numbers at the top of each plot are the five constants, A through E, that define the curve.

The curve approximation may be used to reduce epicenter location errors; however, for the accuracy required in beamforming, it is necessary to divide the earth into small segments and assign each segment a station correction value for each station. This must be done for the 21 LASA subarrays. This has been done by Earth Sciences, a Teledyne Company.[8,9] Using a cell size defined as 15 degrees in azimuth by 500 km in distance it is possible to predict the delay times to within one data sample, or 0.05 seconds for most segments of the earth. Unfortunately, this table contains nearly 5000 entries and presents some problems in programming and storage using small computers.

VI. THE AVERAGE VALUES OF THE STATION CORRECTION

The cause of the station correction, regardless of how it may be defined, can be attributed to inhomogeneities in the earth. However, there is no general agreement on what part of the earth is the major contributor to the station corrections. It shall be shown in this section and later sections of this paper that the major cause of the station residuals is due to the geology of the crust and the geometry of the mantle-crust boundary. This is not to say that the variations within the mantle have no effect, but given a good set of travel time tables, one should not expect mantle variations to manifest themselves as large residuals to those tables. It would seem that any variation from some worldwide average curve would be due to those regions where most geologic processes occur, namely in the crust.

With these thoughts in mind, the author tried to determine what the gross structure of the LASA anomaly might be. It seemed that the DC term of the Fourier series, i.e., the average value of the station correction, would reflect the general trend or structure effecting the station residuals. To get the general picture, contour plots were made of the DC terms that were obtained from the station corrections relative to AØ and the DC terms from the corrections relative to the best fitting plane wave. The results are rather surprising and are quite consistent for both sets of corrections. As can be seen in Figs. 44 and 45, the data contoured very well with the exception of subarray D2 in Fig. 45. This subarray showed a slightly larger value

than would have been expected. From both plots it seems that the gross structure causing the station residuals is an anomaly in the shape of a syncline with its axis trending slightly north of a line through subarrays C4, B4, and C1.

VII. MEASURED VELOCITIES USING LASA

A. Measured Velocities Using the Full LASA Array

Because of the size or aperture of LASA it is possible to measure the apparent velocity of a passing wavefront. This provides the very exciting possibility of actually measuring the first derivative, $dT/d\Delta$, of the travel time curves. From these measurements and related plots, it is possible to determine the actual velocity profile of the earth to a considerable degree of accuracy. A by-product of the study of the station corrections relative to the best fitting plane wave is a measurement of the apparent velocity and the apparent azimuth of a passing wavefront. These measurements, when plotted, reveal some very surprising results.

Using data from approximately 600 events, the author computed the velocity and azimuth of the wavefronts. These events vary in magnitude, depth, and in total number of subarrays reporting P arrivals. Figure 46 is a plot of the measured LASA velocities versus the theoretical J-B velocities. It is very clear that the data separates into two very distinct groups. One group, represented by squares, denotes all events coming from the northwest azimuths, while the second group indicated by the "x" represents events from the southeastern azimuth. The separation of the data into two groups was a complete surprise and it now poses many problems in the interpretation of the $dT/d\Delta$ curve. Figure 47 shows the same data represented as an error to the J-B velocity curve. On the vertical axis the value of LASA velocity minus J-B

velocity is plotted while the horizontal axis is the J-B velocity. This figure indicates that the velocity measurements from the northwest are very nearly equal to the theoretical velocities predicted from J-B while events from the southeast, represented by "v," give values lower than J-B values. The large scatter seen at velocities beyond 21 km/sec may be attributed to effects of the earth's core, or to effects of the anomaly under LASA.

B. Effect of Reducing the LASA Aperture

An investigation into the effects of reducing the LASA aperture lead to some surprising results. One would expect that reduction of the LASA aperture would introduce more scatter into the velocity measurements, but the data should still trend about the two groups defined in Fig. 46. This would be true if the anomaly under the array had a uniform effect upon the entire array. From Figs. 44 and 45 it seems that the gross feature of the anomaly is not uniform under the array and it may therefore effect velocity measurements obtained from smaller aperture arrays.

In an attempt to determine the aperture effect on velocity measurements, an array of 100 km aperture was used. This array was achieved by simply omitting all F subarrays from velocity computations. The resulting velocity measurements are plotted versus the J-B velocity in Fig. 48 and the error of the measured velocities is plotted in Fig. 49. In comparing Fig. 48 with Fig. 46 it is easy to see that the two velocity groups are still clearly defined. The real effect in reducing the aperture is to further separate these two velocity groups. When the aperture is further reduced

to approximately 50 km, achieved by removing both the E and F subarrays, the separation becomes more severe, as seen in Figs. 50 and 51. It is easy to see that as the aperture is decreased the scatter is increased, as one would expect, but the trend of the data from the southeast moves to lower and lower values of velocity and becomes quite different from values of velocity measured from the northwest. Further reductions in aperture produced an increase in scatter but no apparent change of the velocity separations.

The conclusion drawn from these results seems to be that the LASA anomaly appears to be centered near the center of the array, possibly near the point indicated by the contours in Figs. 45 and 46. If this is true, then velocity measurements made with the outer F and E subarrays should be closer to J-B velocities than measurements made by an array that included the inner subarrays. Figure 52 is a plot of the velocity measurements made by using only the four F subarrays. Here, there is little or no apparent separation in the data from the northwest and the southeast.

VIII. AZIMUTH DETERMINATIONS

One effect that has not been mentioned thus far is the effect of an azimuth anomaly. By azimuth anomaly the author is referring to the errors made by LASA in the determination of the azimuth to the epicenter. This is a very interesting anomaly and should yield more information on the location of the source of the station residuals than any other measurement made by LASA. In considering some of the causes of an azimuth error one might imagine that horizontal variations in the mantle could cause some bending of the wavefront, horizontal refraction, and cause LASA to see the wave coming from some directly slightly different from the true azimuth. The cone of waves travelling from the epicenter to LASA attains its widest separation when it reaches LASA, namely 200 km. If the azimuth anomaly is attributed to effects within the mantle, then the lateral variations must be rather severe since the cone of waves is internally sampling only a few tens of kilometers. It would seem that a more reasonable solution would be to attribute an azimuth anomaly, especially if it is a large anomaly, to effects within the crust.

The error in the azimuth determinations using the full LASA array are shown in Fig. 53. The four symbols used represent the same range of distance that was described earlier. The scatter may be considered a problem, but there is a definite trend in the data. Azimuth errors of about six degrees are quite common, although most errors are less.

The result of reducing the LASA aperture was seen to have dramatic effects on velocity measurements, but no such surprising results were obtained from the azimuth measurements. Figure 54 shows the azimuth error for a 100 km aperture array. Here the error has reached eight degrees and the data seems to indicate that the error relation to the true azimuth is in the form of a sine function with a maximum at an azimuth of 75 degrees and a minimum at about 250 degrees. A further reduction of LASA aperture produced azimuth errors well over 10 degrees but still maintained the same sine relationship with the two azimuths. Figure 55 is a plot of the azimuth errors made by a 50 km array identical to the 50 km array used in the velocity analysis.

It would seem that errors of this magnitude are simply too large to be explained by mantle variations. The more reasonable assumption is that crustal effects or mantle-crust boundary effects are the cause.

IX. STRUCTURAL IMPLICATIONS FROM THE STATION CORRECTIONS

There have been several attempts to interpret the station correction data and velocity measurements in terms of discontinuities within the mantle rather than due to features within the crust.[10, 11] Some of the results presented here would seem to indicate that to attribute the station residuals to effects within the mantle without first knowing the finer structure beneath the array could lead to erroneous conclusions about mantle variations.

As a first approach to learning the shape and extent of the anomaly one might consider the crust as being a uniformly layered feature that is not contributing in any major way to the station correction. Because the eastern section of Montana is known to be a rather uniformly layered area and due to the absence of any profound geologic structures, it would seem that the crust under the array may be considered fairly uniform. There may be, however, small local anomalies that will affect a single station and result in an additional station error superimposed on general effect of the anomaly.

The synclinal structure that seems to be indicated in Figs. 45 and 46 can be achieved with some reasonable changes in the depth to the Moho. If one assumes a velocity contrast of 6.0 and 8.0 km/sec at the Moho, then in order to explain the changes along a cross section along subarrays F4, B4 and F2, one need only make the depth to the Moho under subarray B4 about 10 km deeper than under the F2 and F4.

This would correspond to about a five to six degree slope in the Moho from F4 to B4 and from F2 to B4. Since this cross section seems to be perpendicular to the trend of the structure and is therefore along the region of steepest slope, one need not require more than a six degree slope in the Moho in order to explain the entire feature by means of a dipping boundary at the base of the crust. Similarly, if one tries to explain the anomaly by a near surface effect such as the interface between a 3.0 and a 6.0 km/sec layer then it would require a three kilometer increase in thickness of the lower velocity layer under subarray B4. This would correspond to an interface slope of about one degree from subarray F2 to subarray B4.

At this point, the anomaly may be better understood using only selected sections of LASA rather than the entire array. Consider, for example, the section that lies wholly on the southeast limb of the anomaly and the section that lies entirely on the northwest limb. It would seem that if this synclinal structure is correct, then the southeast group of subarrays would measure lower velocities from South American than from the northwest while the northwest group would measure just the reverse. Figures 56 and 57 show velocity measurements made using the southern group of subarrays. Note that events from the south give lower velocity measurements than those from the northwest. The data from a group of subarrays lying on the northwest limb are shown in Figs. 58 and 59. Although there does not seem to be a well defined split in the data, one can see that events from the northwest are slower than events from the southeast. There actually is a reversal in the relative position of the two velocity

groups as shown in Figs. 56 and 58, thus further supporting the synclinal shape of the anomaly.

The azimuth anomaly associated with each group of stations presents additional support to the author's contention of a crustal or mantle boundary based anomaly. The azimuth errors made by the southeastern group of stations are shown in Fig. 60. The values of the error range from + 10 degrees to − 10 degrees and exhibit a fair amount of scatter. Such a sizable residual is just too large to attribute to mantle effects. The zero crossings of the azimuth error would correspond to the directions of dip of the interface causing the anomaly. The zero crossings seem to be near 135 and 330 degrees, which is in good agreement with the direction of dip of the southeast limb indicated in Figs. 44 and 45. Furthermore, when the same data is used on the northwestern group of stations the azimuth error data shows the same relative magnitude but the errors are essentially inverted, similar to the results obtained for velocity. A plot of the azimuth errors for the northwestern group of stations is shown for Fig. 61. It is now quite easy to see that the azimuth error is independent of epicenter and dependent on LASA. Together with these errors and the velocity measurements it is difficult to postulate an anomaly at any other location than within the crust or at the crust-mantle boundary.

These plots seem to strengthen the idea that the anomaly is shaped in the form of a syncline, whose axis trends northeasterly and whose center is slightly north of the center of LASA. If one were to infer the lateness or earliness of a station from

this concept of a synclinal anomaly and then compare that inference with the actual performance of the station, as plotted in Figs. 12 through 43, one would find general agreement with the actual data. All this seems to indicate that the general structure of the anomaly is fairly definite. The remaining fine structures can now be approached, then finally the mantle variations can be learned. It is important to note, however, that refraction surveys conducted in the area of the Montana LASA do not clearly indicate any structure similar to the one obtained from teleseismic data and presented in this report.[12, 13]

X. CONCLUSIONS

Since the installation of the Montana LASA the field of seismology gained a new, complex system that can aid in the investigation of features deep within the earth. One of the areas in seismology which has benefitted from the Large Aperture Seismic Array is the investigation of travel time curves and their derivatives. Data generated from the array has been used in an analysis of station corrections and the $dT/d\Delta$ measurements.

It has been found that the station corrections or station residuals can be a complex function of epicenter, travel path and receiver effects. Attempts to define the station correction relative to the J-B travel time curve showed the corrections to be too large and produced too much scatter to be useful in predicting delay times across the array. Defining the station correction relative to a site within the array proved to be a useful means of approximating delay times across the array and an aid in introducing correction to epicenters obtained from the array. Because of the accuracy required in predicting delay times needed for beamforming, the station corrections were examined relative to the plane wave approximations of the wavefront. These corrections proved reasonably good for most areas of the world. However, for the accuracy needed in beamforming it appears that corrections must be applied to each particular seismic region.

Because of the aperture of LASA it is possible to measure the actual $dT/d\Delta$ of the travel time curves. It was these measurements that gave the first indication of

the structure of an anomaly under LASA. It soon became apparent that this structure is strongly affecting all travel time data derived from LASA. An idea of the size and extent of the anomaly can be obtained from the plots of the station corrections and plots of $dT/d\Delta$ measurements. The structure indicated from the data is in the shape of a syncline with the axis trending northeasterly from subarray B4. Further investigation is necessary to determine the depth to this structure and some of the finer features in the crust. With the knowledge of the geologic structures under LASA more accurate studies can be made into the properties of the mantle and core.

ACKNOWLEDGMENT

I would like to take this opportunity to express my sincerest thanks to Dr. E. J. Kelly for his continued encouragement, suggestions and patience and also to Profs. N. M. Toksöz and A. Gangi of M.I.T. for their suggestions. My sincerest appreciation to Dr. Paul E. Green for his suggestions and encouragement.

The body of this report was presented as a Master's thesis to the Department of Geophysics, Weston Observatory, Boston College.

REFERENCES

1. M. Otsuka, Azimuth and Slowness Anomalies of Seismic Waves Measured on the Central California Seismographic Array, Part I, Observations, Bull. Seismol. Soc. Am., 56, 223-239, February 1966.

2. L. R. Johnson, Measurements of Mantle Velocities of P Waves with Large Arrays, Doctoral Thesis, California Institute of Technology, 1966.

3. M. Niazi, Corrections to Apparent Azimuth and Travel Time Gradients for a Dipping Mohorovicic Discontinuitie, Bull. Seismol. Soc. Am., 56, 491-509, April 1966.

4. E. J. Kelly, Limited Network Processing of Seismic Signals, M.I.T., Lincoln Laboratory Group Report 1964-44, 1964.

5. H. W. Briscoe, R. M. Sheppard, Jr., A Study of the Capability of a LASA to Aid the Identification of a Seismic Source, M.I.T., Lincoln Laboratory Technical Note 1966-38, 1966.

6. P. E. Green and R. V. Wood, Jr., Large Aperture Seismic Array Capabilities, M.I.T., Lincoln Laboratory Technical Report No. 421, 1966.

7. H. S. Travis, Interpolated Jeffreys and Bullen Seismological Tables, The Geotechnical Corporation, Technical Report No. 65-35, 162, 1965.

8. E. F. Chiburis, LASA Travel Time Anomalies for Various Epicentral Regions, Seismic Data Laboratory Report No. 159, 1966.

9. D. E. Frankowski, Travel-Time Anomalies at LASA, Seismic Data Laboratory Report No. LL-6, 1967.

10. M. A. Chinnery, M. N. Toksöz, P Wave Velocities in the Mantle below 700 km, Bull. Seismol. Soc. Am., 57, 199-226, May 1967.

11. M. N. Toksöz, M. A. Chinnery, D. L. Anderson, Inhomogeneities in the Earth's Mantle, The Geophysical Journal, 13, 31-59, July 1967.

12. C. A. Borcherot, J. C. Roller, Preliminary Interpretation of a Seismic Refraction Profile Across the Large Aperture Seismic Array, Montana, National Center for Earthquake Research, Technical Letter NCER-2, May 1967.

13. J. S. Steinhart, Explosion Studies of Continental Structures, Doctoral Thesis, University of Wisconsin, 1960.

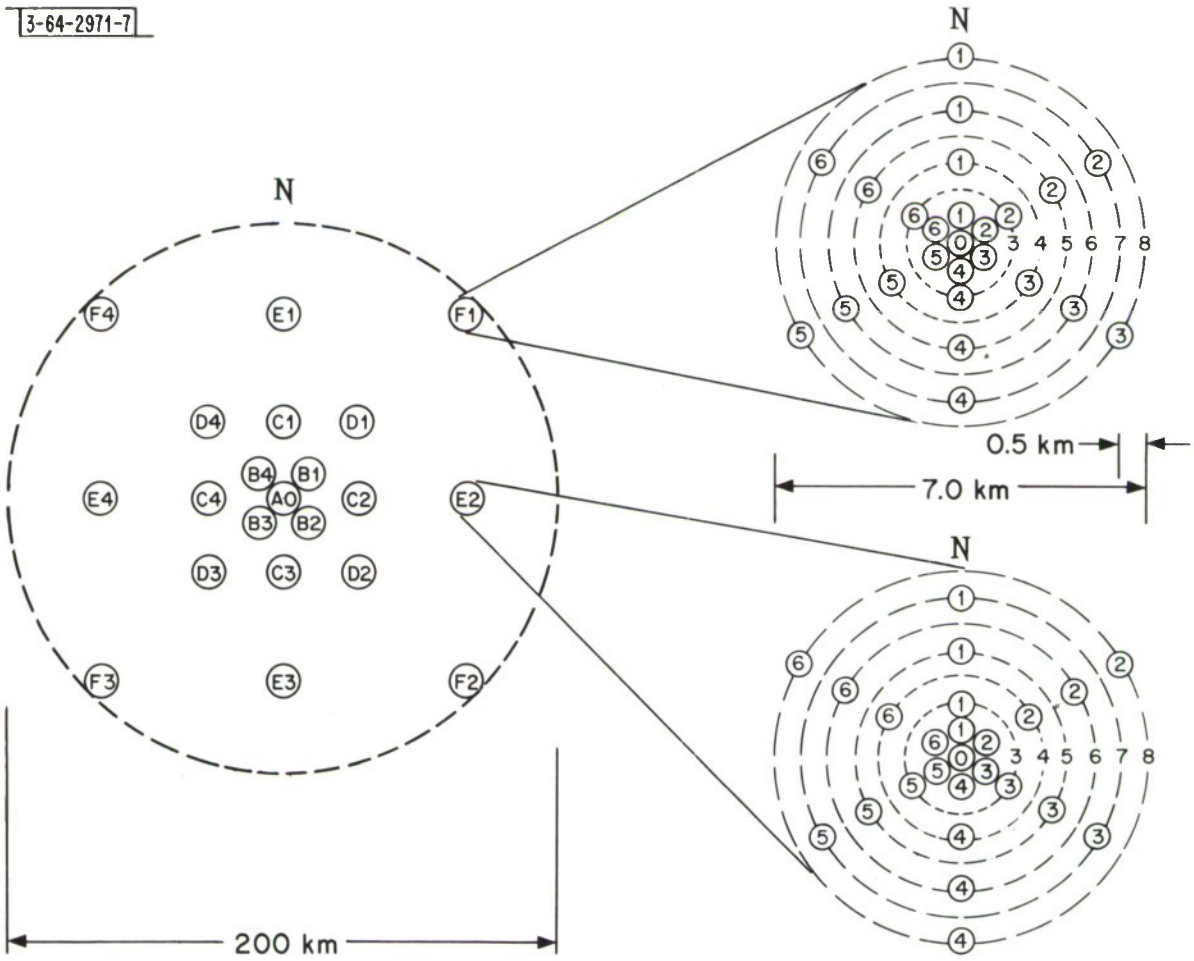

Fig. 1. LASA geometry.

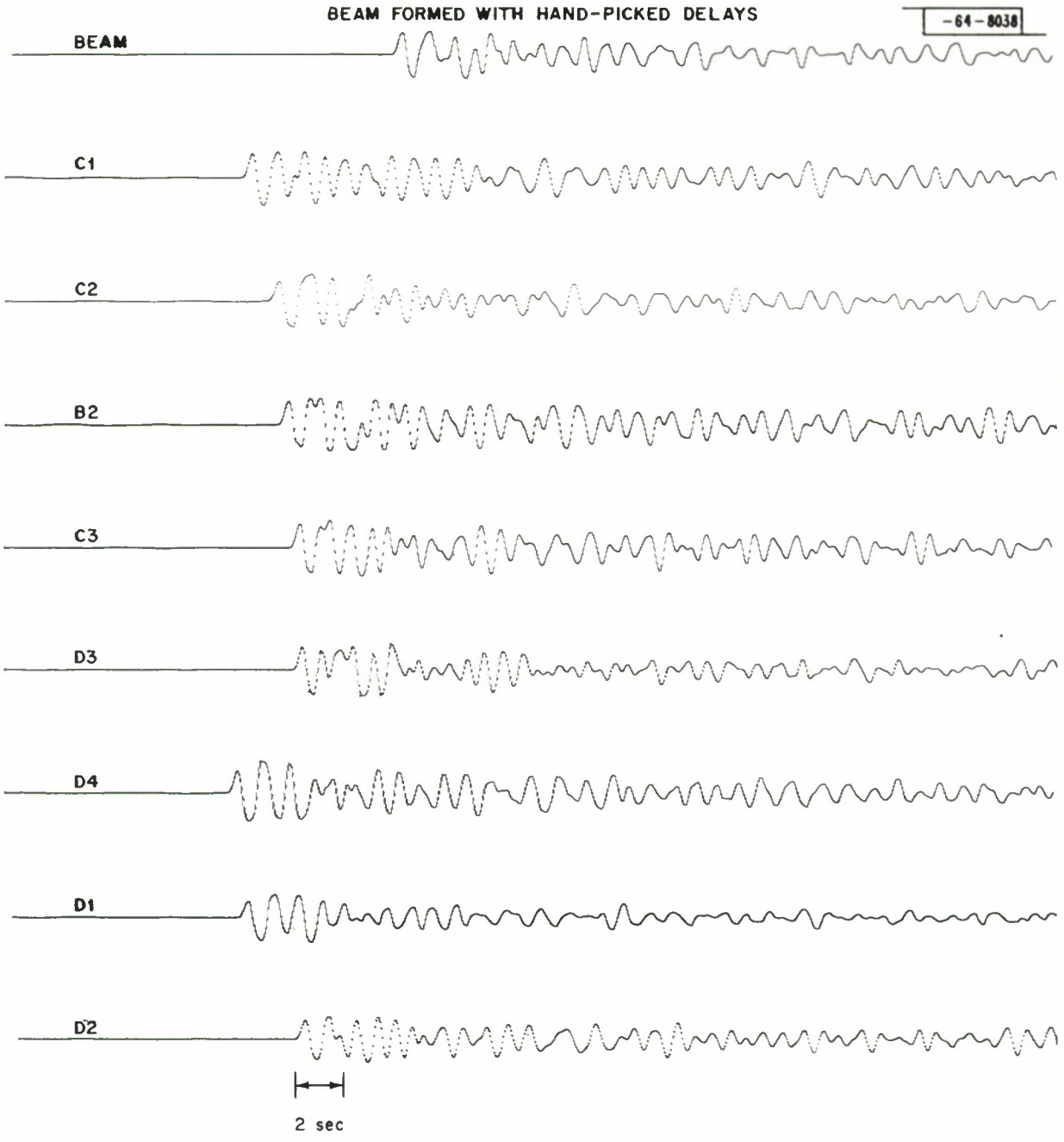

Fig. 2. LASA beam using measured delays.

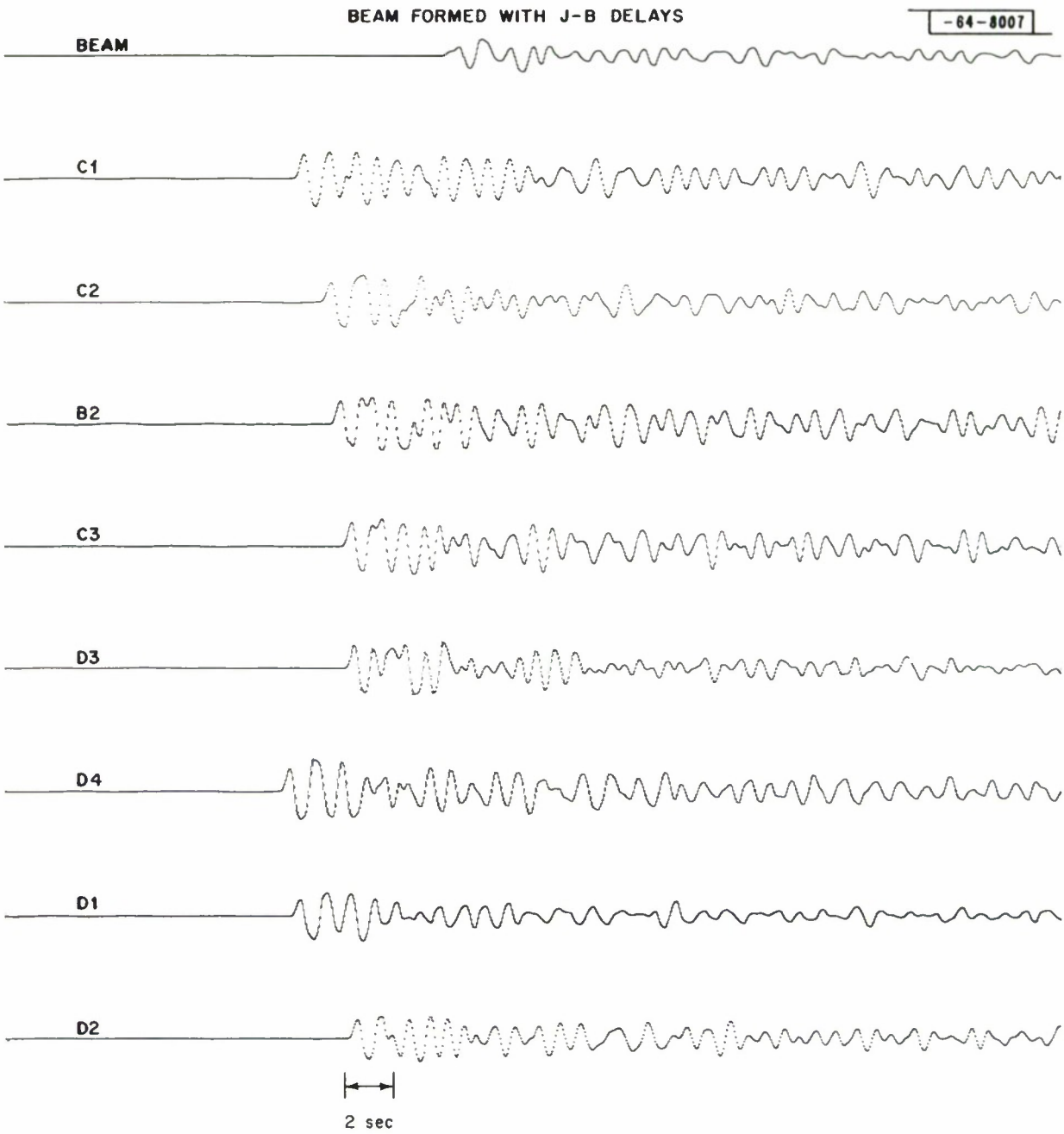

Fig. 3. LASA beam using theoretical delays.

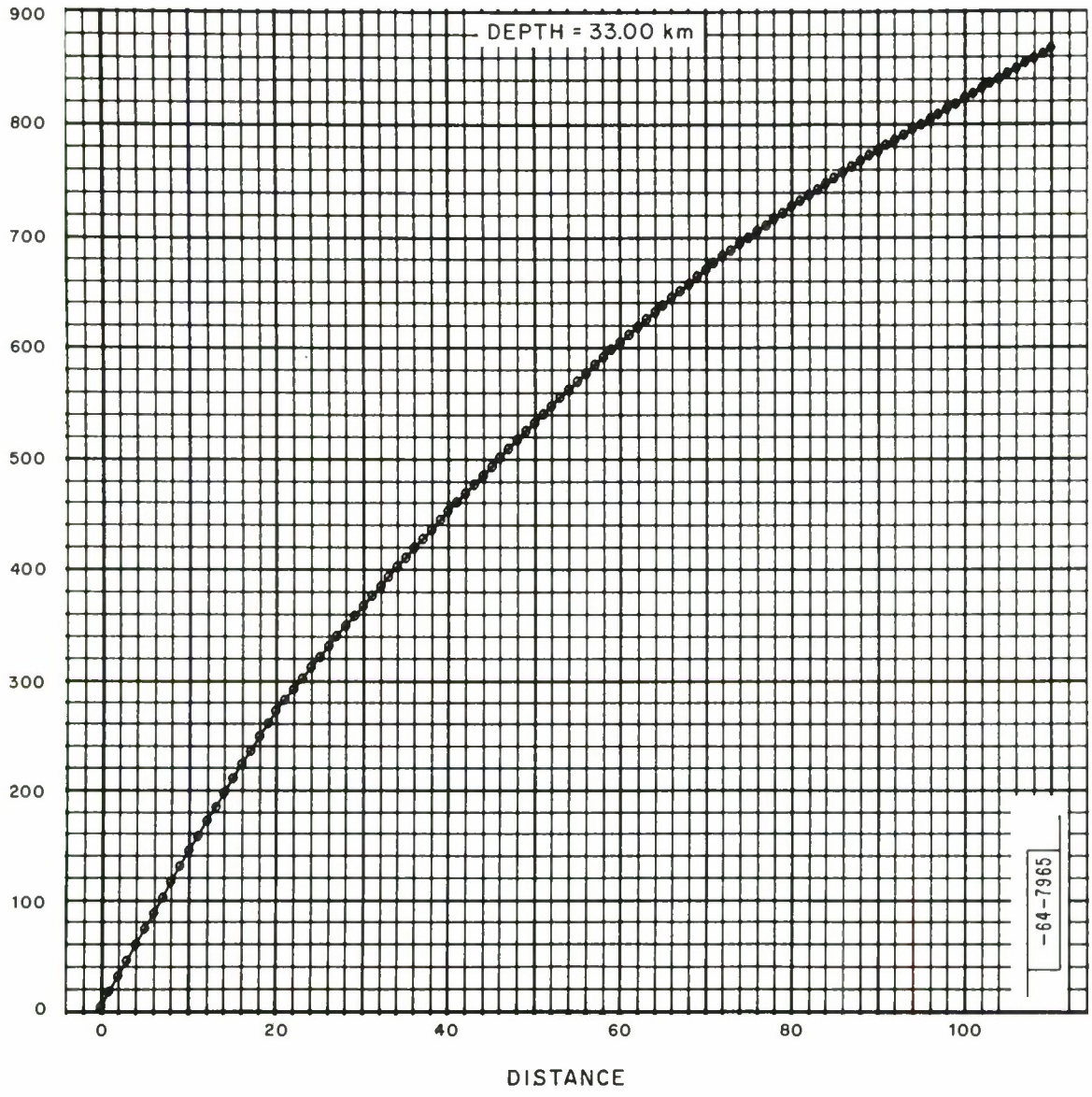

Fig. 4. J-B travel time curve for a depth of 33 km.

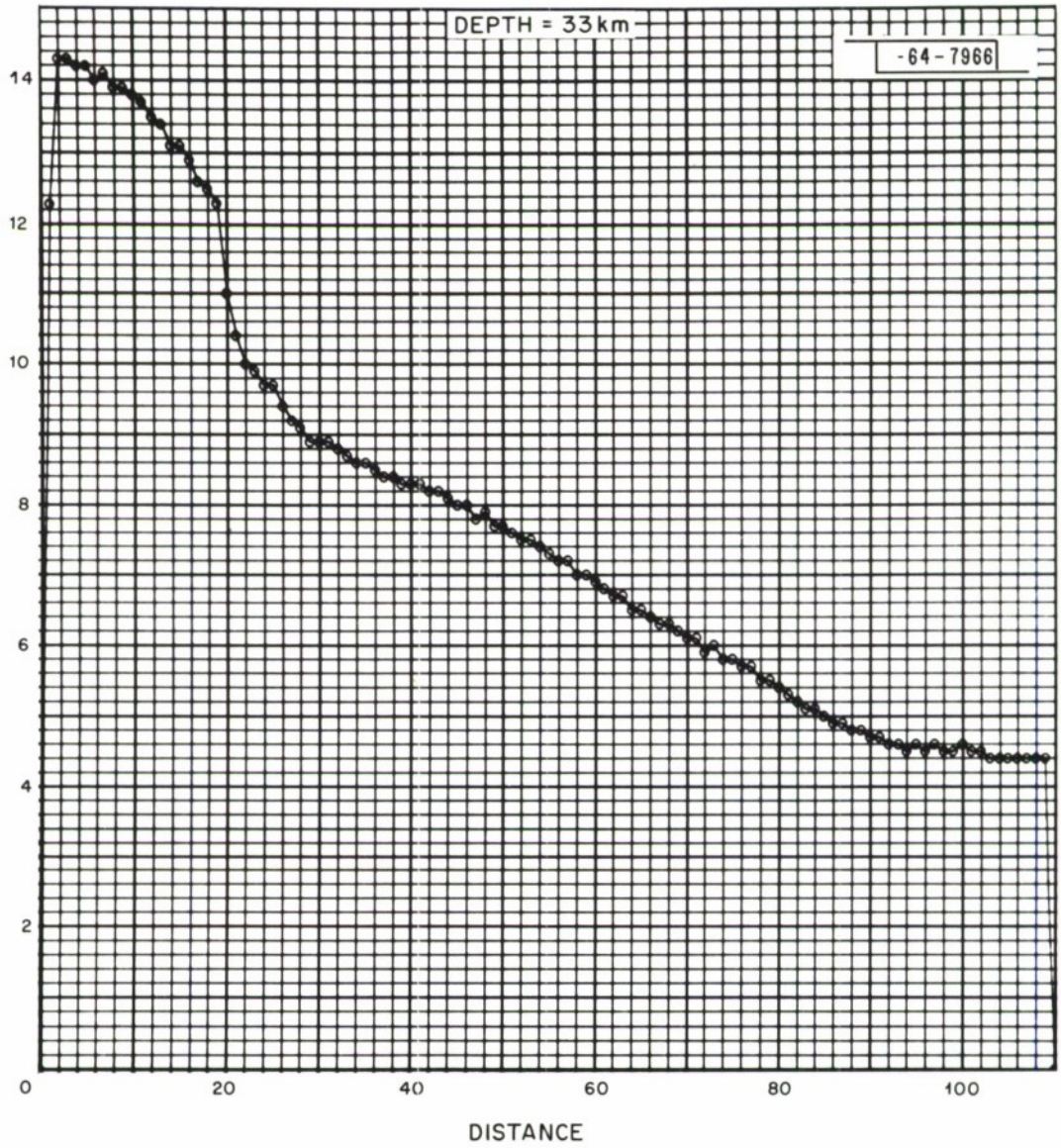

Fig. 5. $dT/d\Delta$ of J-B travel time curve.

Fig. 6. $d^2T/d\Delta^2$ of J-B travel time curve.

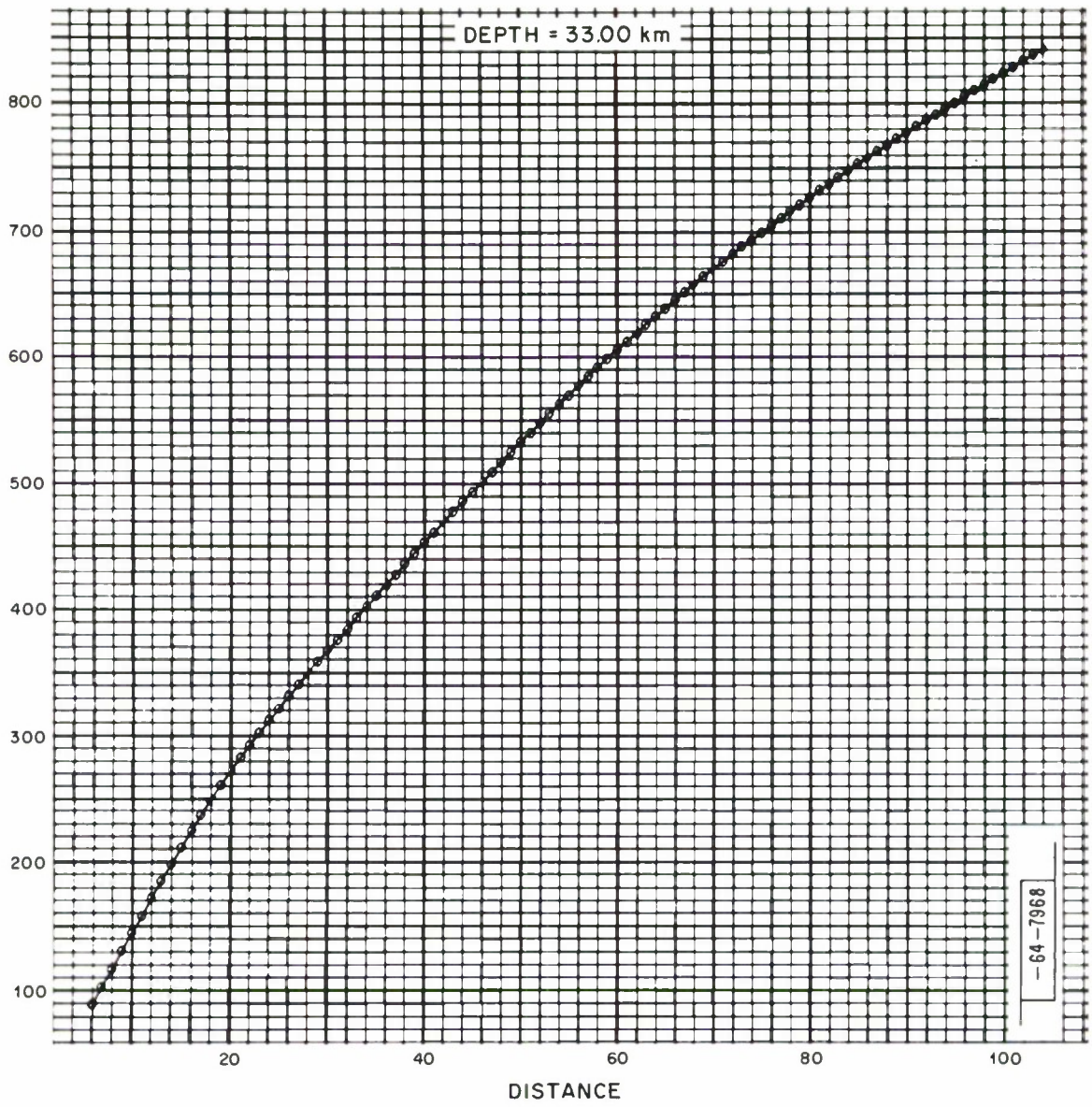

Fig. 7. Smoothed J-B travel time curve.

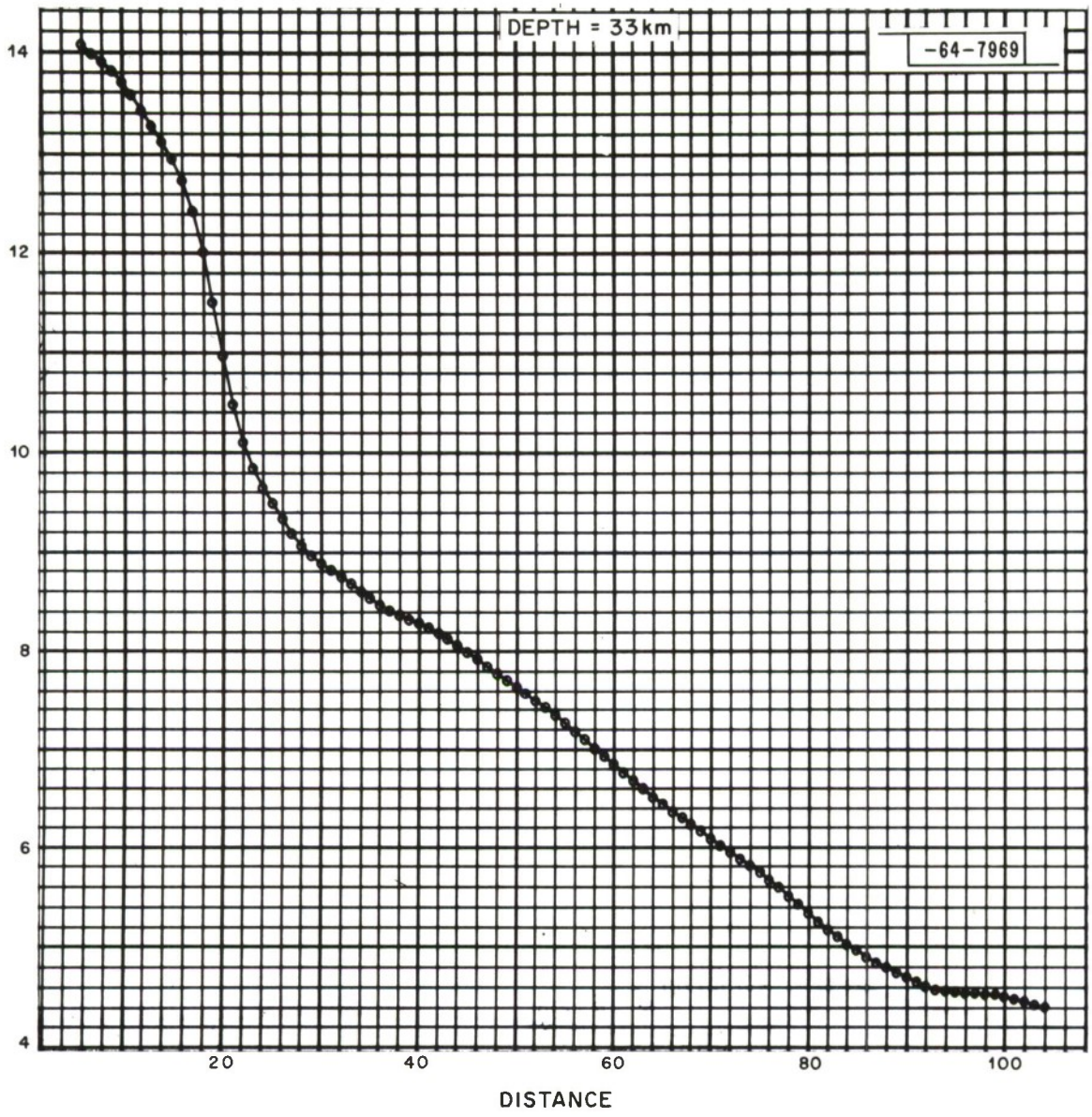

Fig. 8. $dT/d\Delta$ of smoothed J-B travel time curve.

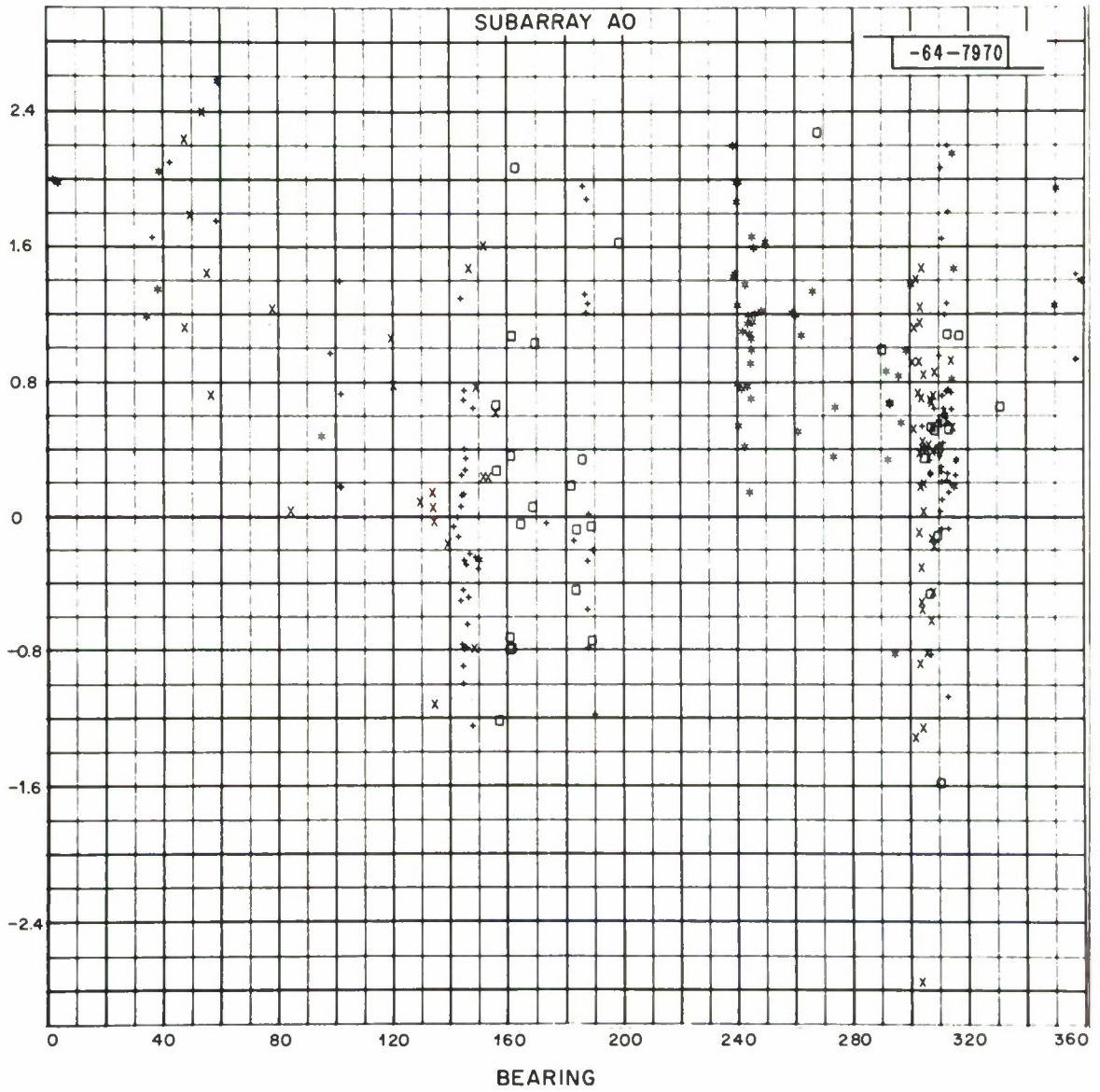

Fig. 9. Residual to J-B travel times for AØ.

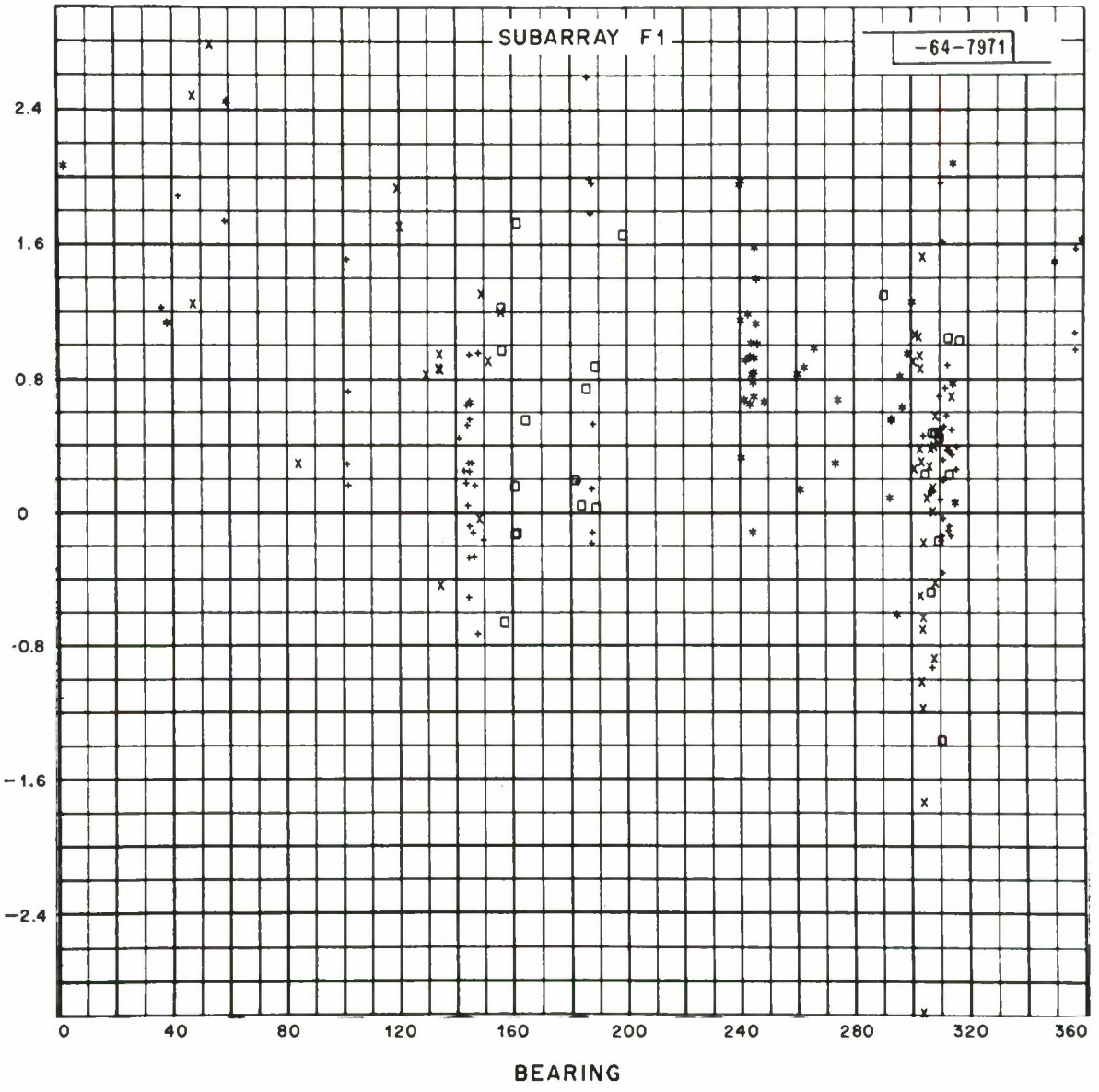

Fig. 10. Residual to J-B travel times for F1.

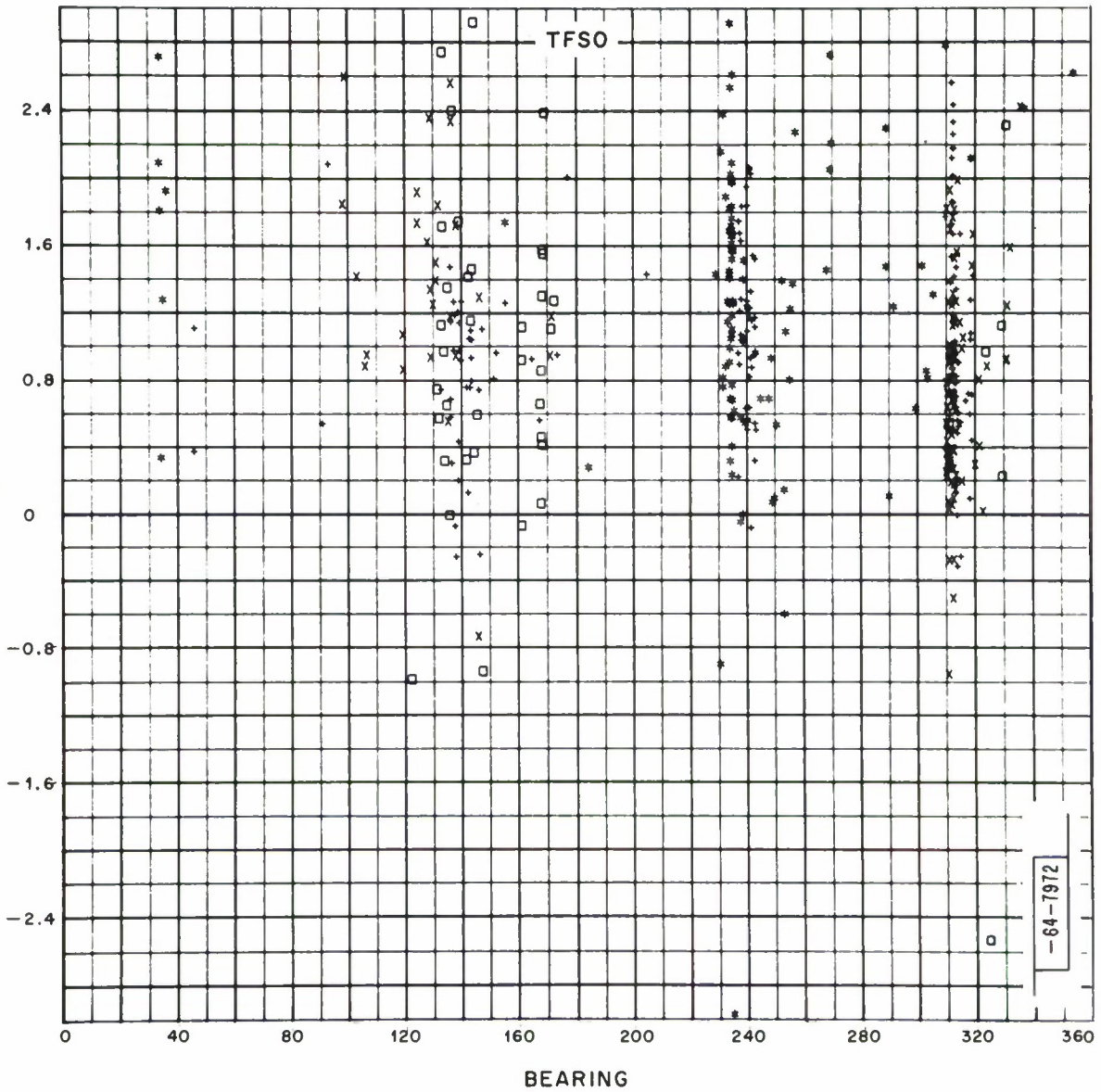

Fig. 11. Residual to J-B travel times for TFSO.

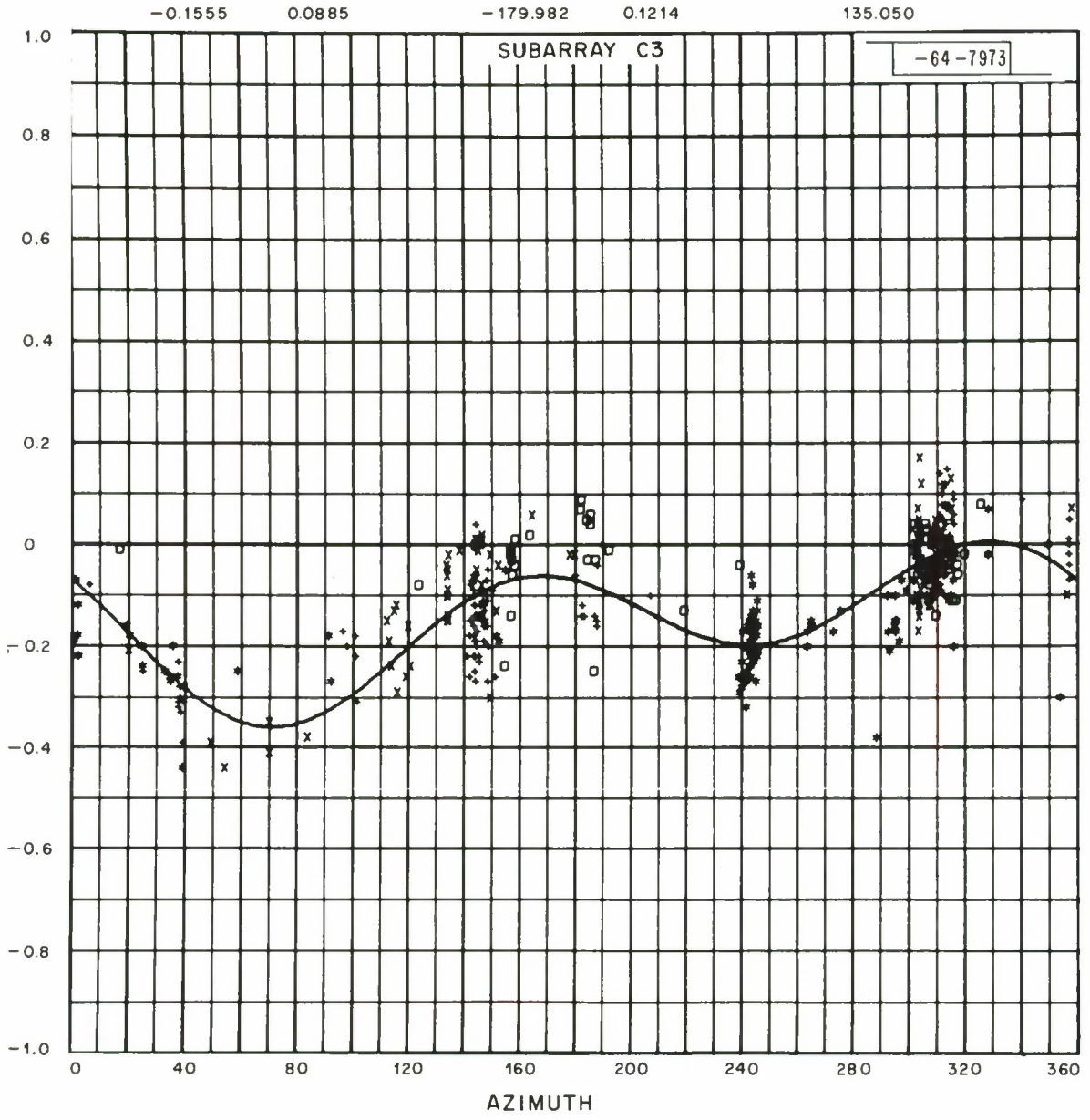

Fig. 12. Relative residuals vs azimuth for C3.

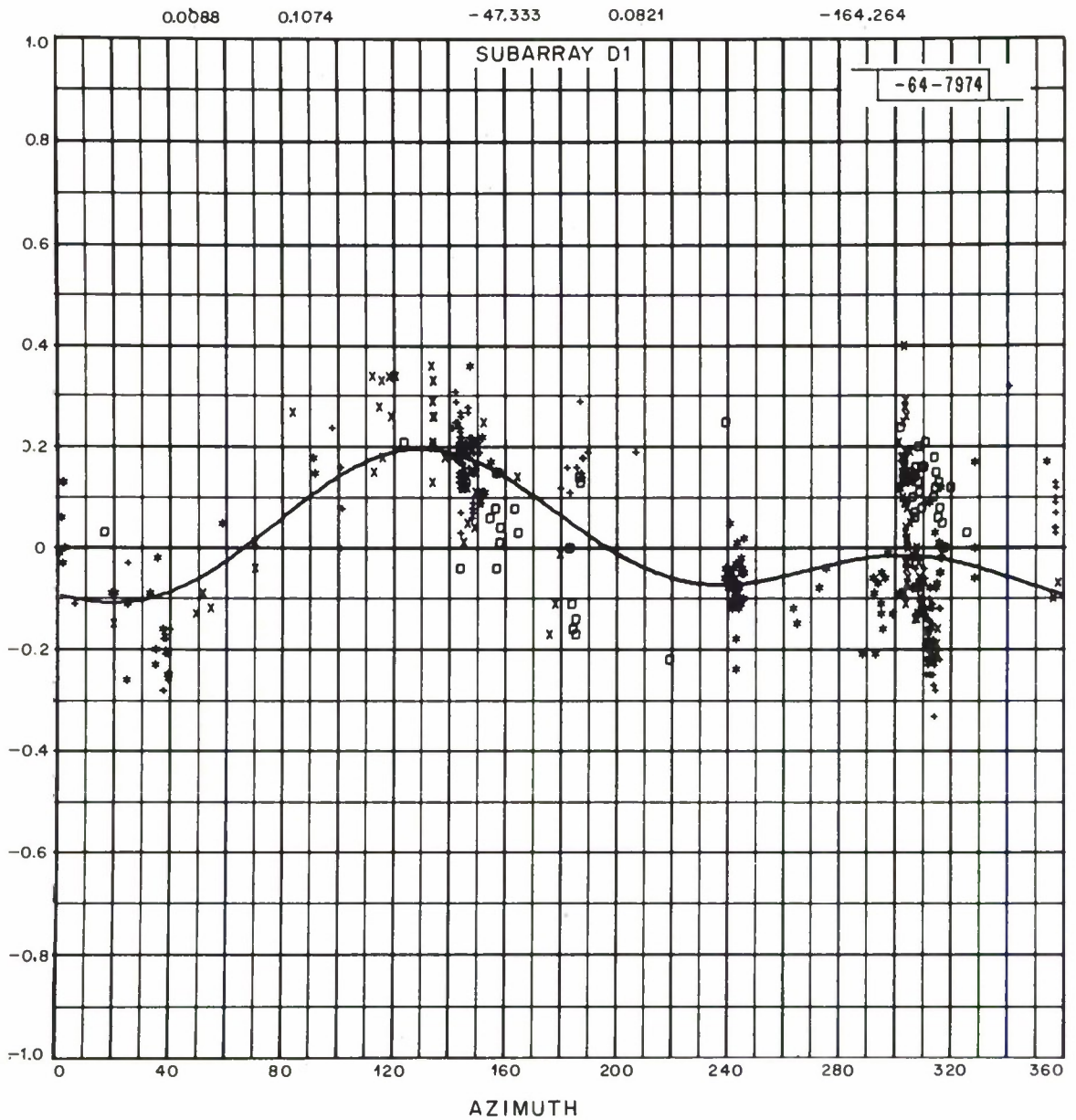

Fig. 13. Relative residuals vs azimuth for D1.

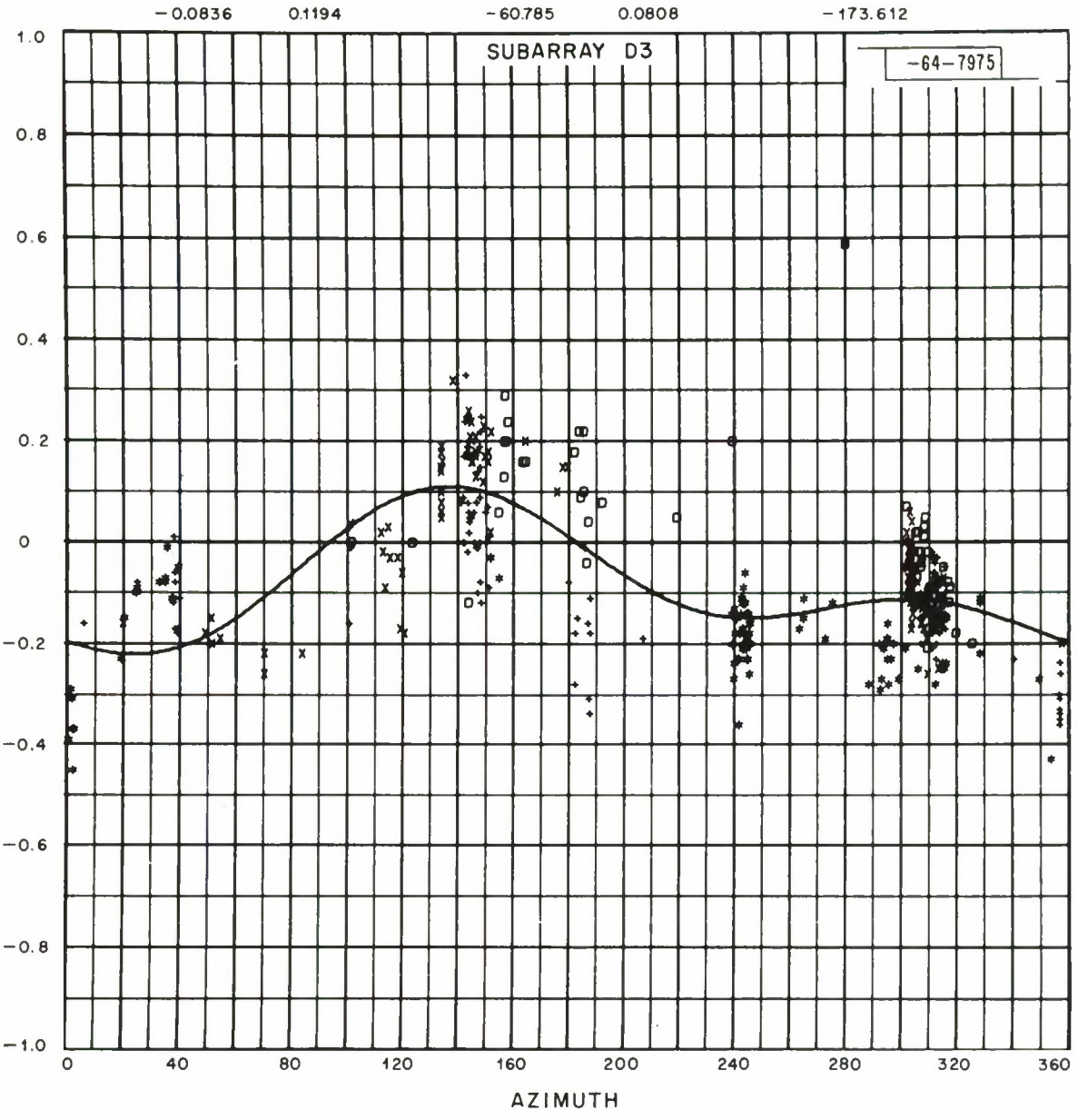

Fig. 14. Relative residuals vs azimuth for D3.

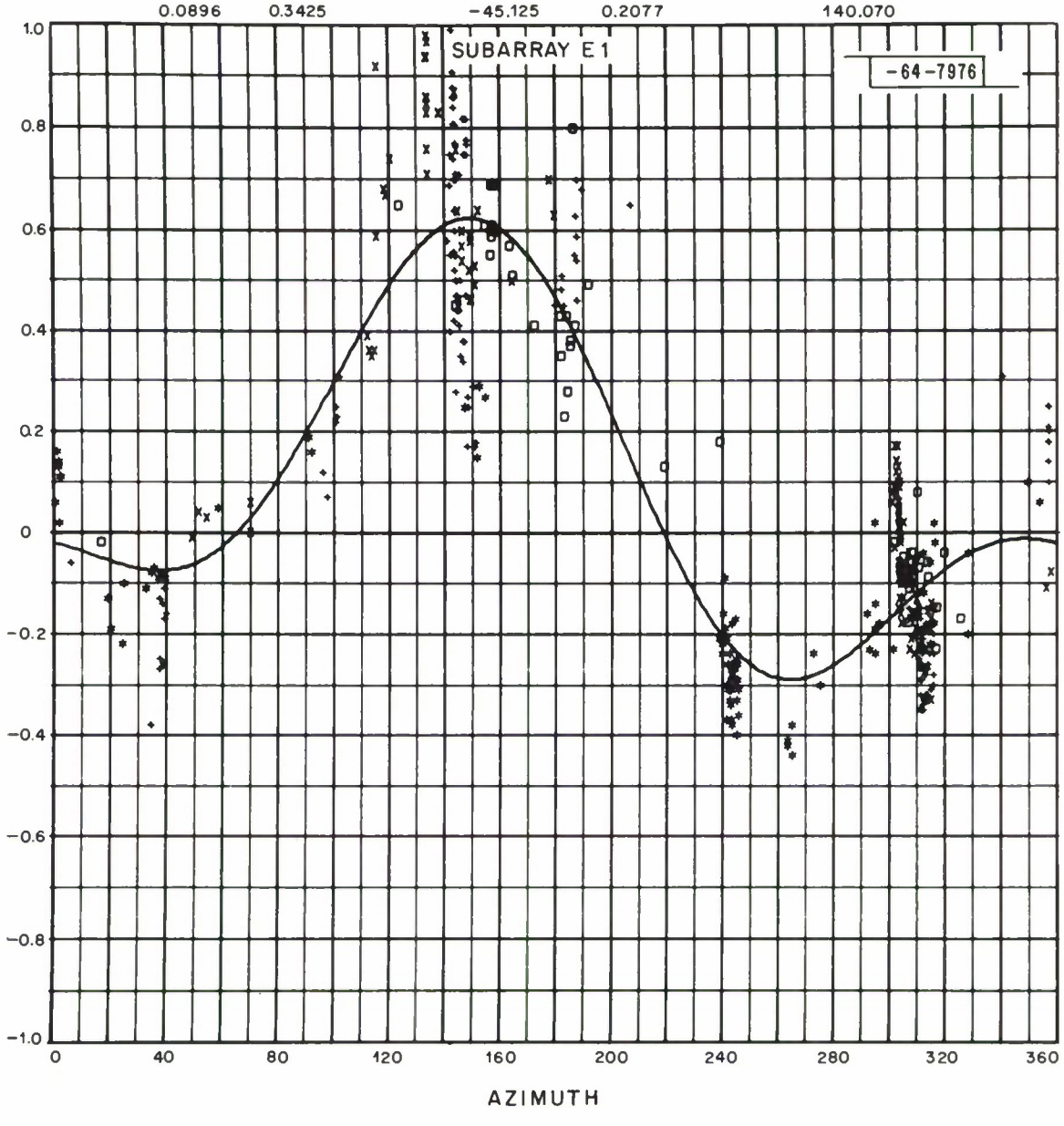

Fig. 15. Relative residuals vs azimuth for E1.

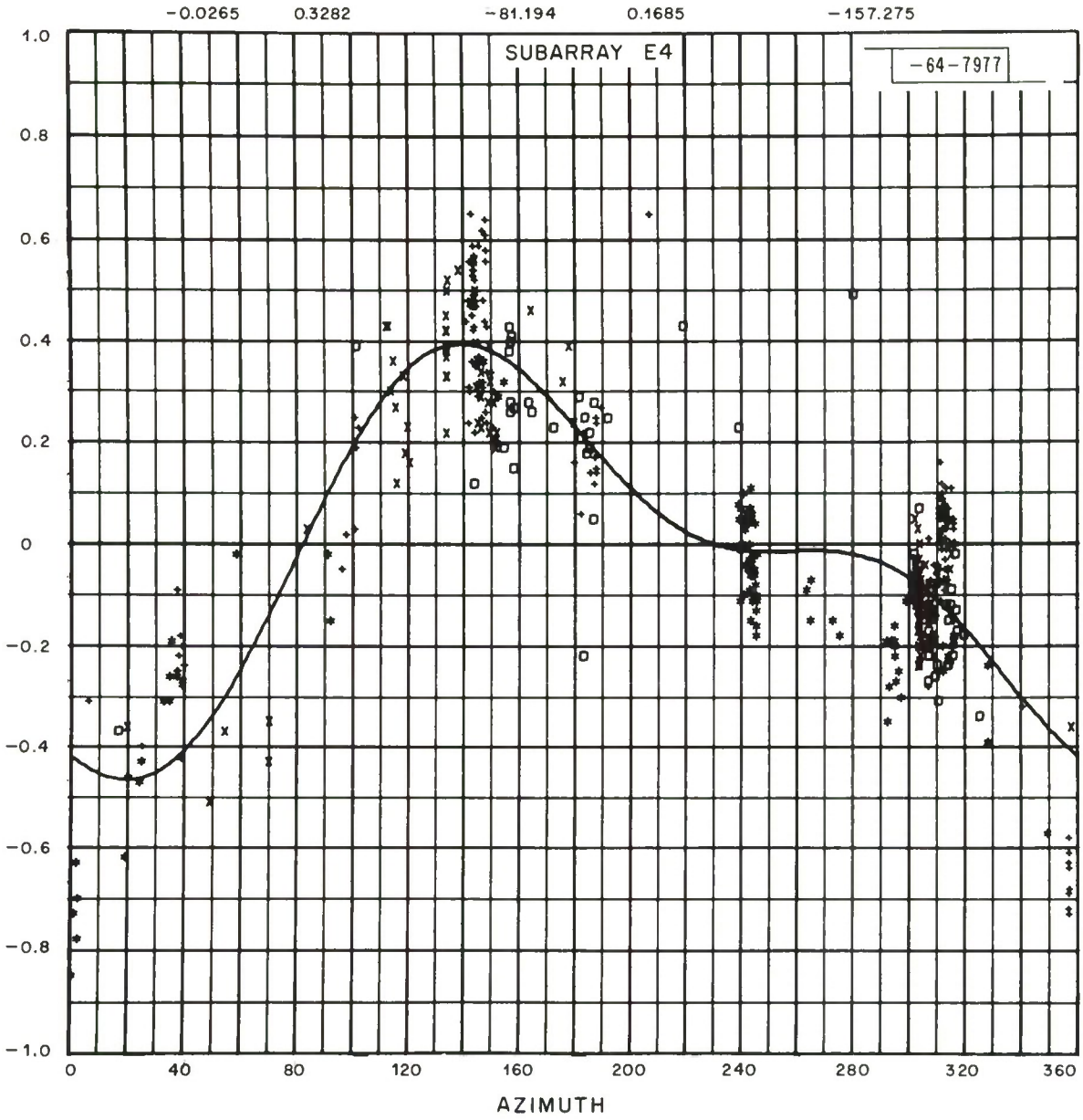

Fig. 16. Relative residuals vs azimuth for E4.

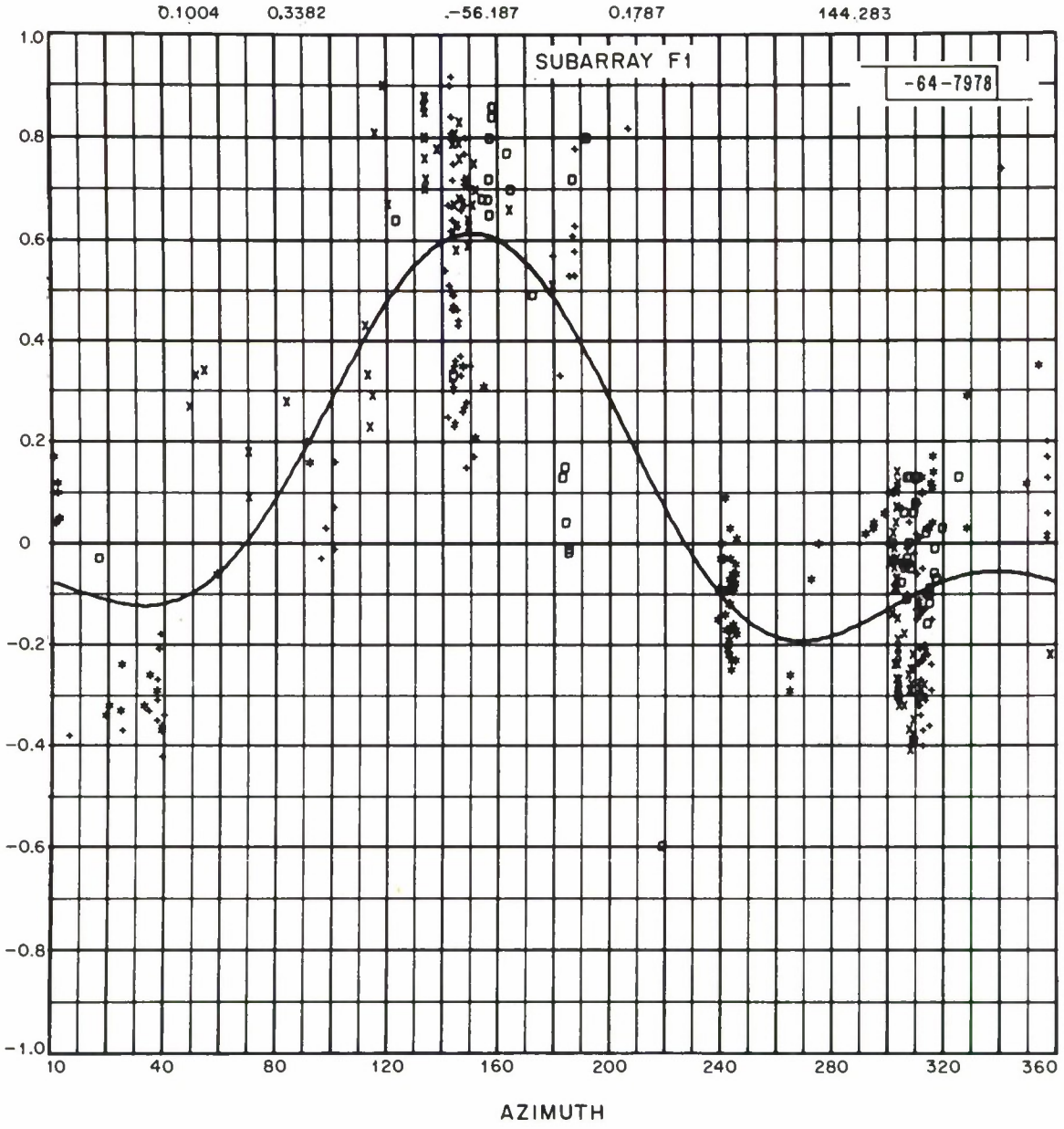

Fig. 17. Relative residuals vs azimuth for F1.

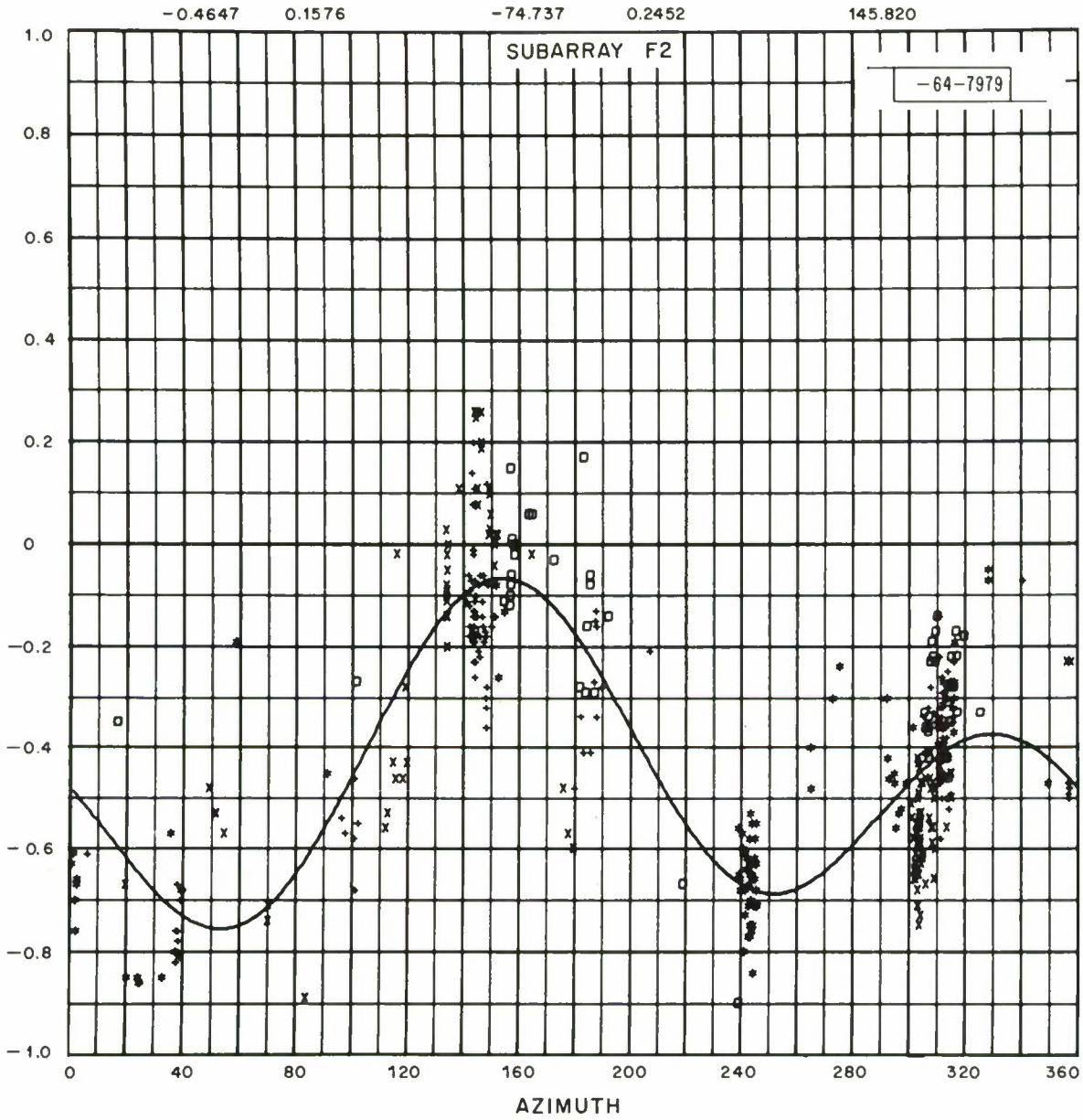

Fig. 18. Relative residuals vs azimuth for F2.

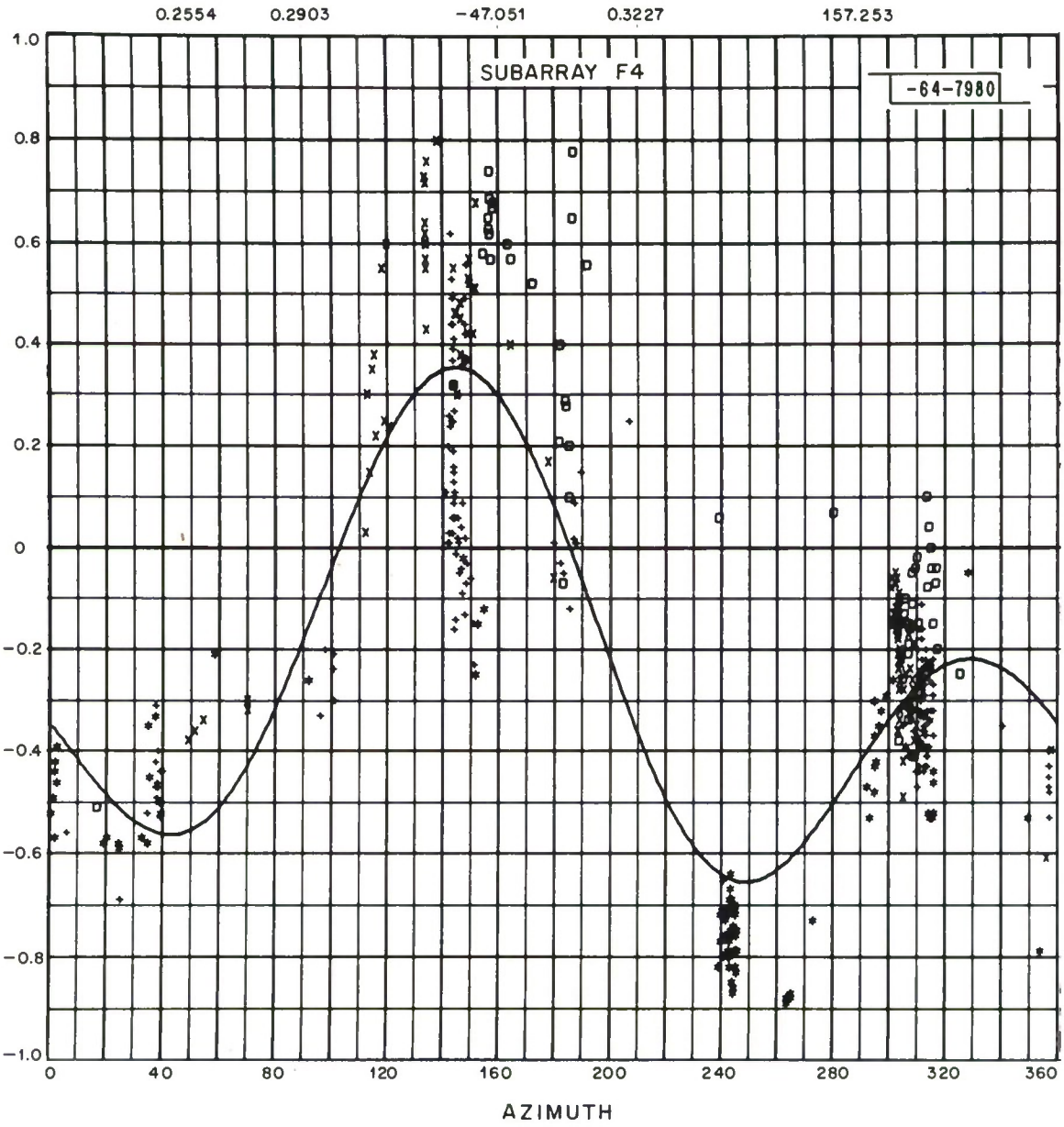

Fig. 19. Relative residuals vs azimuth for F4.

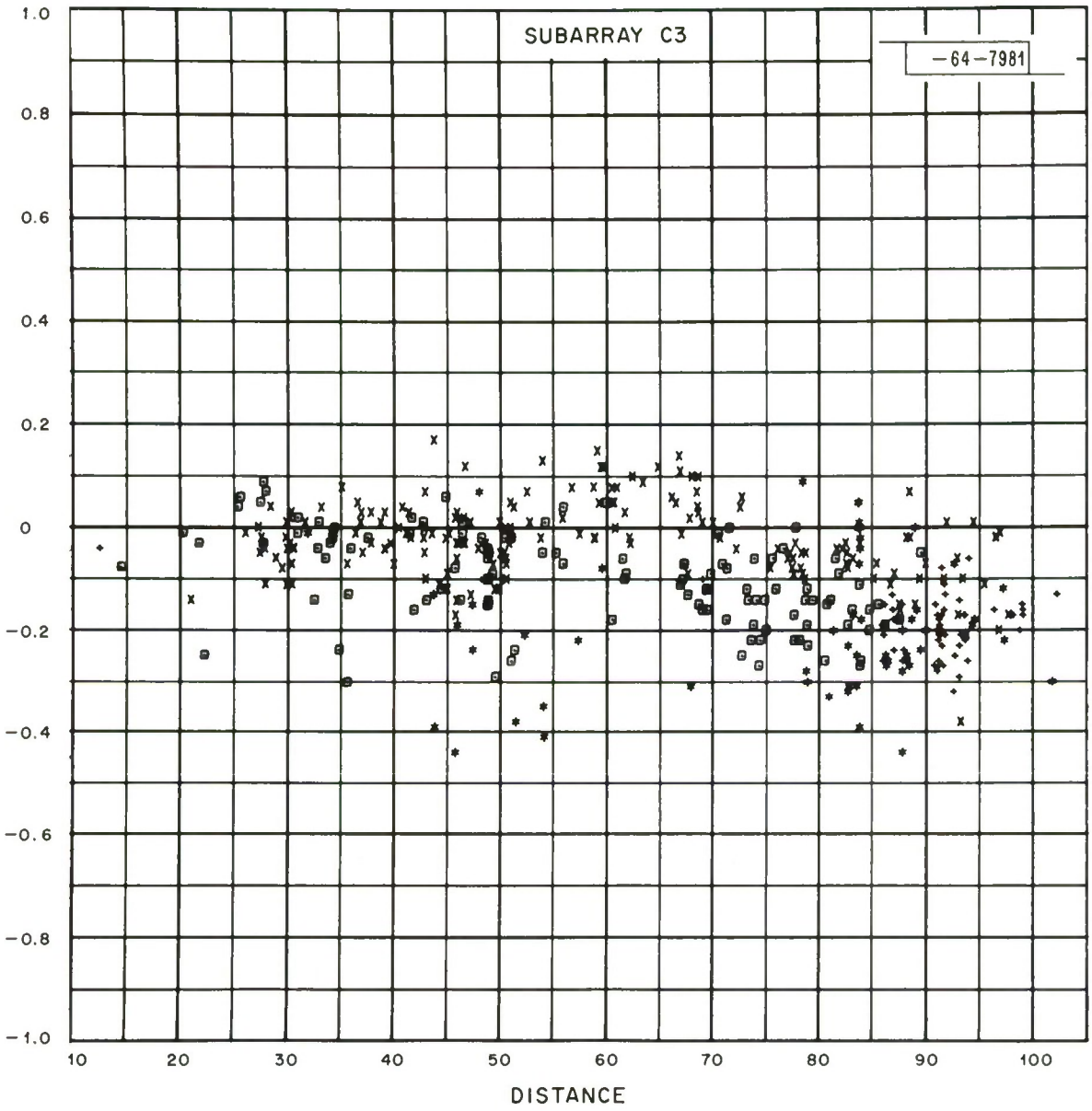

Fig. 20. Relative residuals vs distance for C3.

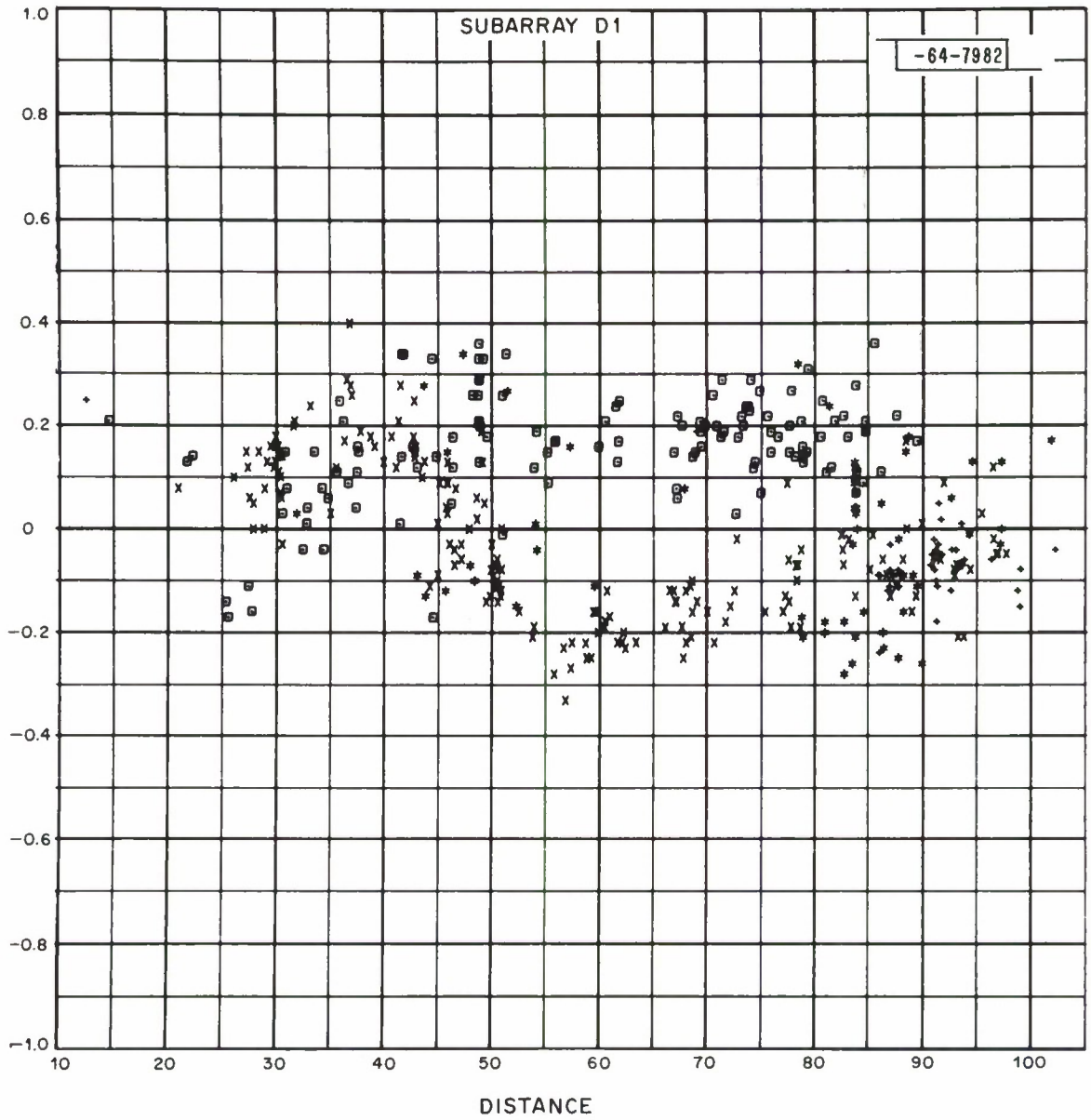

Fig. 21. Relative residuals vs distance for D1.

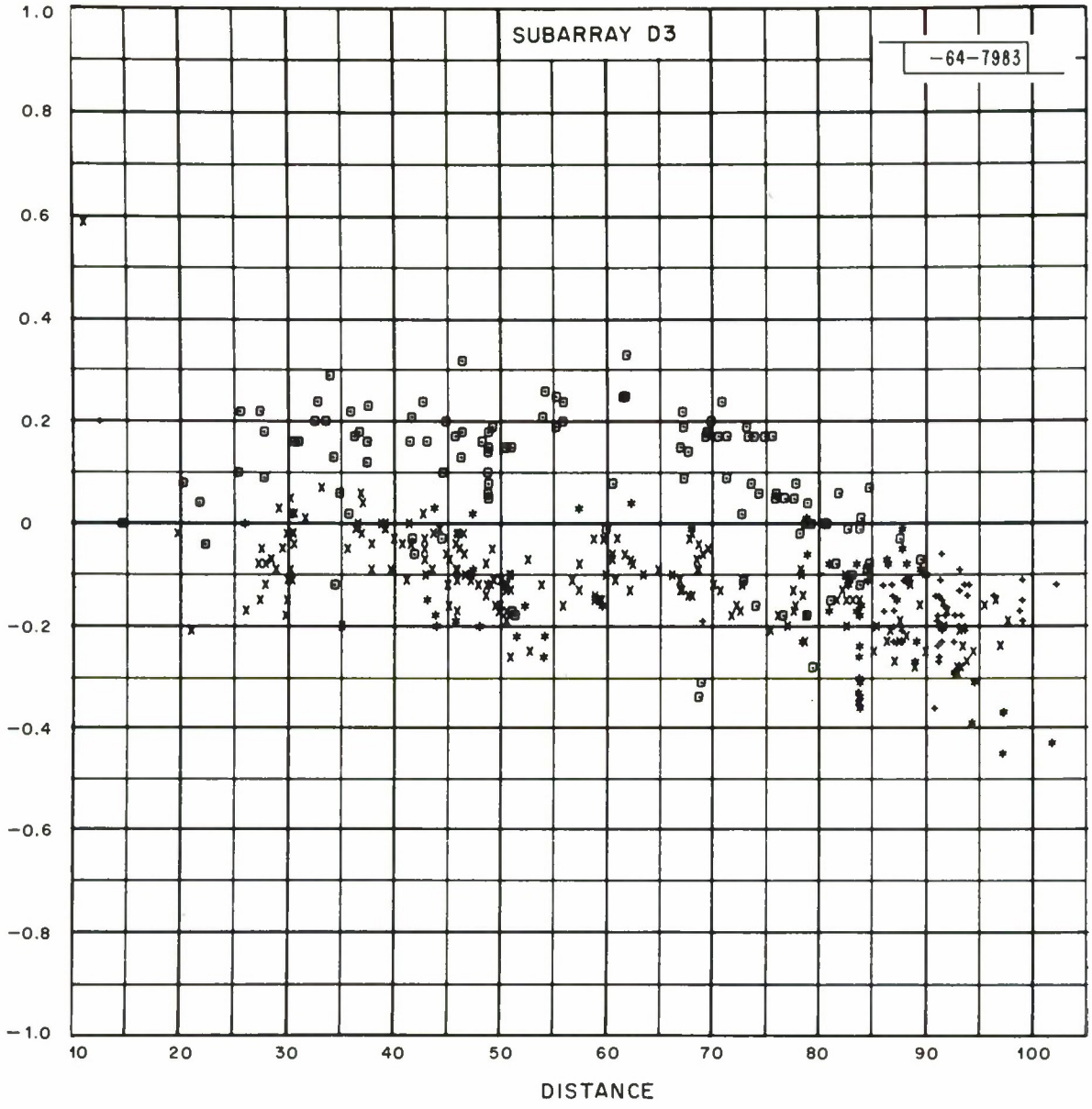

Fig. 22. Relative residuals vs distance for D3.

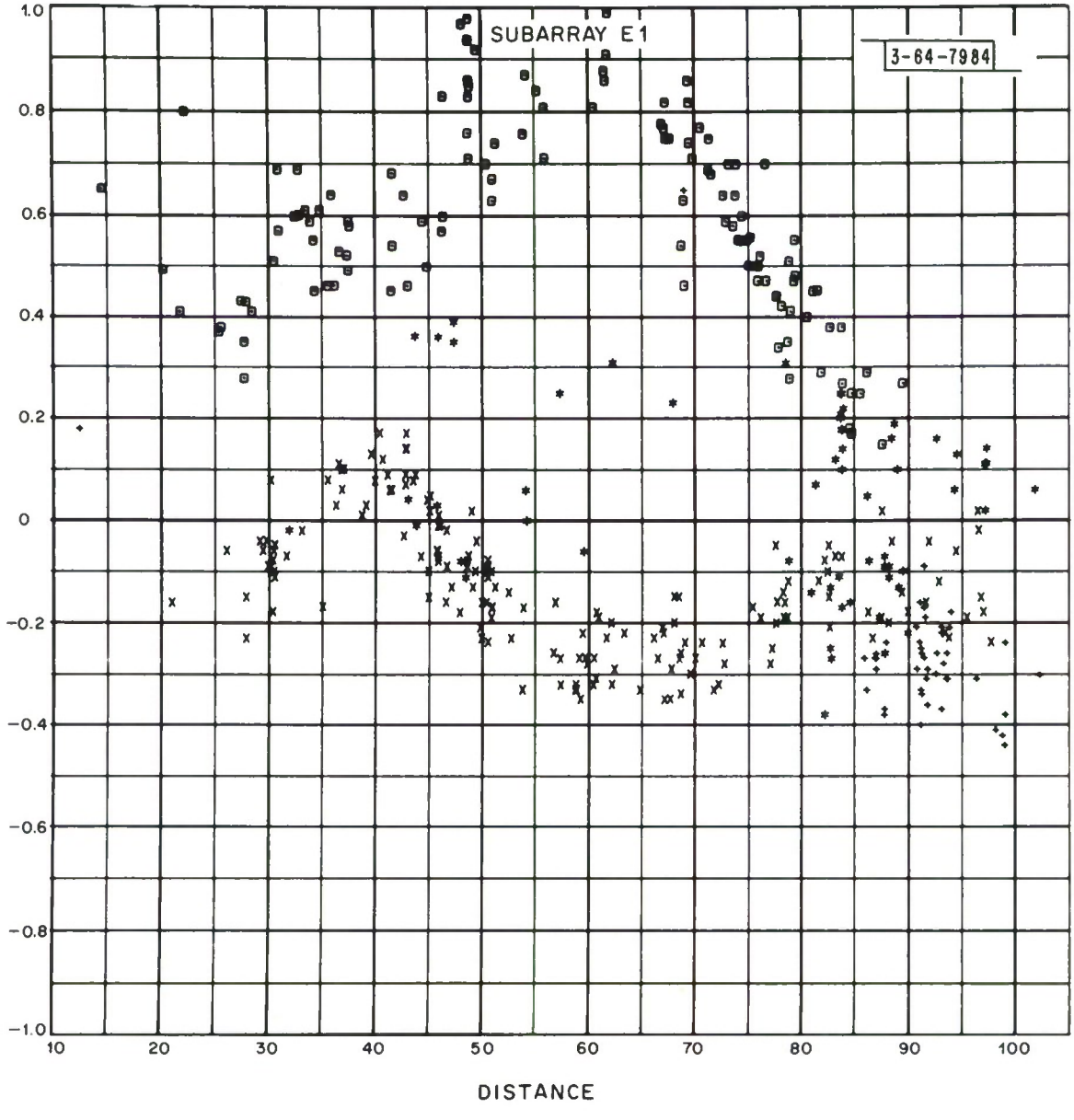

Fig. 23. Relative residuals vs distance for E1.

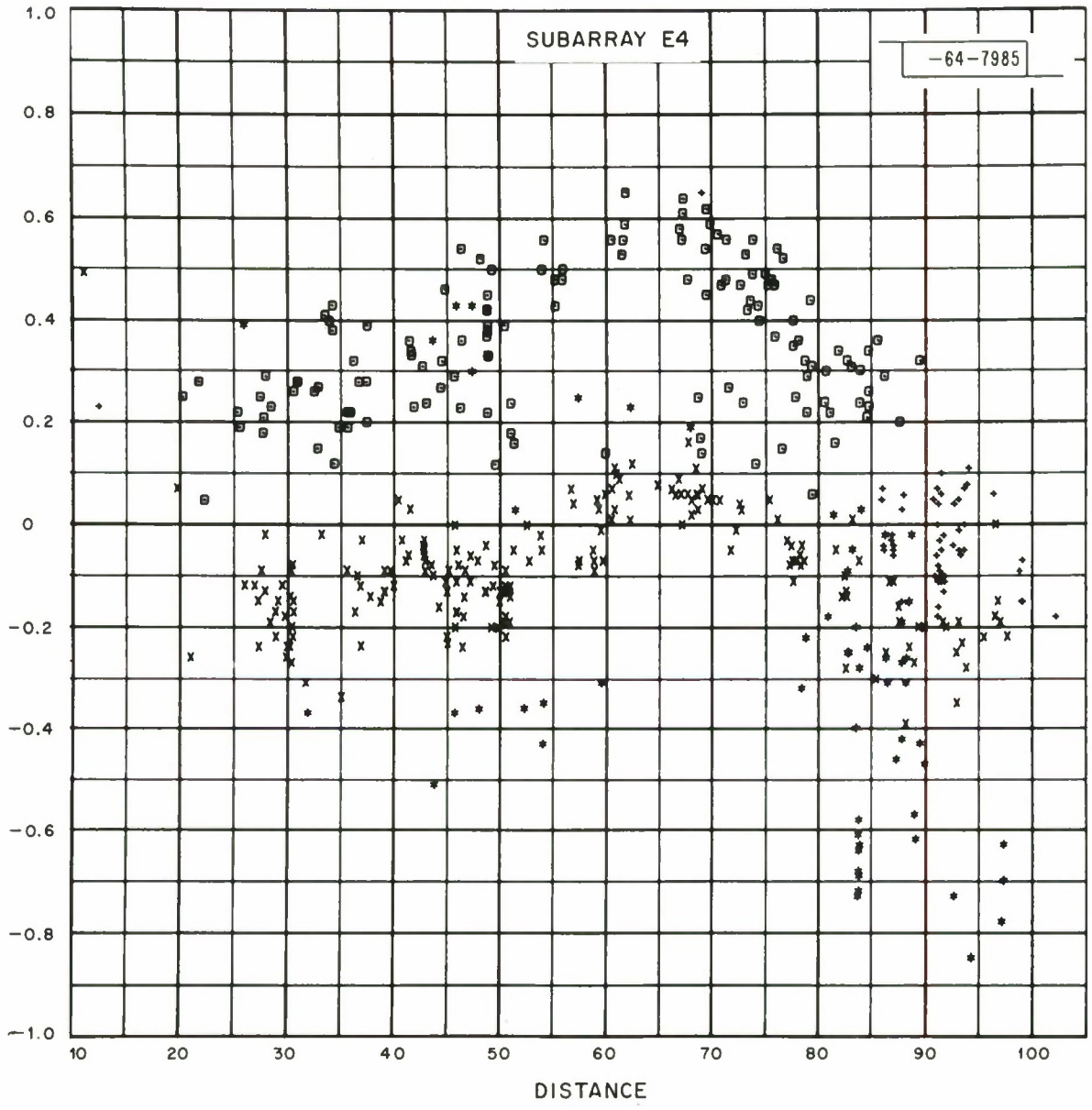

Fig. 24. Relative residuals vs distance for E4.

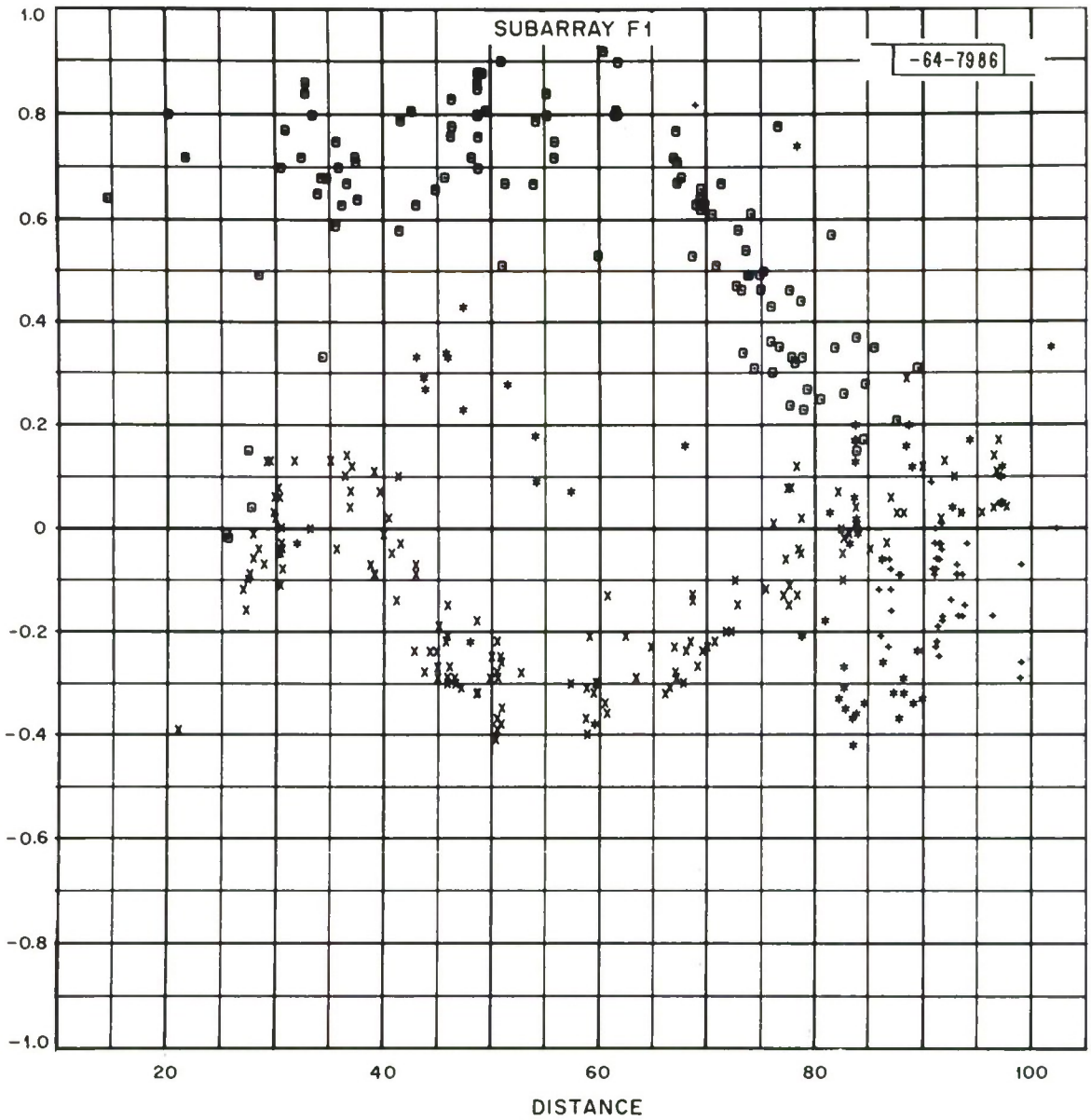

Fig. 25. Relative residuals vs distance for F1.

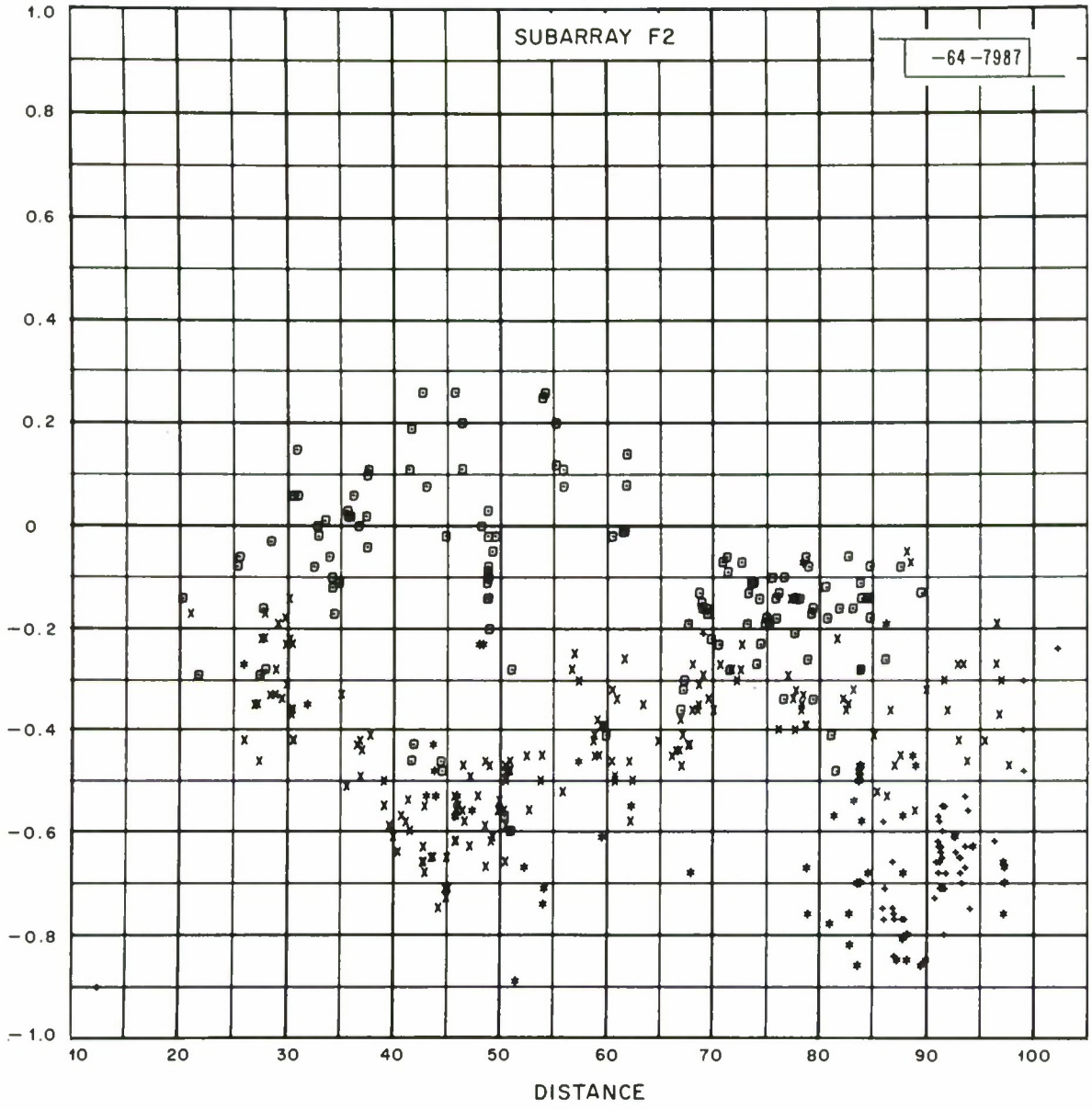

Fig. 26. Relative residuals vs distance for F2.

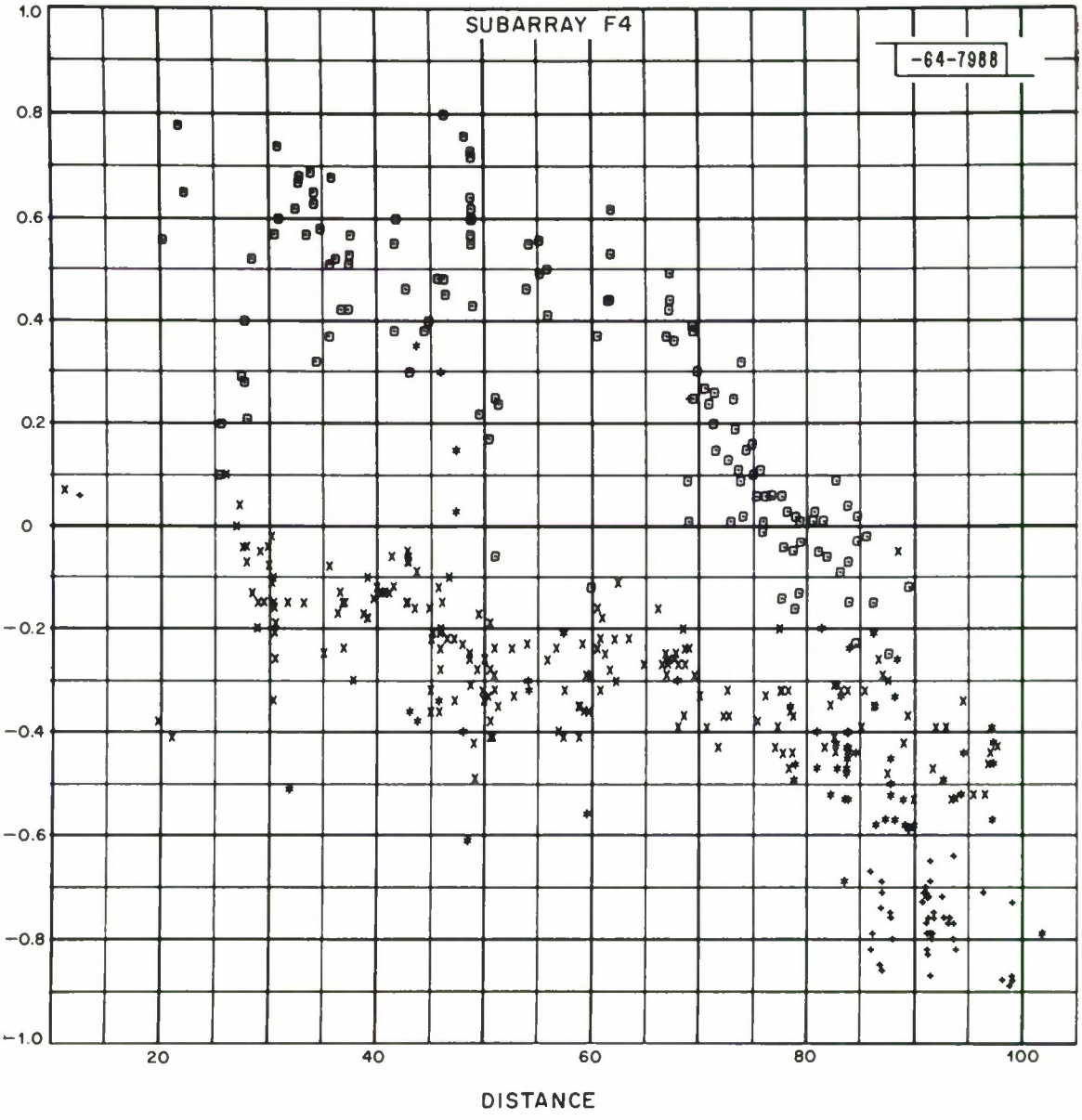

Fig. 27. Relative residuals vs distance for F4.

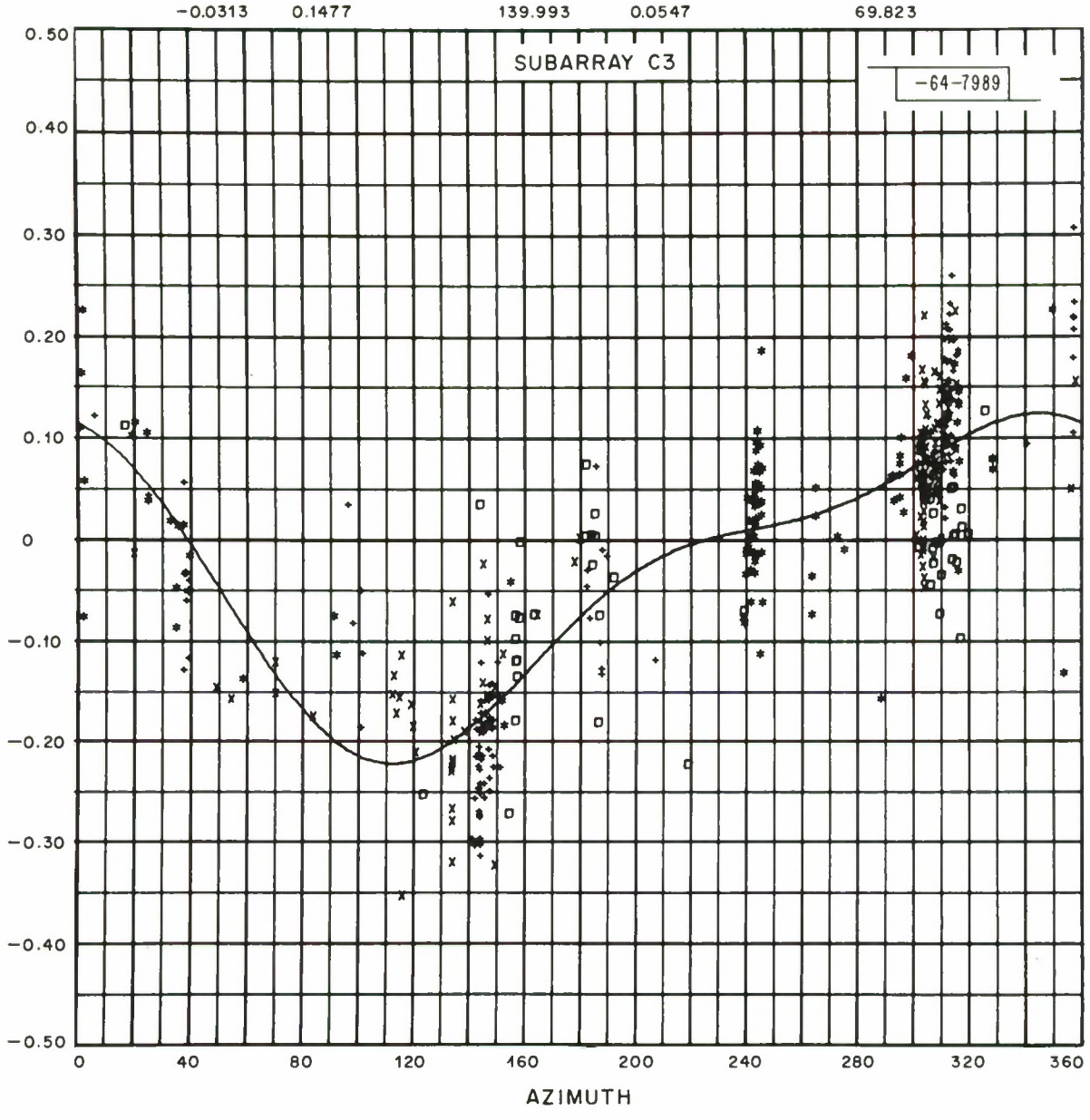

Fig. 28. Plane wave residuals vs azimuth for C3.

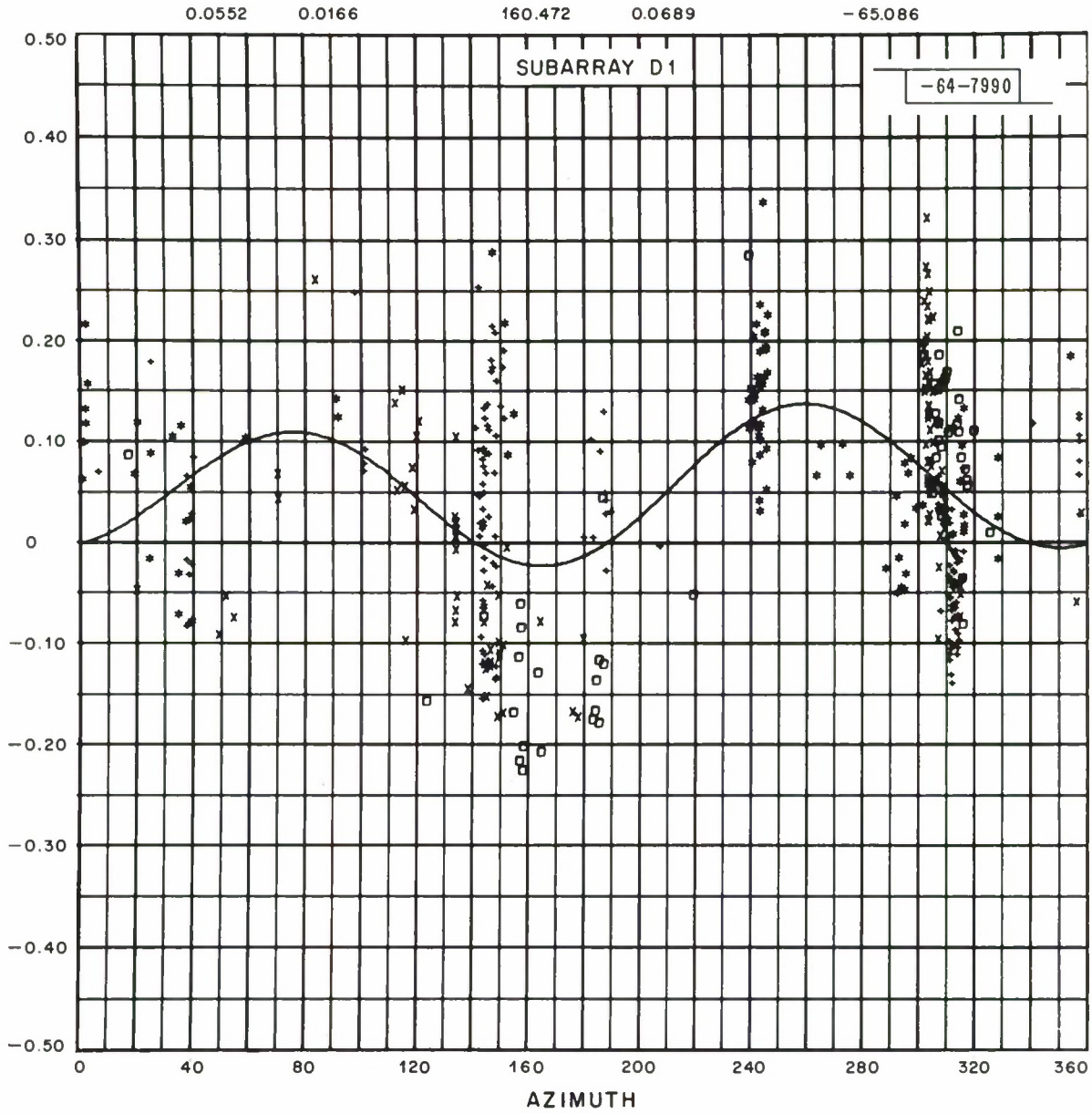

Fig. 29. Plane wave residuals vs azimuth for D1.

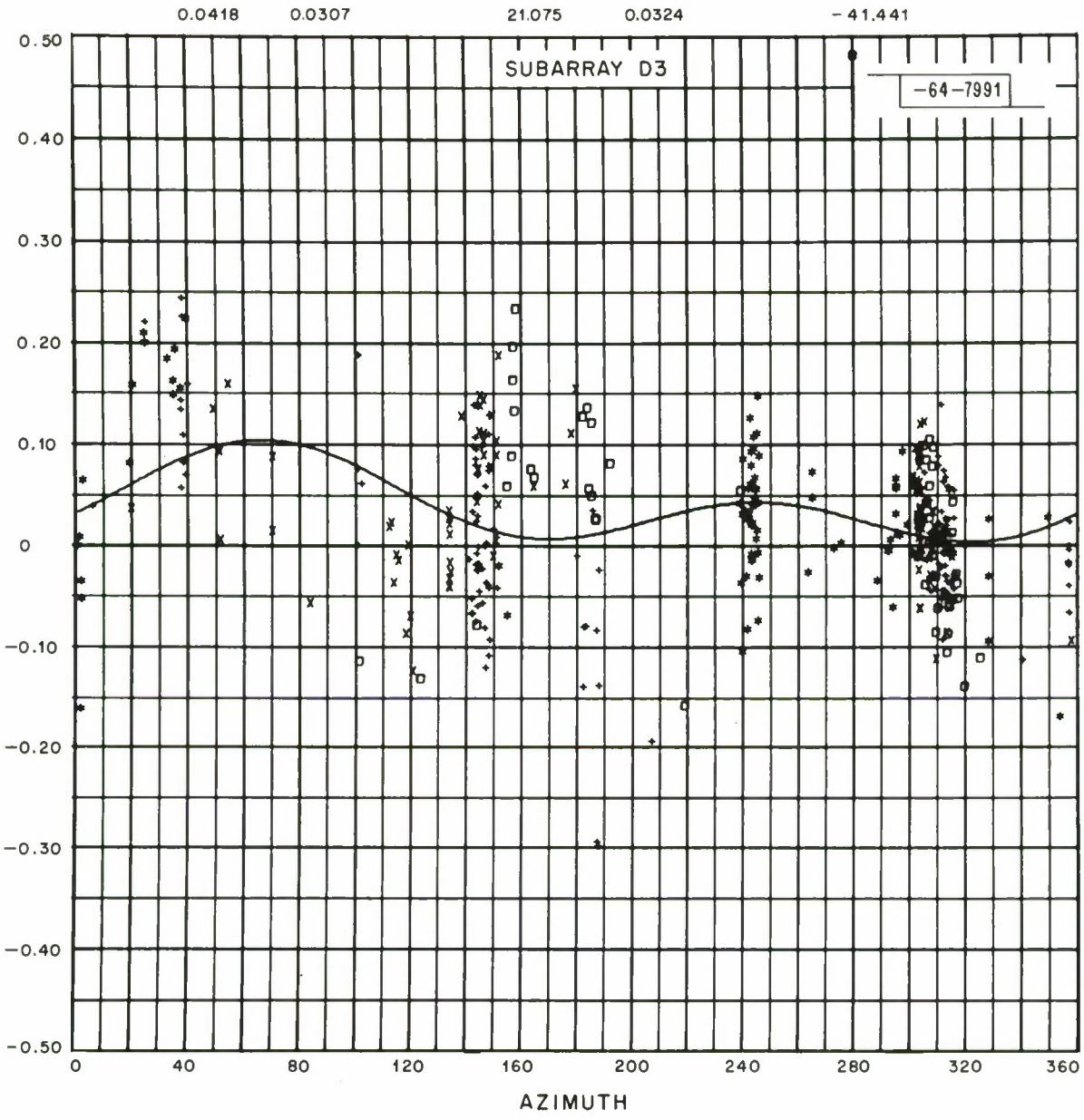

Fig. 30. Plane wave residuals vs azimuth for D3.

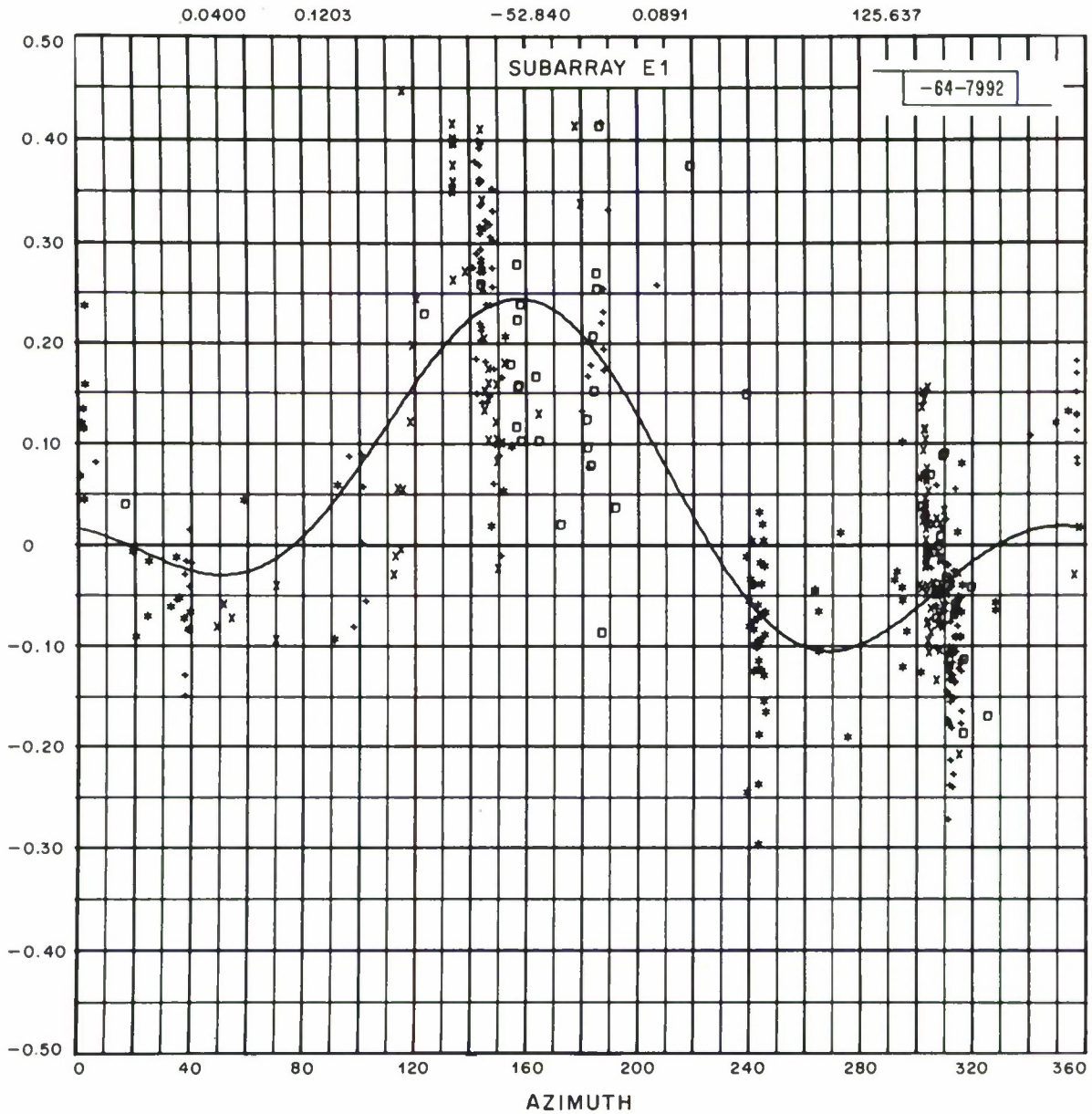

Fig. 31. Plane wave residuals vs azimuth for E1.

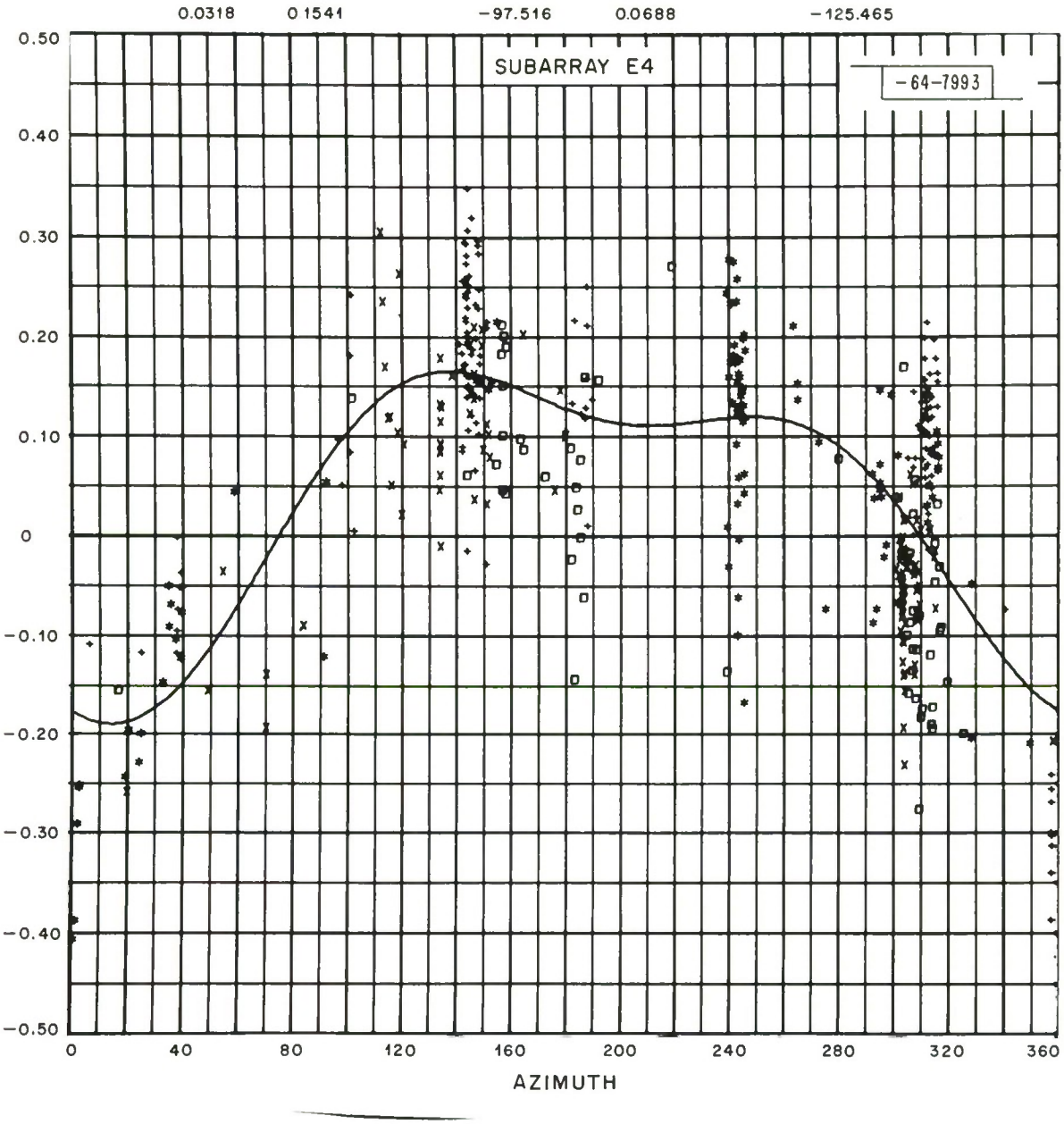

Fig. 32. Plane wave residuals vs azimuth for E4.

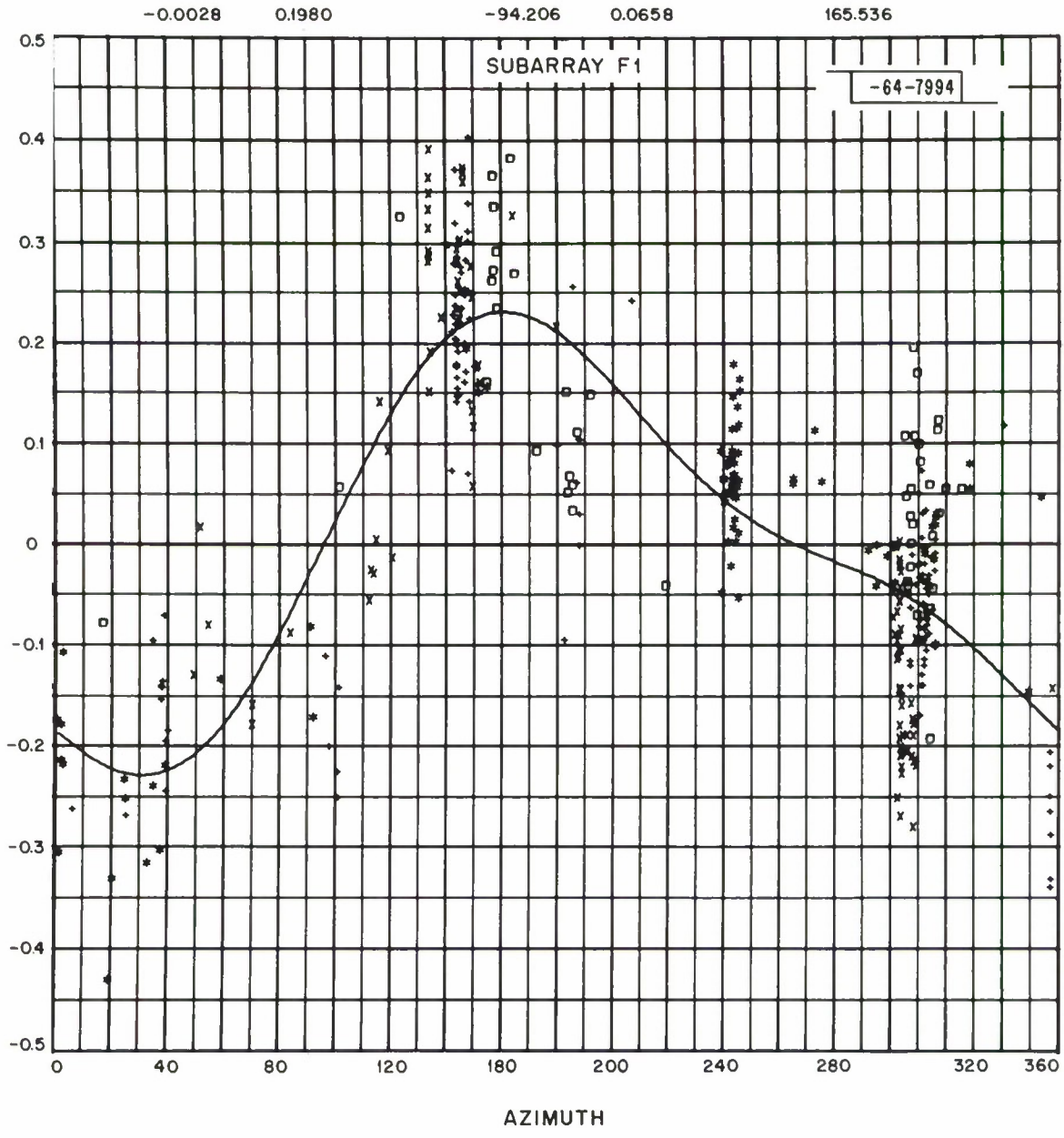

Fig. 33. Plane wave residuals vs azimuth for F1.

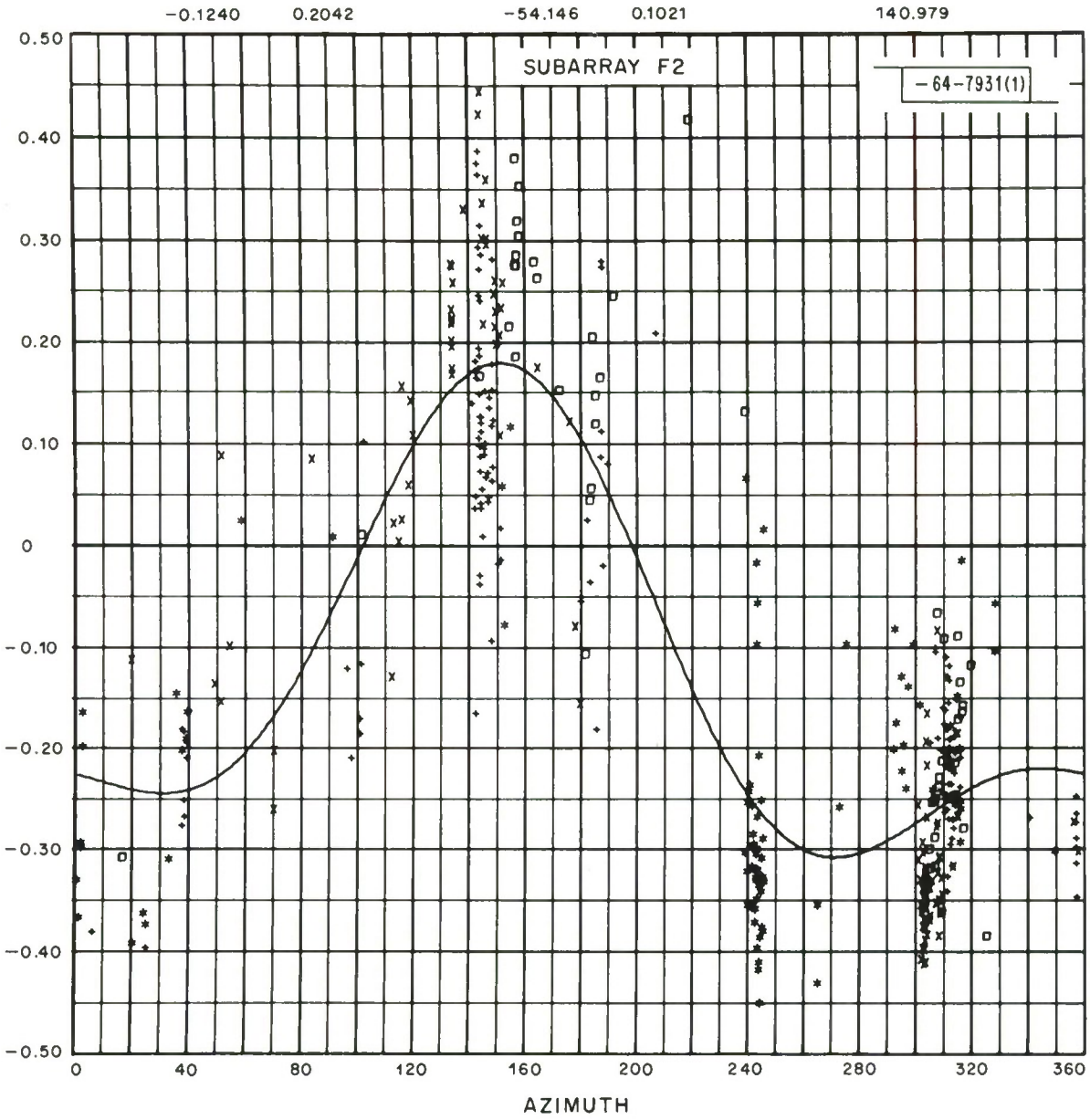

Fig. 34. Plane wave residuals vs azimuth for F2.

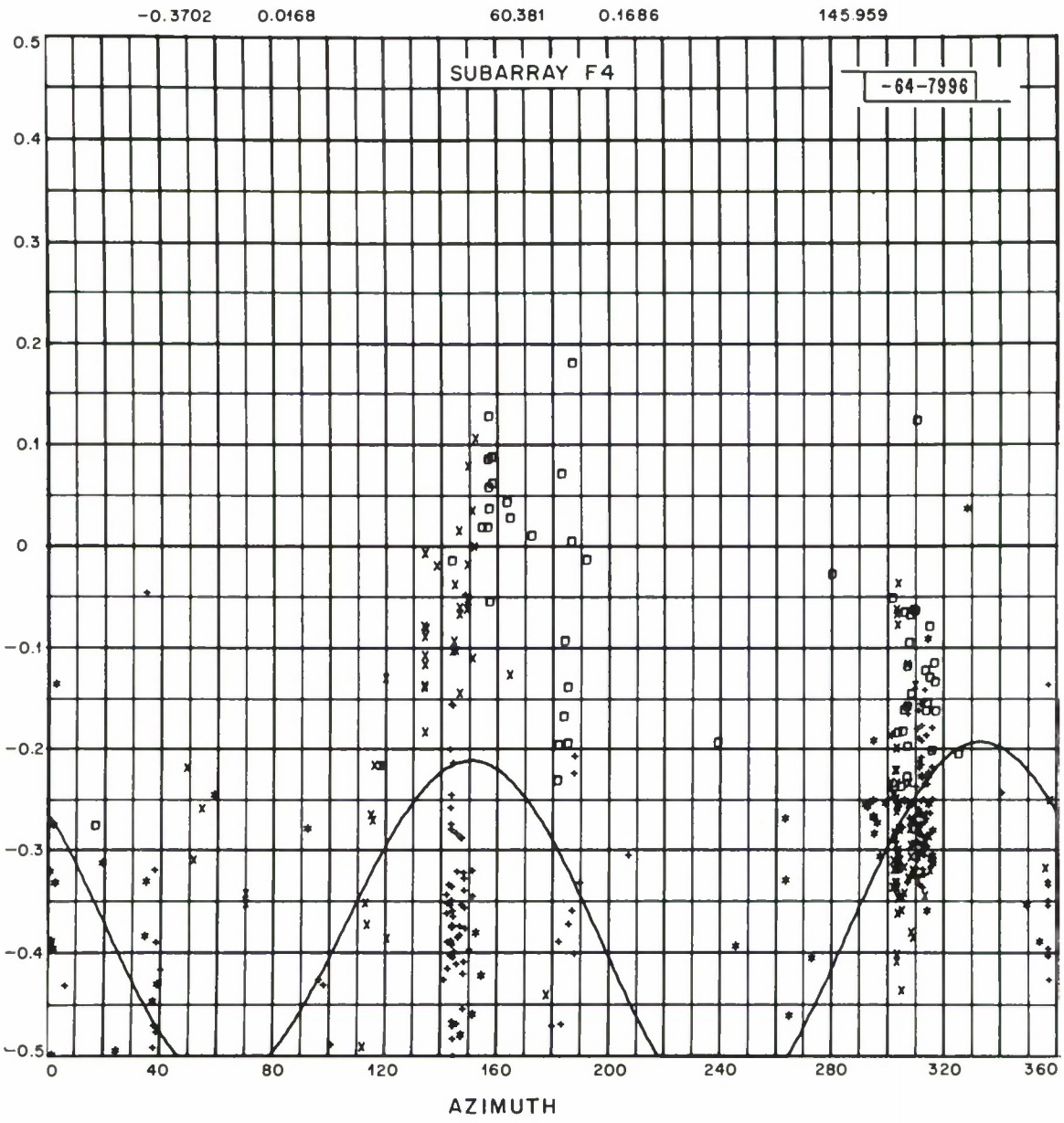

Fig. 35. Plane wave residuals vs azimuth for F4.

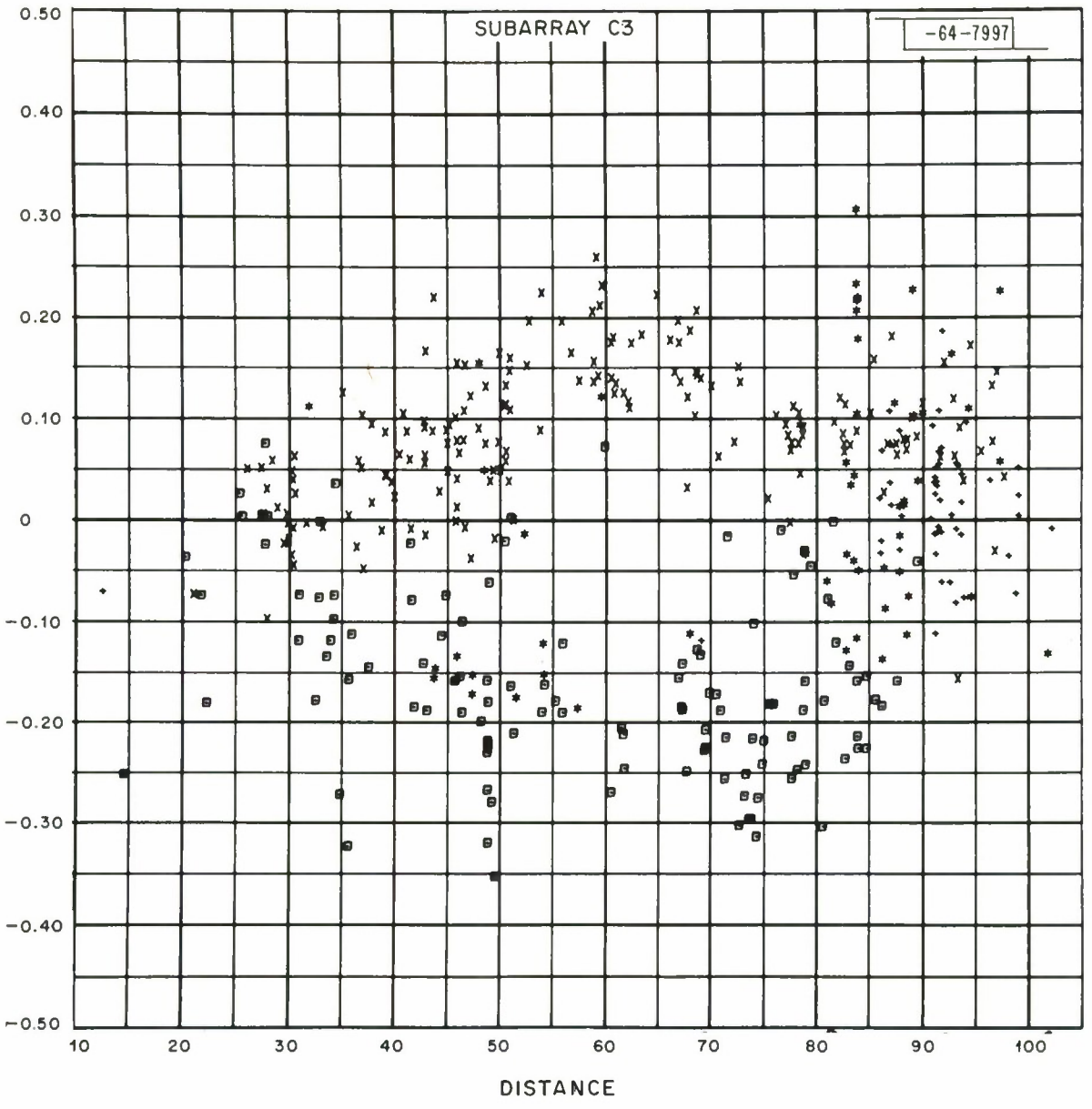

Fig. 36. Plane wave residuals vs distance for C3.

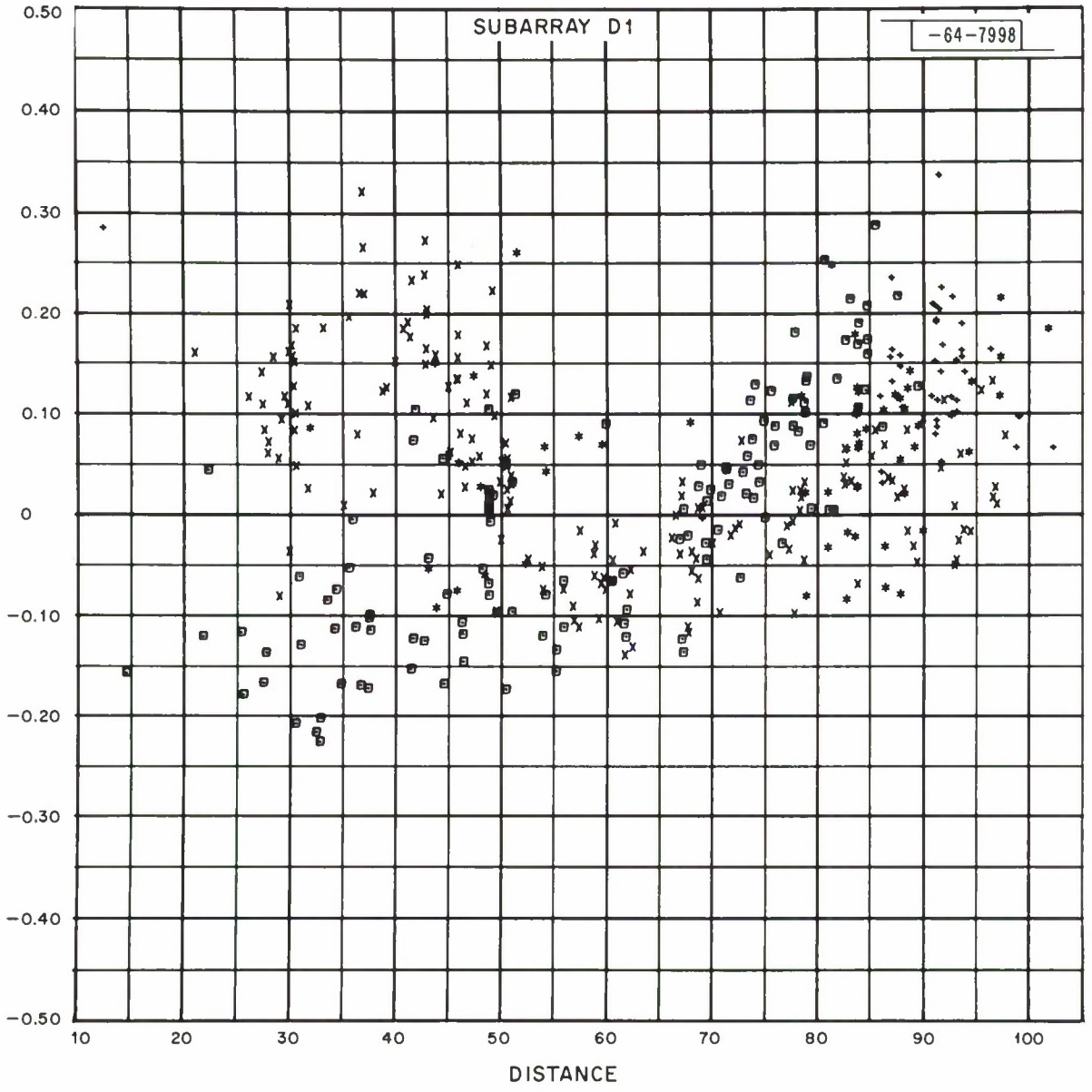

Fig. 37. Plane wave residuals vs distance for D1.

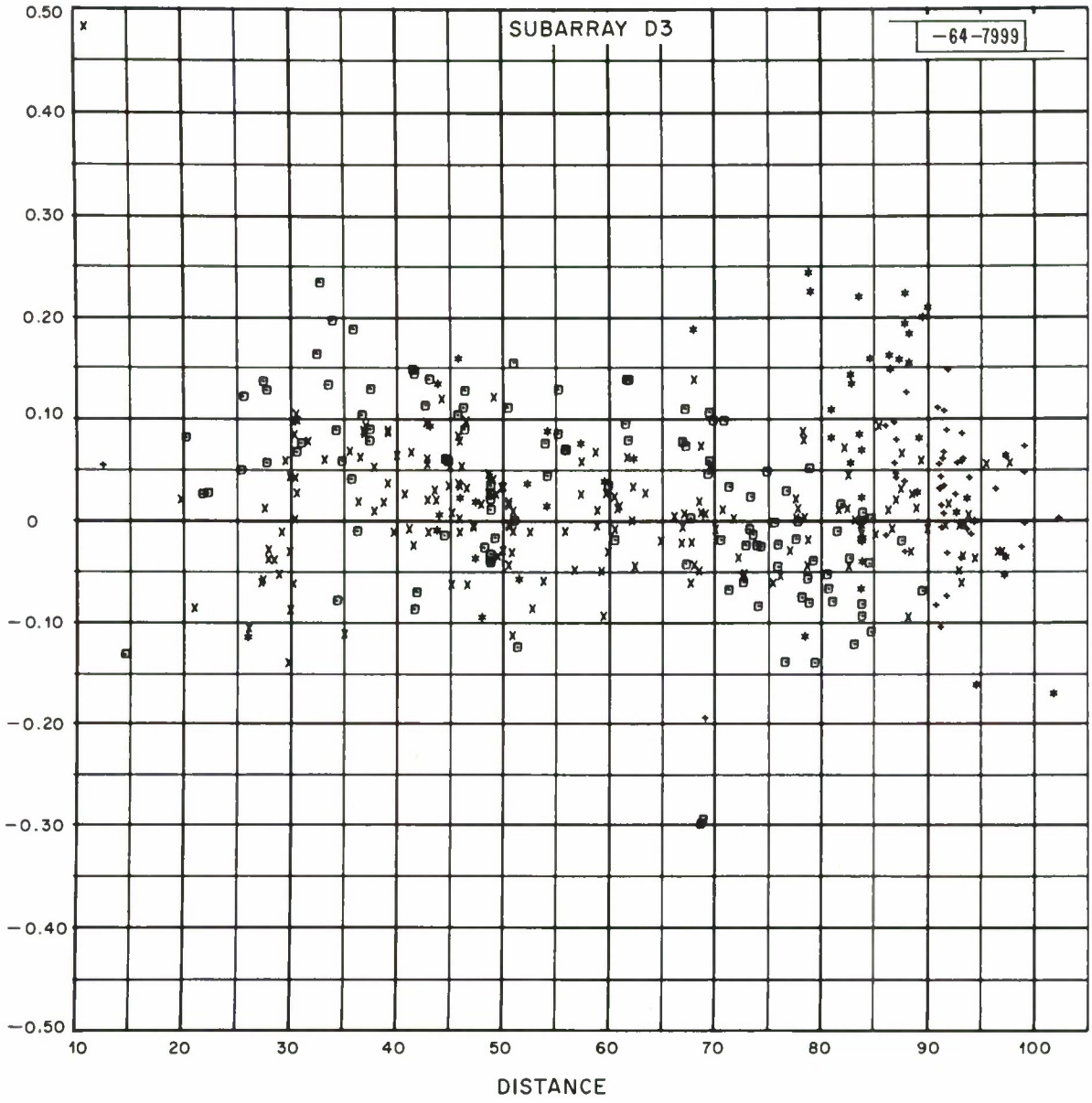

Fig. 38. Plane wave residuals vs distance for D3.

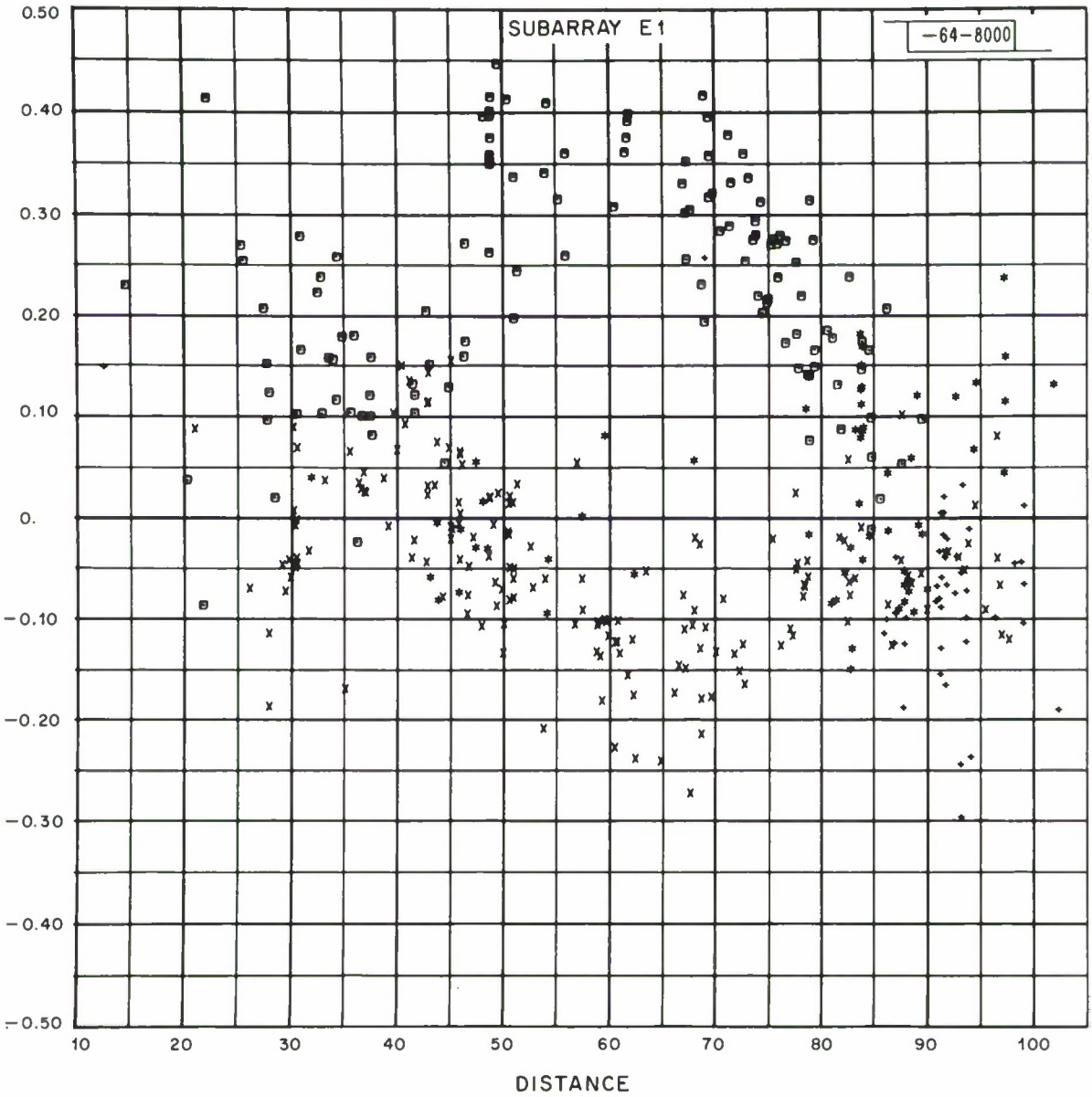

Fig. 39. Plane wave residuals vs distance for E1.

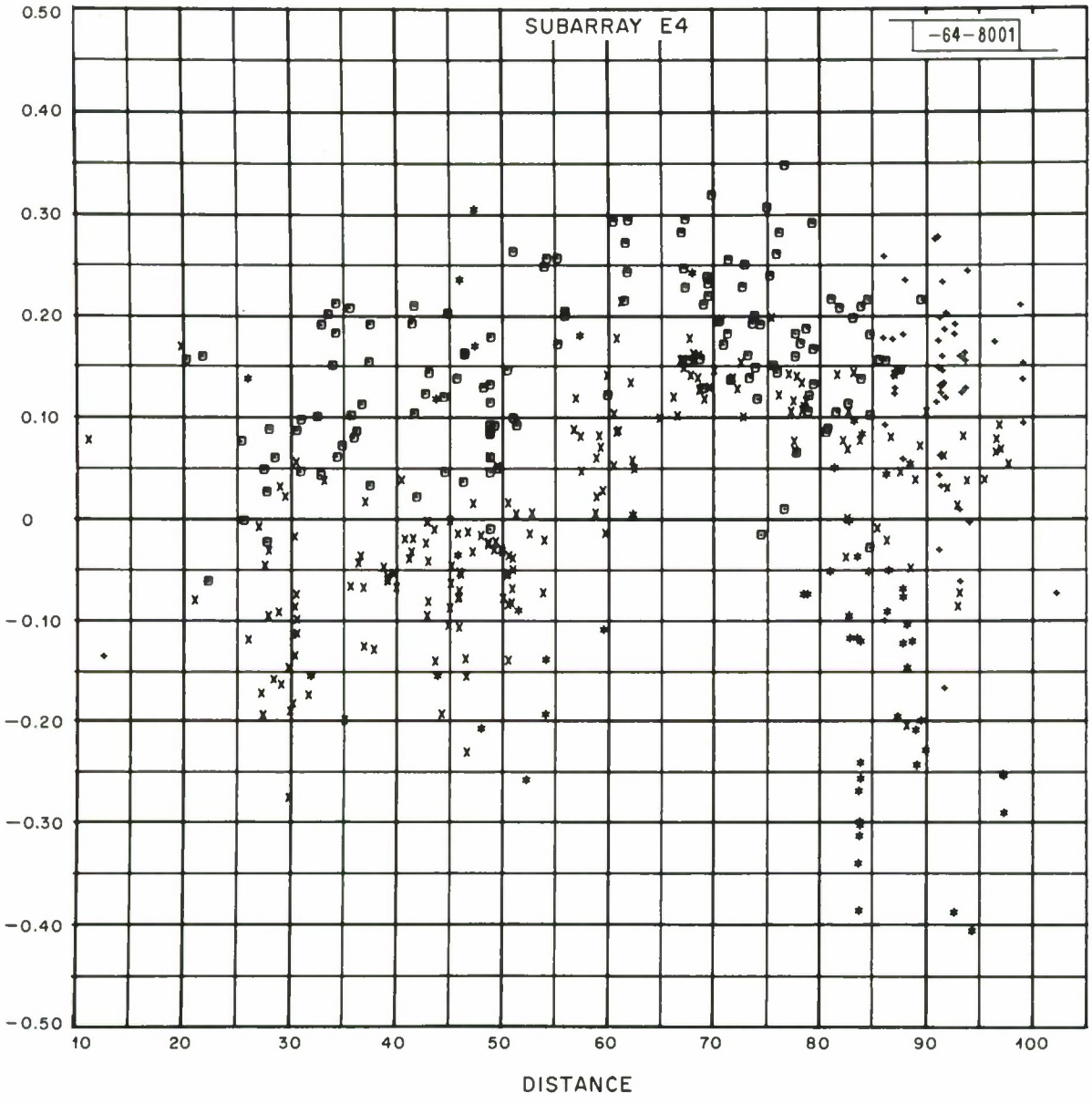

Fig. 40. Plane wave residuals vs distance for E4.

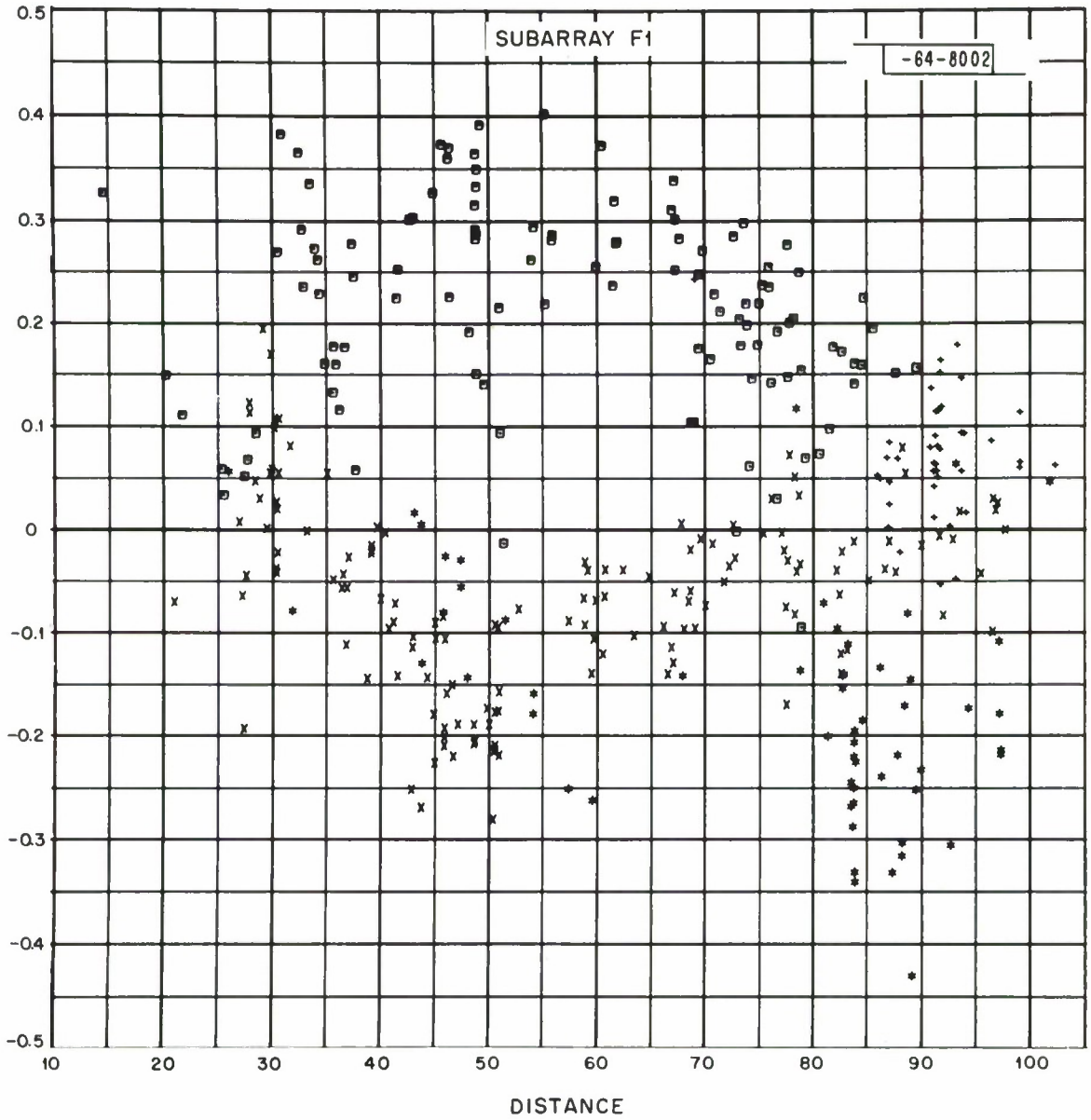

Fig. 41. Plane wave residuals vs distance for F1.

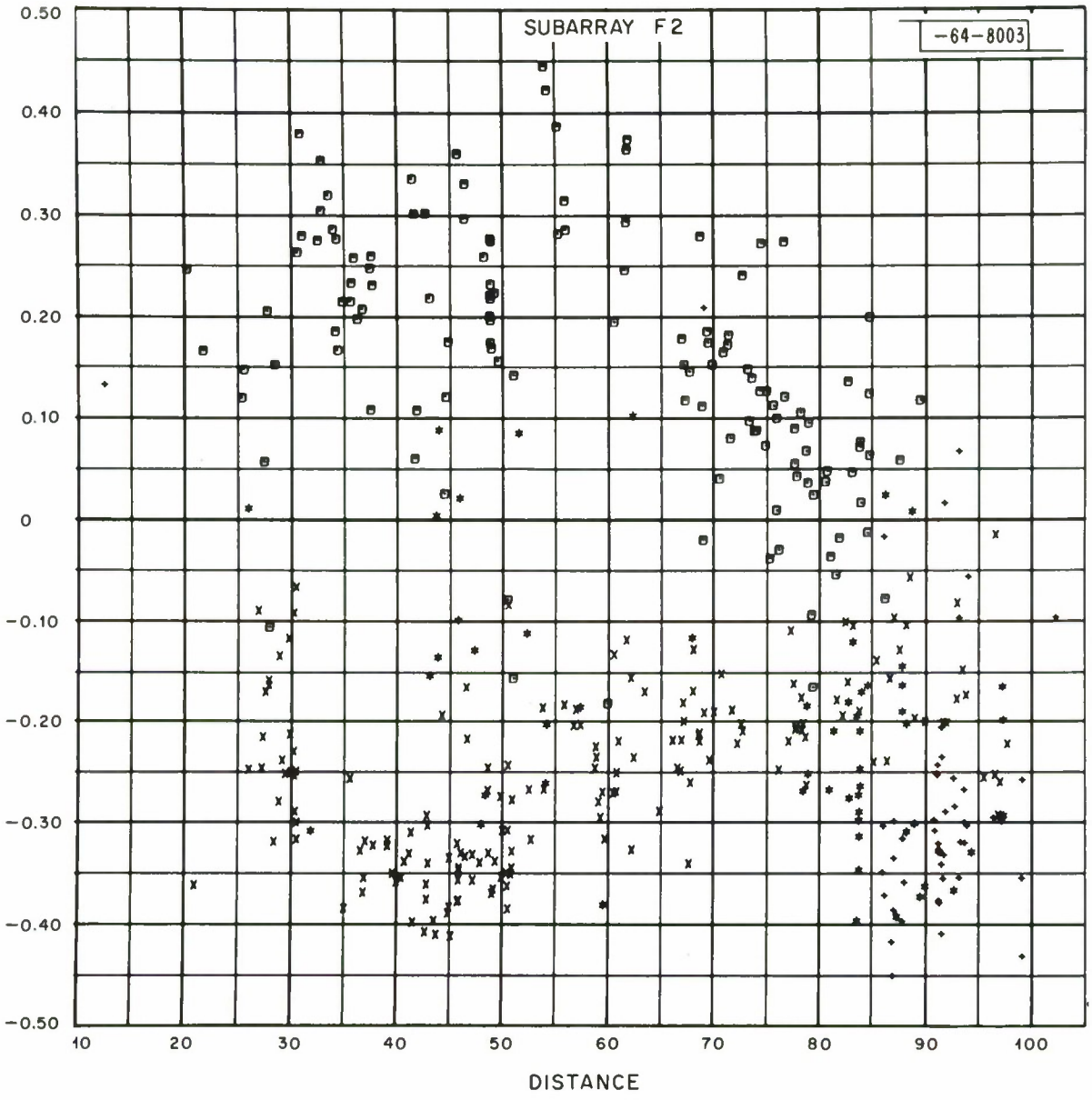

Fig. 42. Plane wave residuals vs distance for F2.

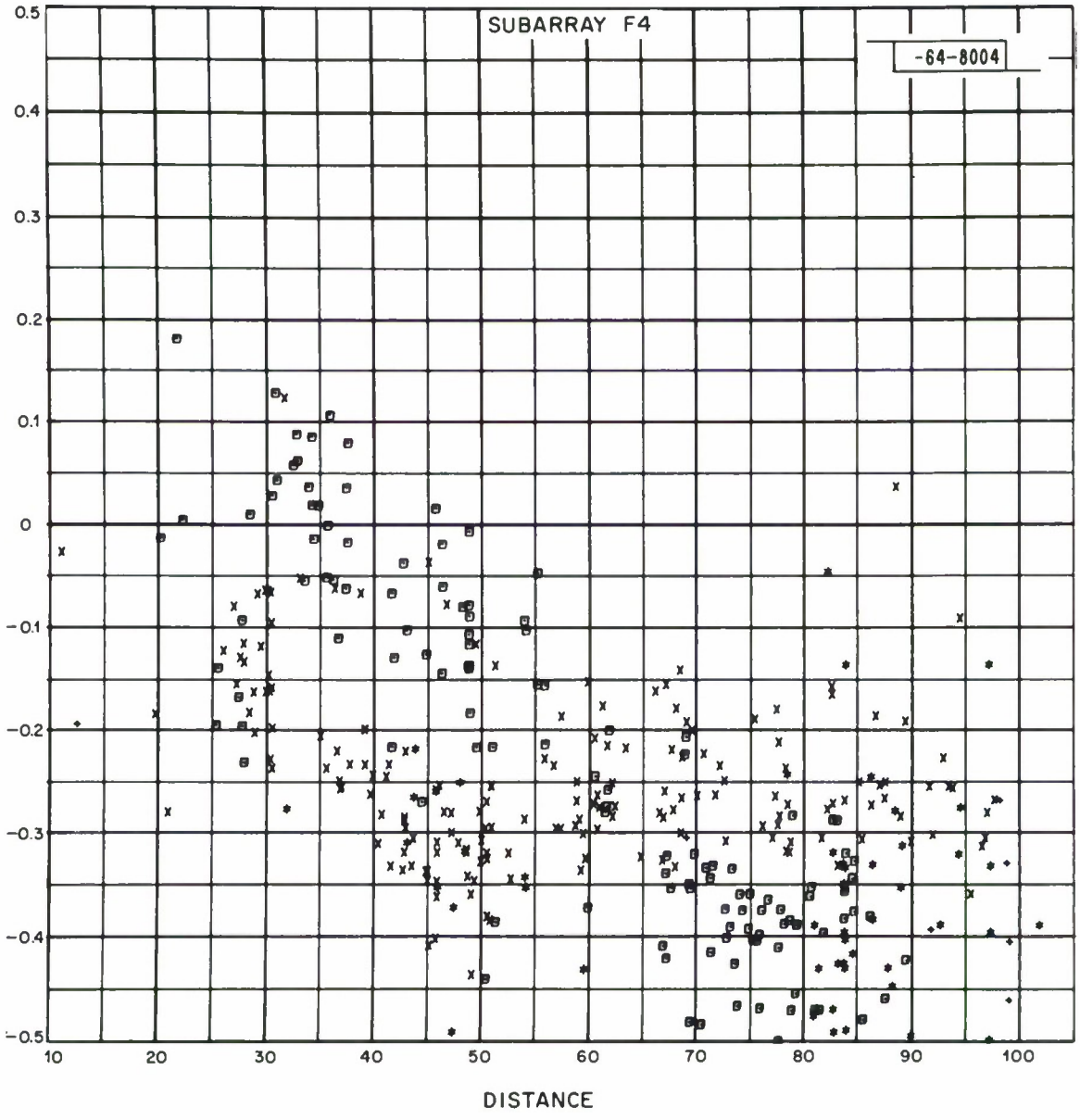

Fig. 43. Plane wave residuals vs distance for F4.

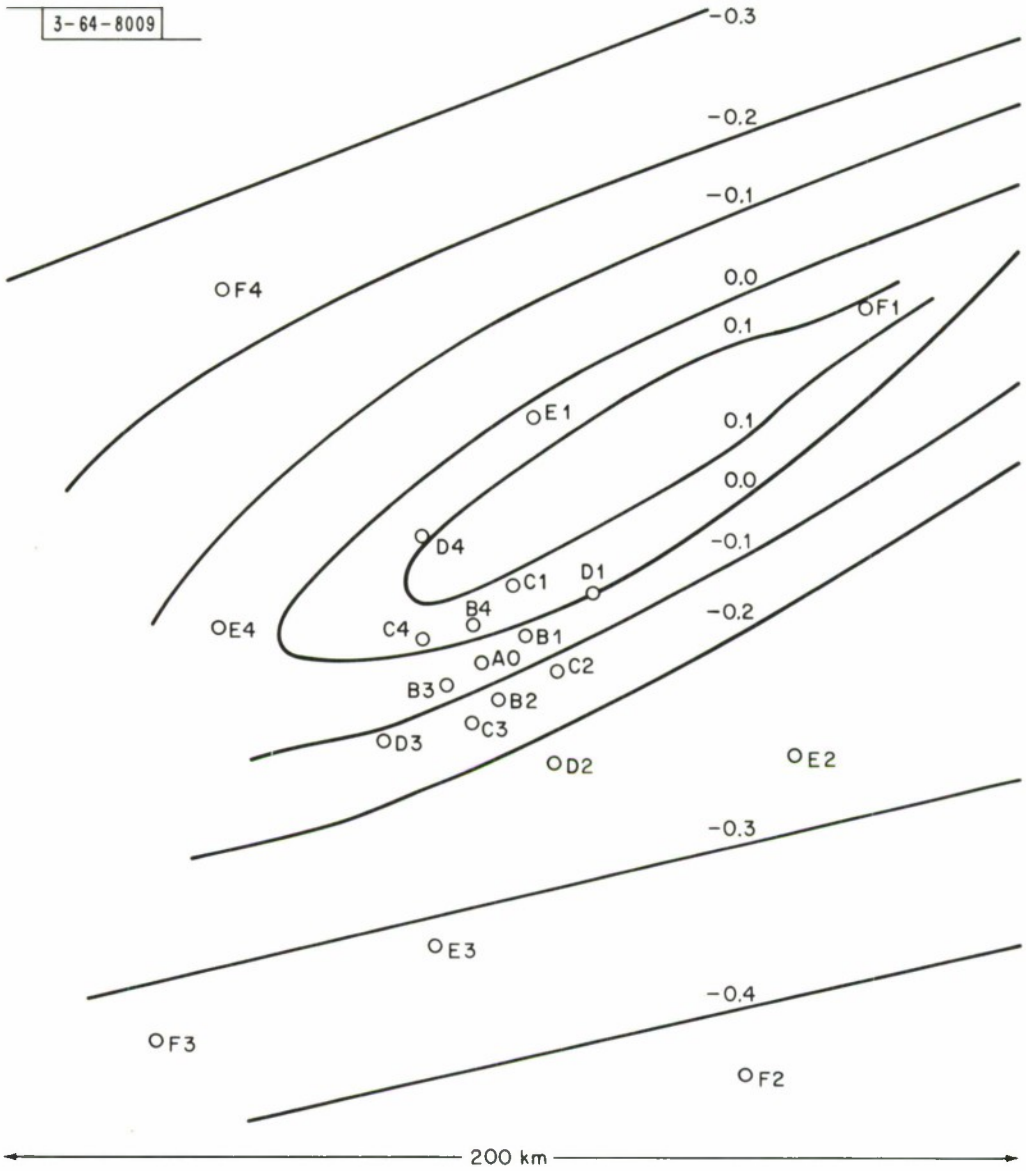

Fig. 44. Contours of average relative corrections.

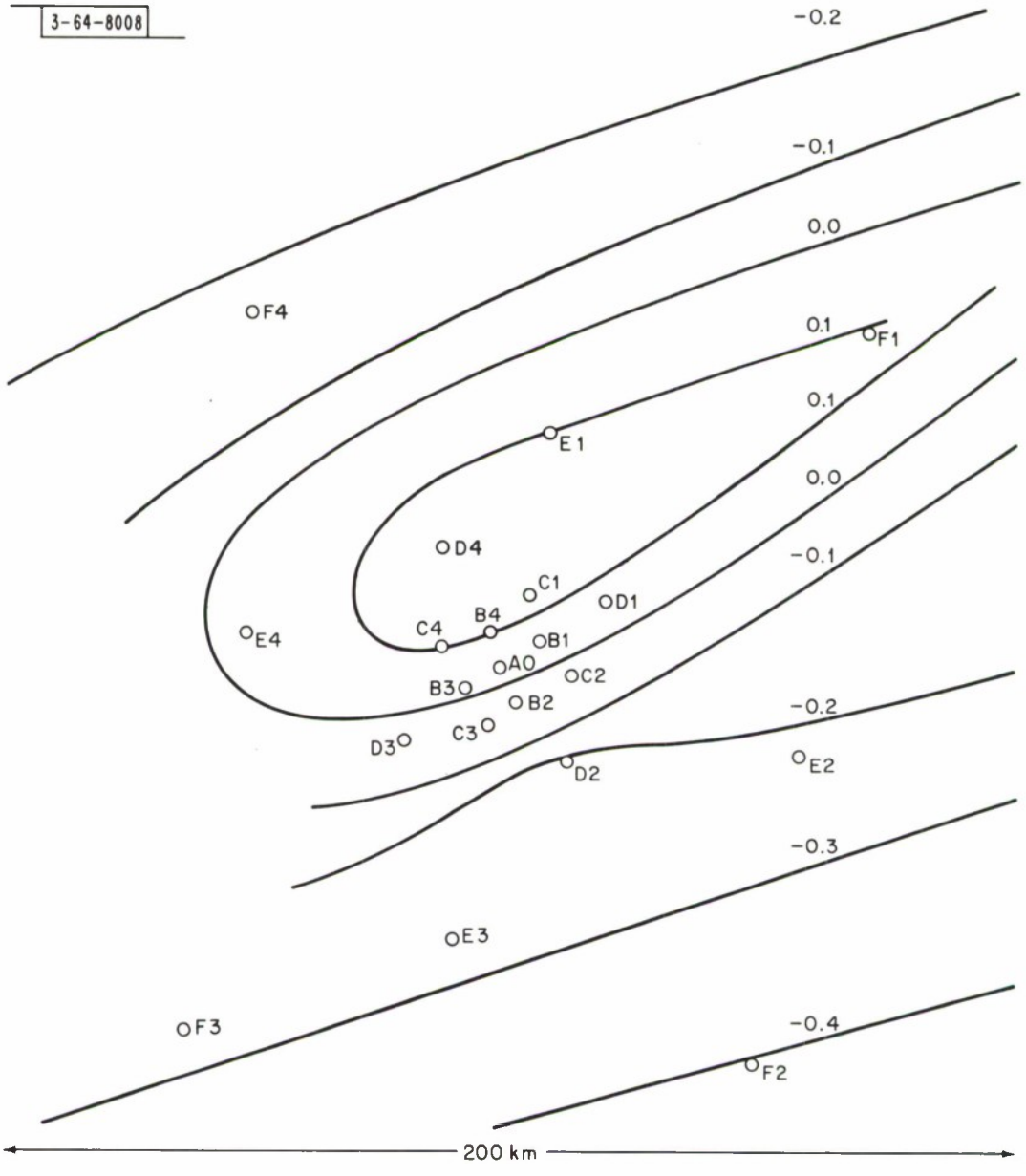

Fig. 45. Contours of average plane wave corrections.

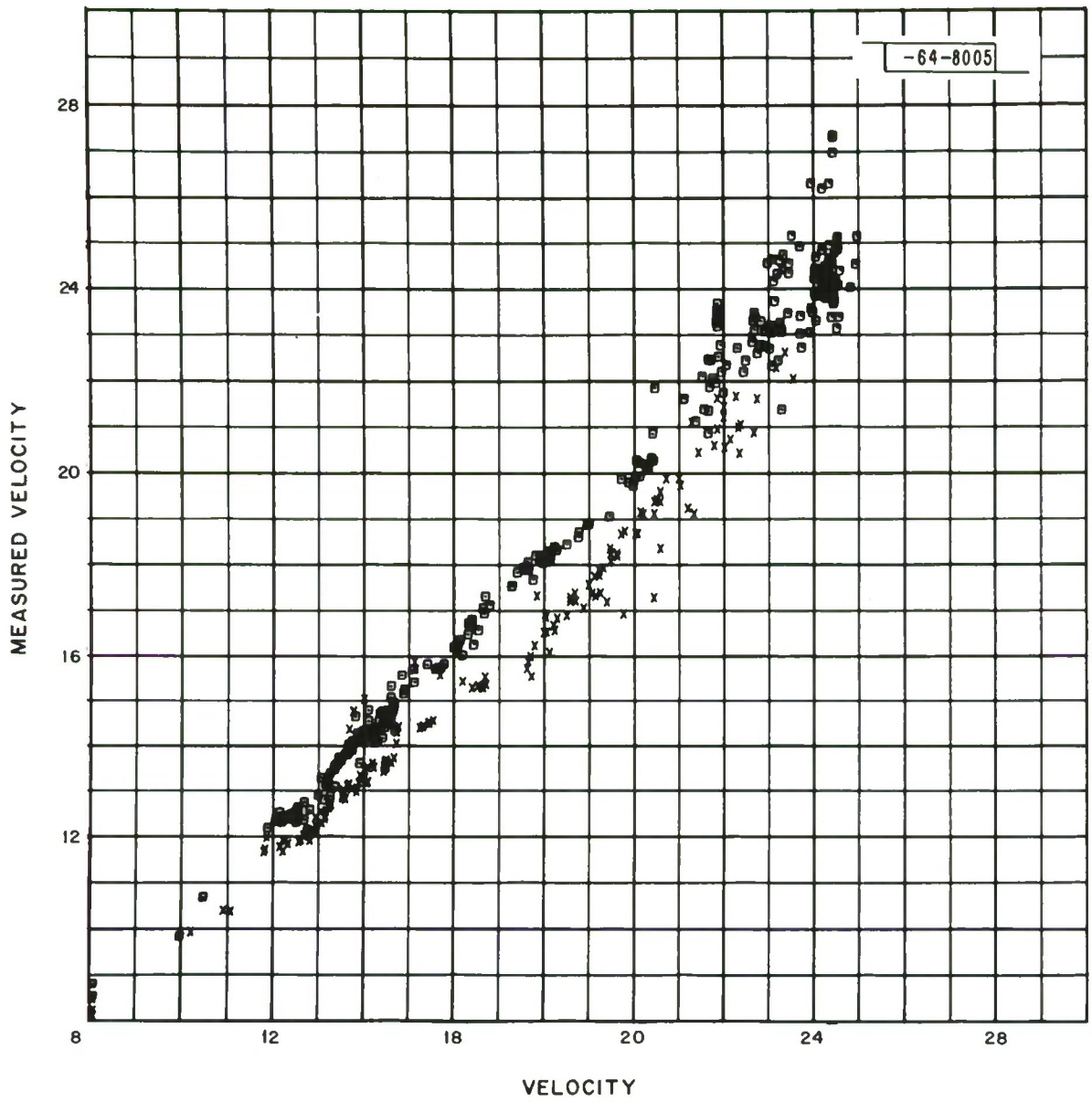

Fig. 46. Measured $dT/d\Delta$ values for P waves.

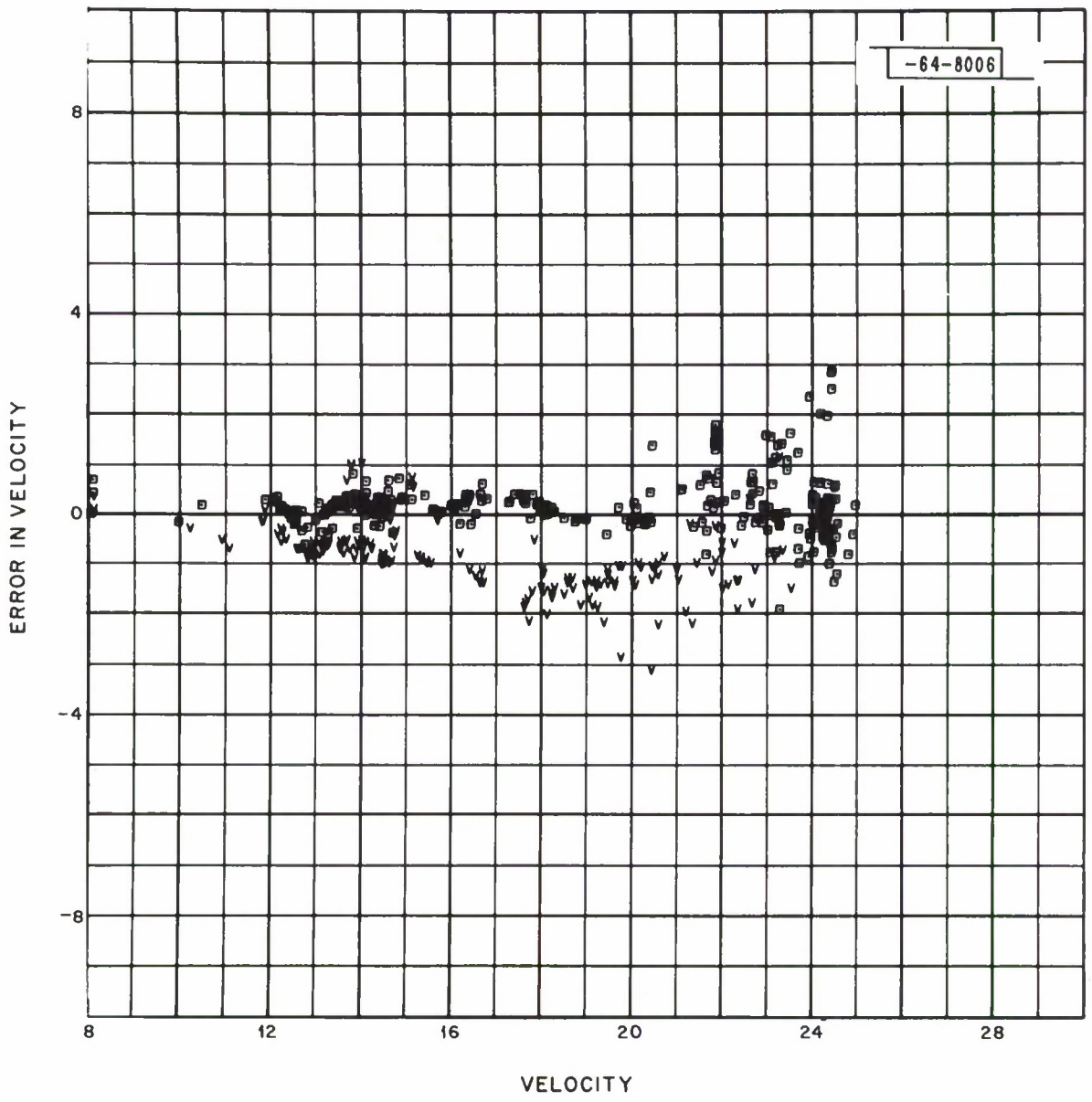

Fig. 47. Deviations in measured dT/dΔ from J-B dT/dΔ values.

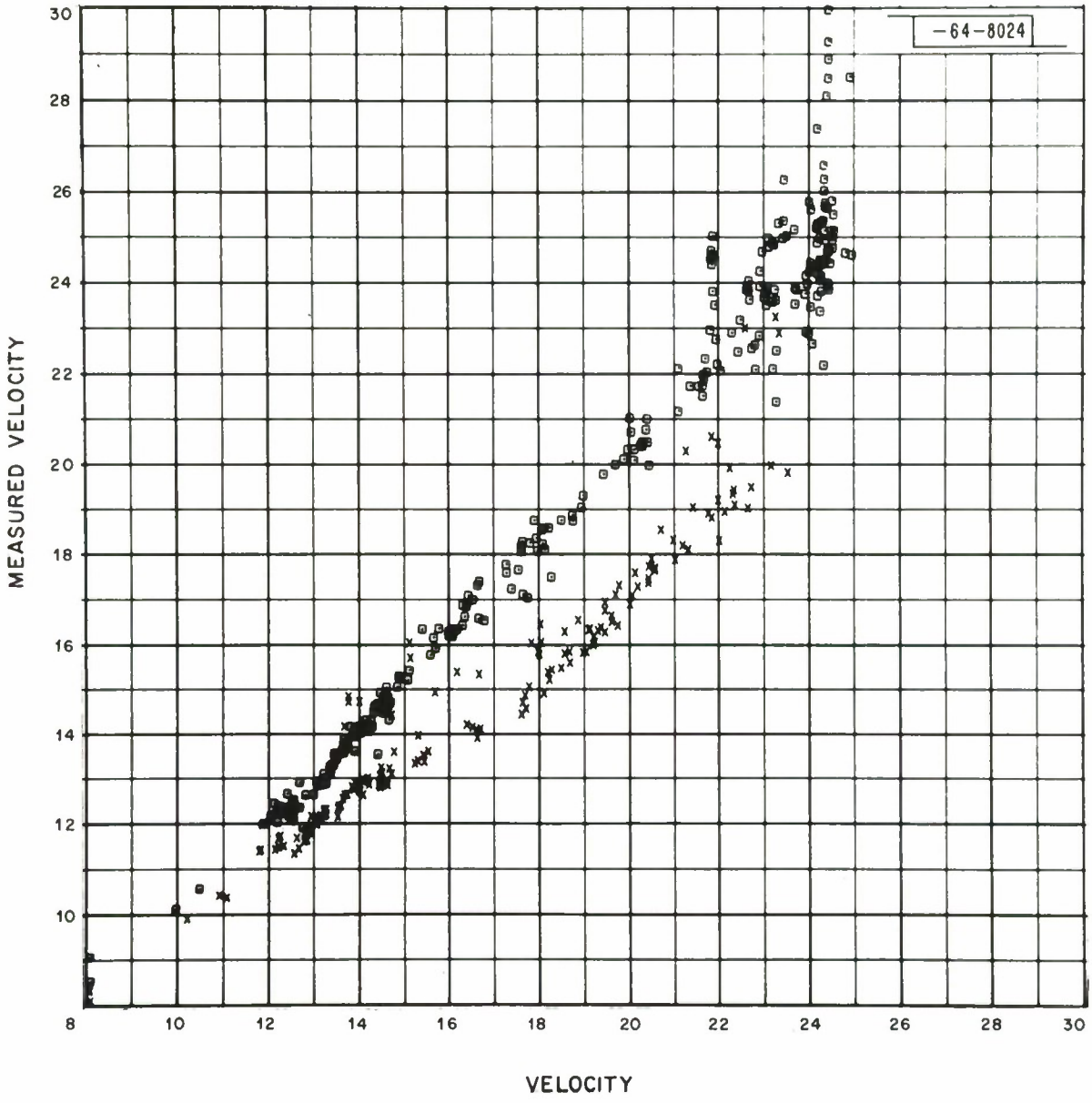

Fig. 48. Measured dT/dΔ using 100 km aperture array.

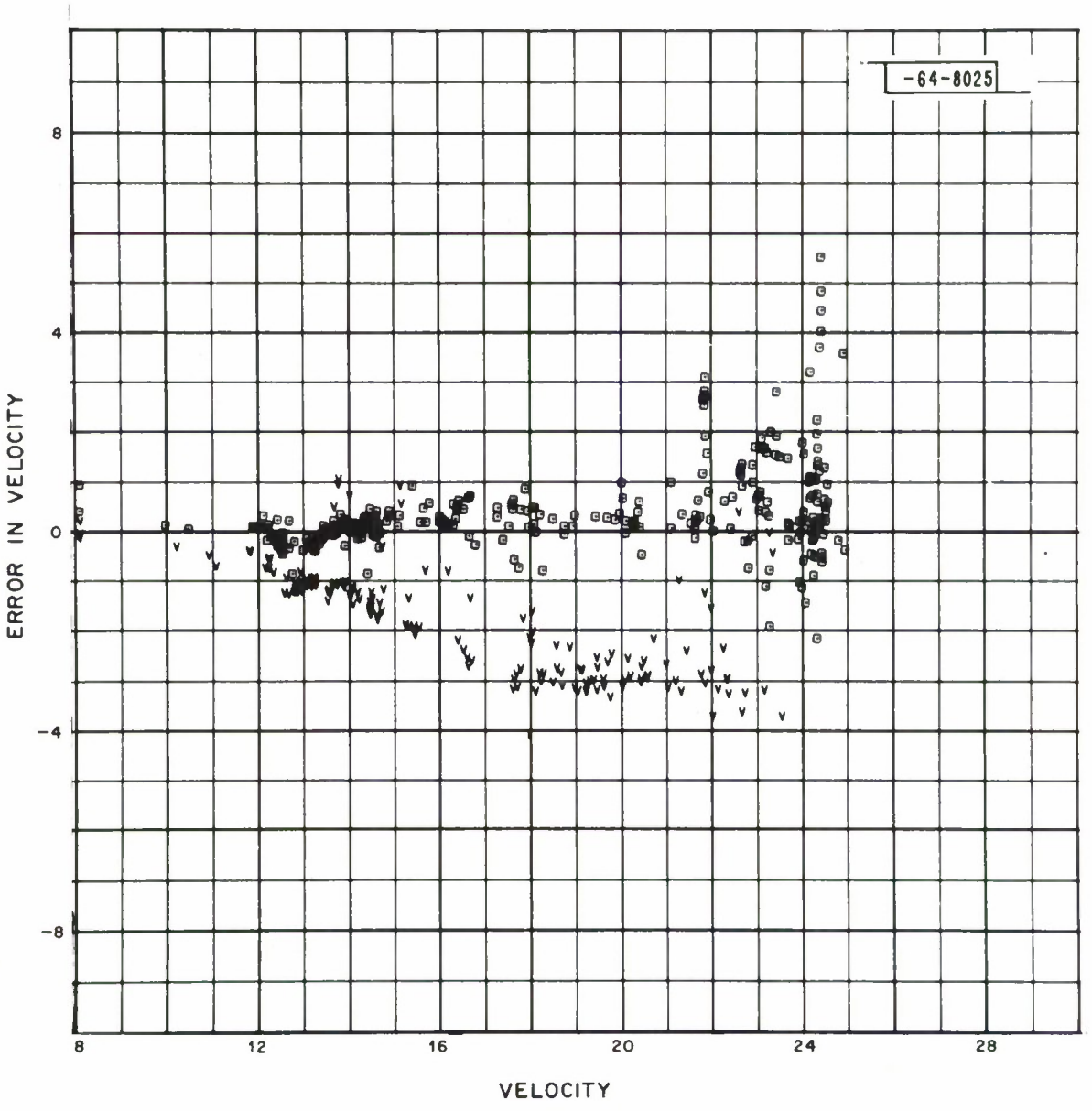

Fig. 49. Deviations in $dT/d\Delta$ of 100 km aperture from J-B $dT/d\Delta$.

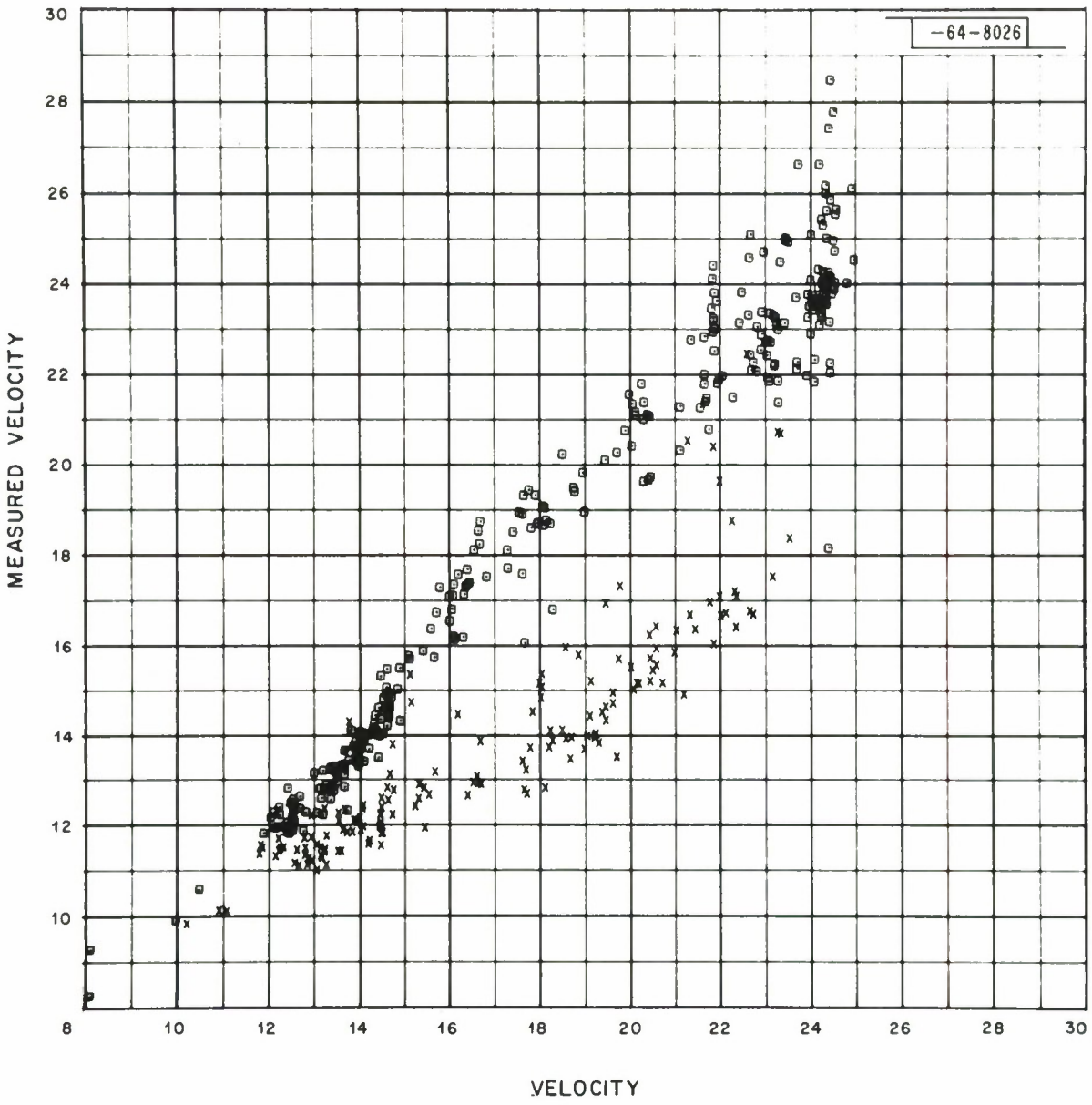

Fig. 50. Measured $dT/d\Delta$ using 50 km aperture array.

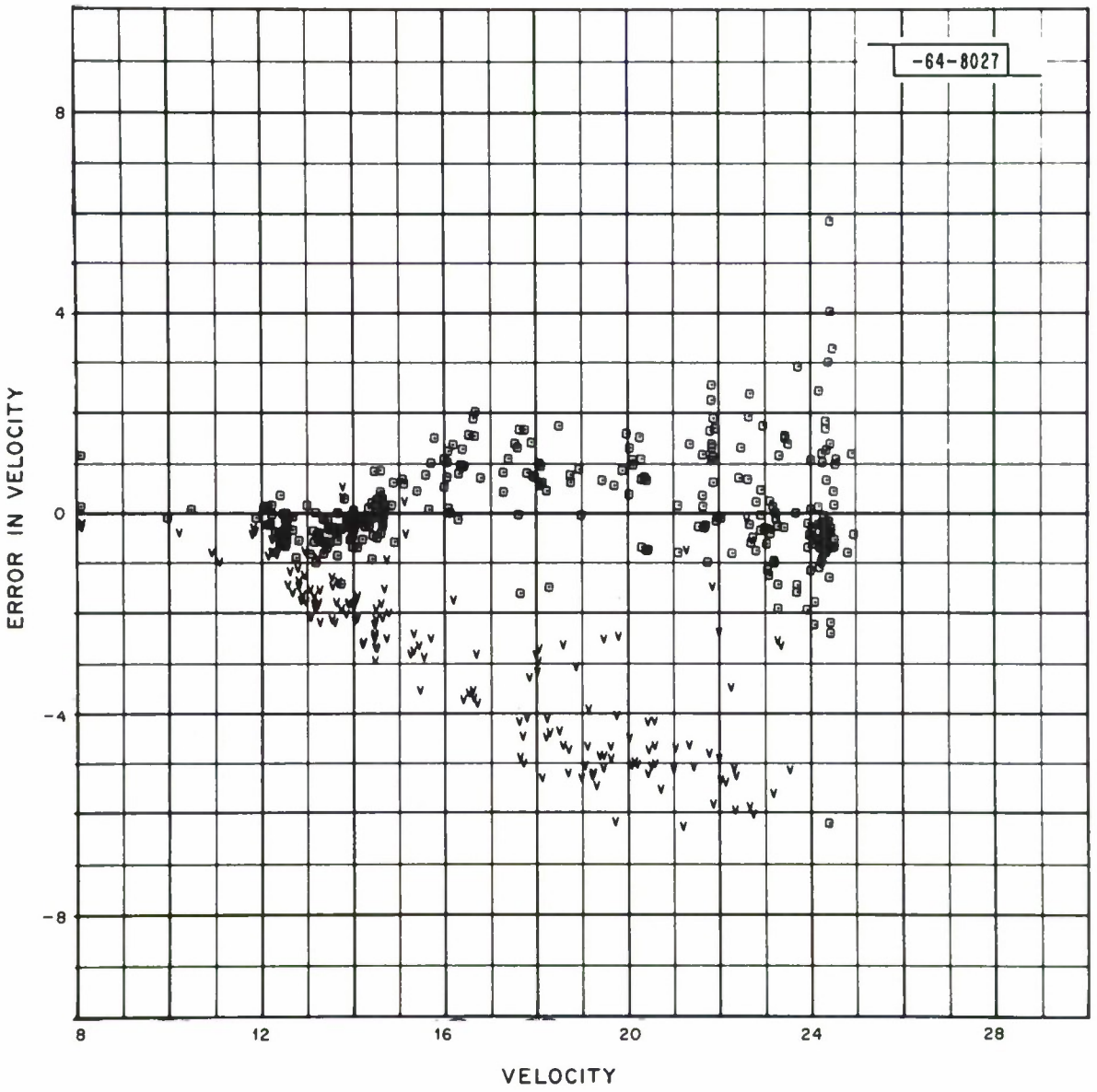

Fig. 51. Deviations in $dT/d\Delta$ of 50 km aperture from J-B $dT/d\Delta$.

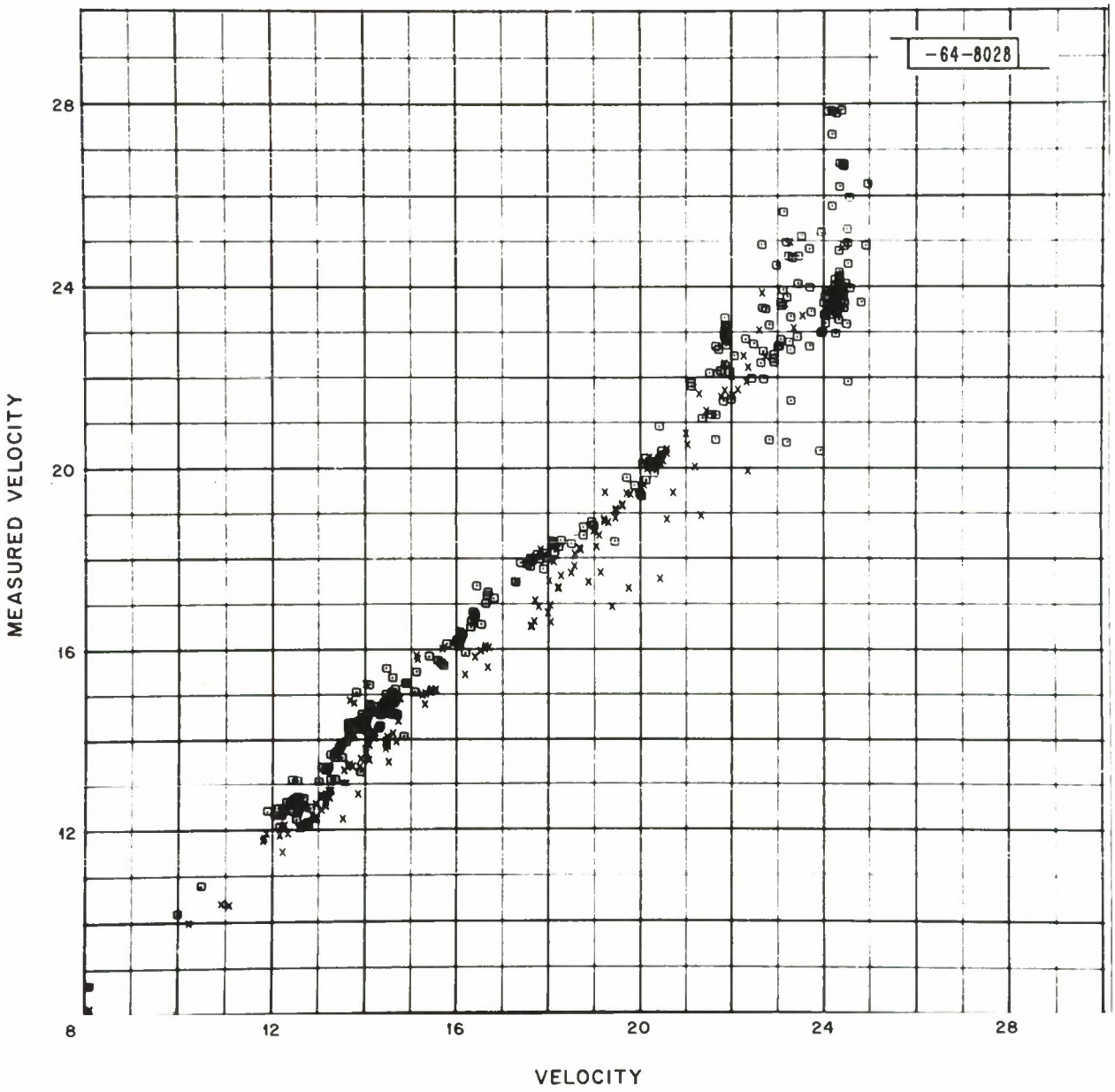

Fig. 52. Measured dT/dΔ using F ring only.

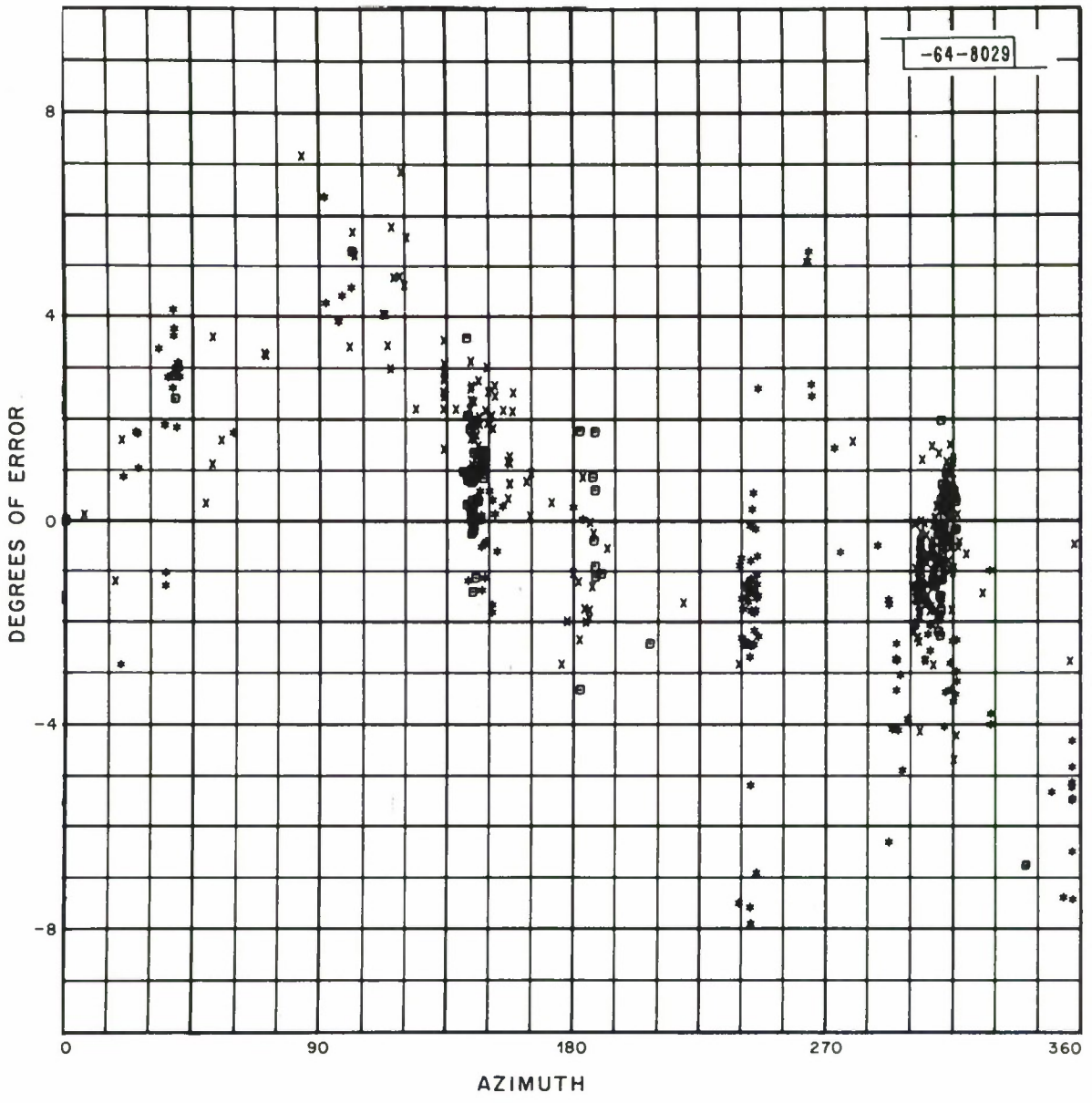

Fig. 53. Azimuth errors produced by LASA.

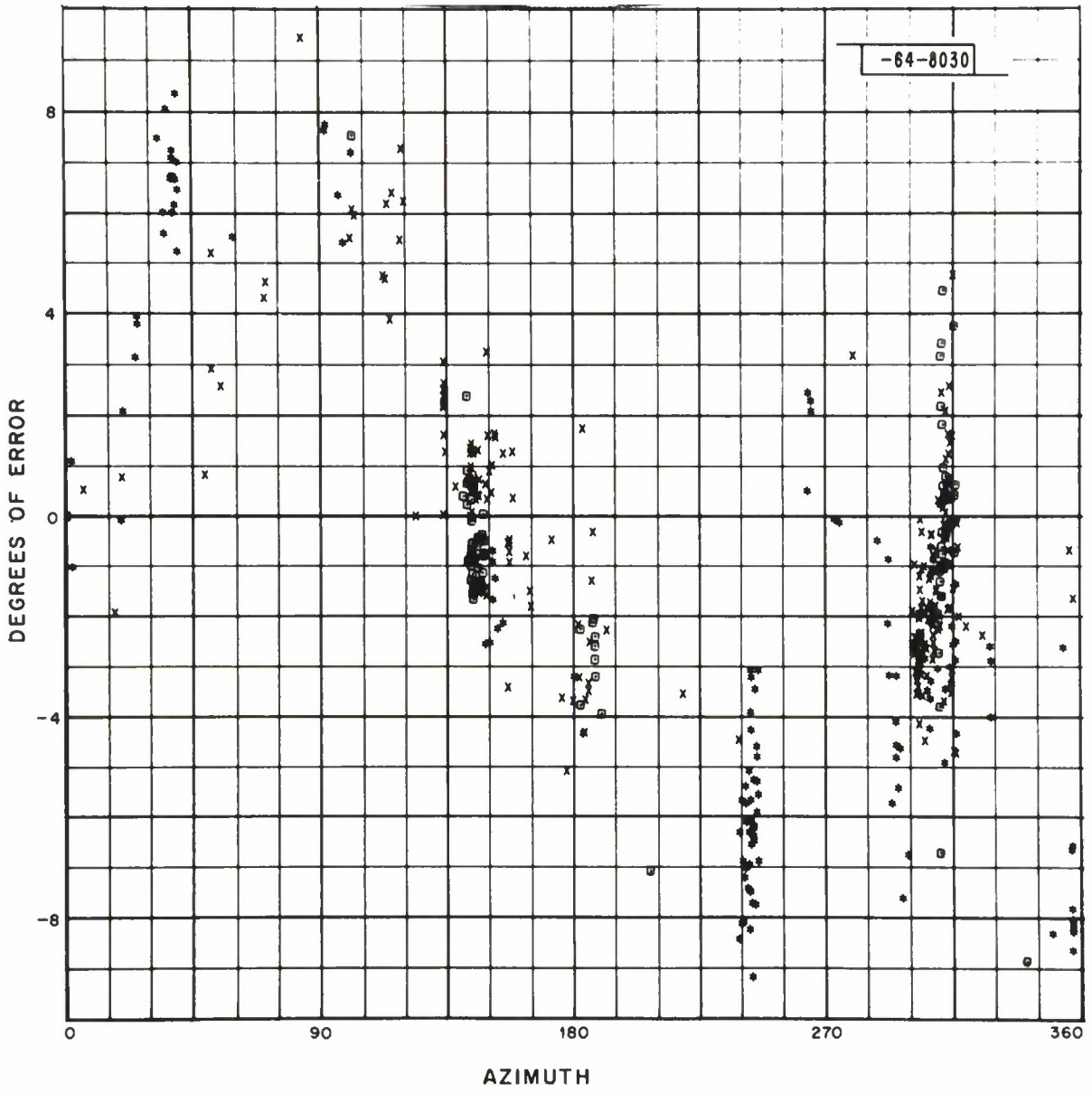

Fig. 54. Azimuth errors produced by 100 km array.

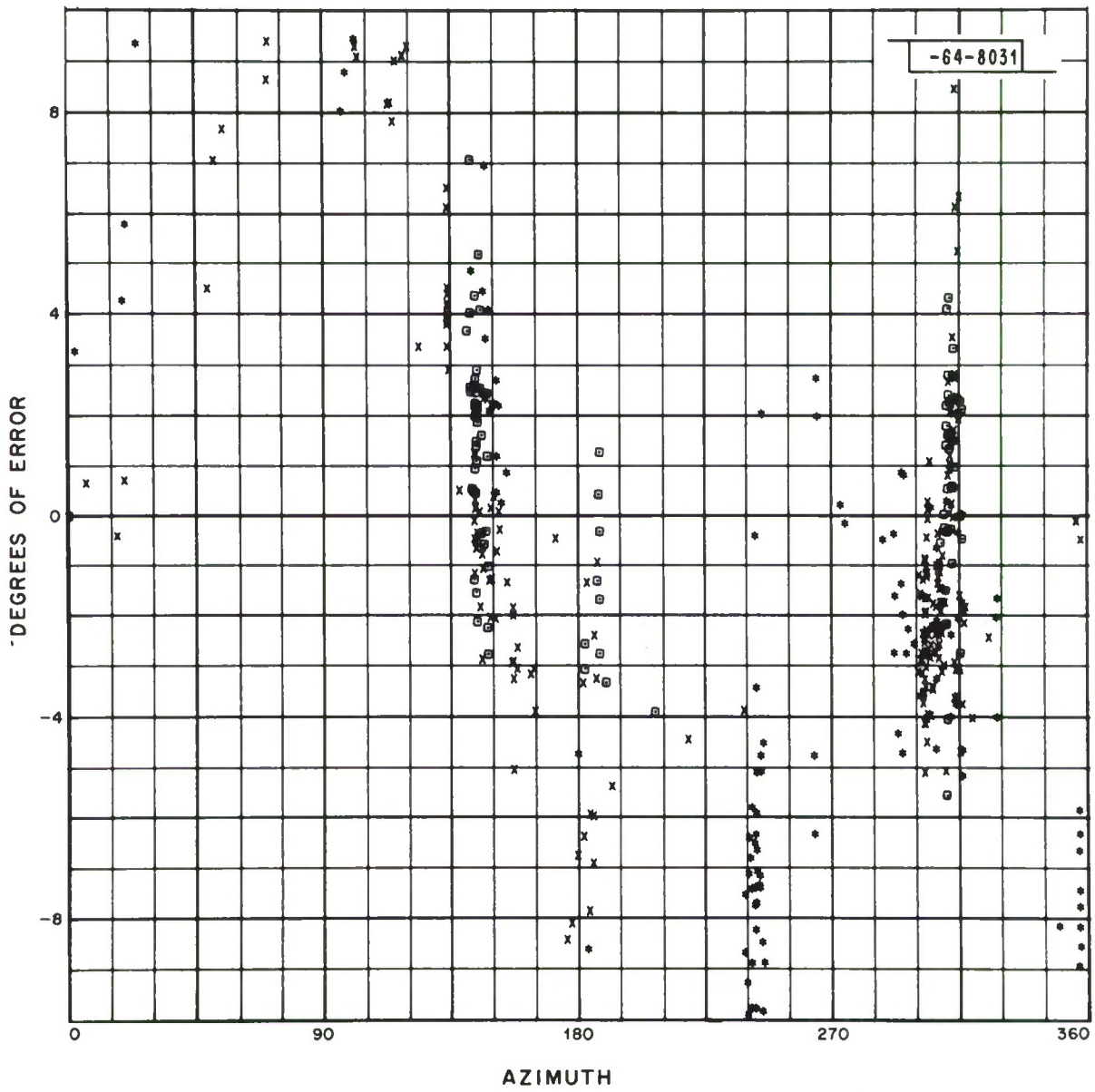

Fig. 55. Azimuth errors produced by 50 km array.

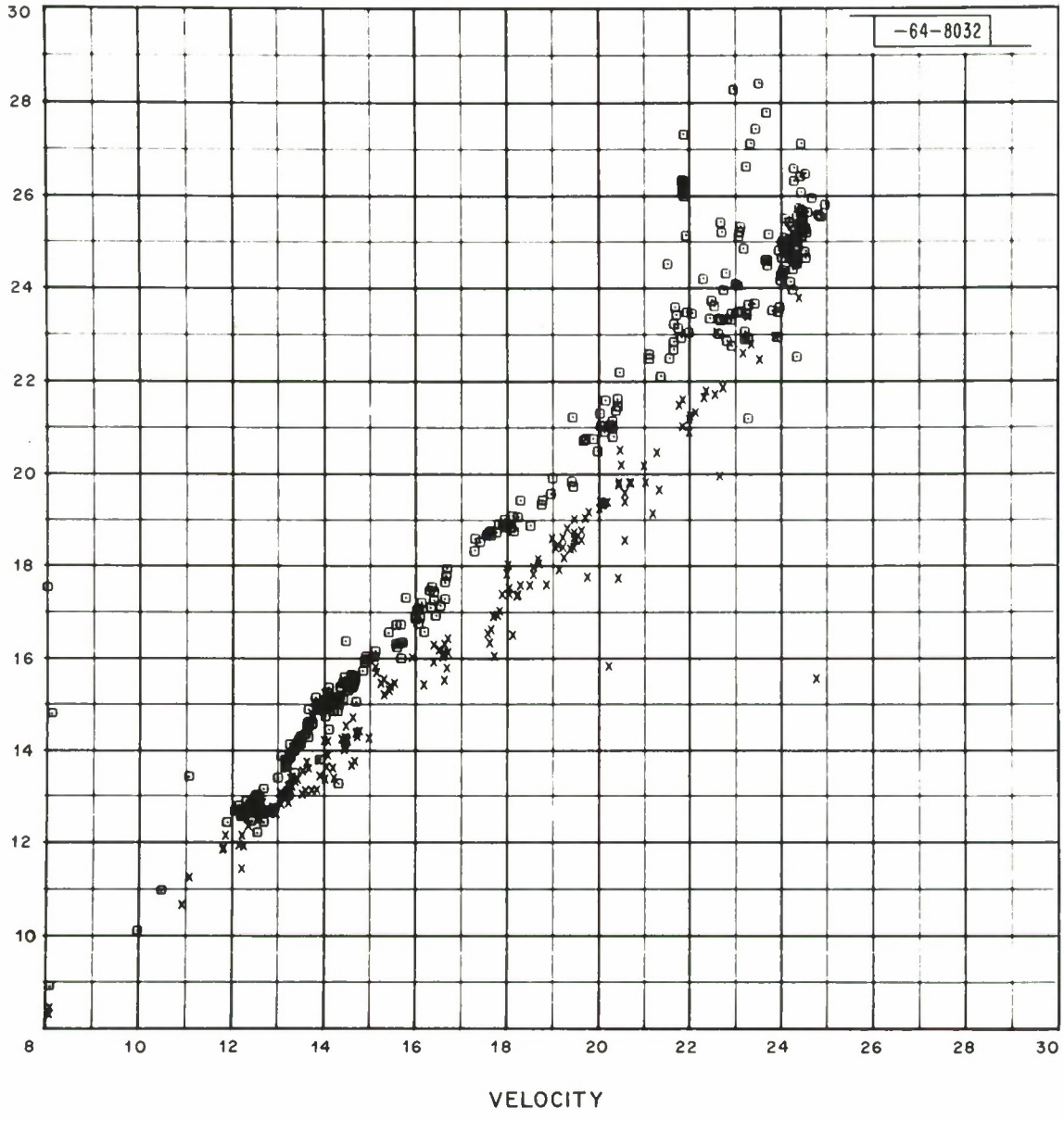

Fig. 56. Measured dT/dΔ using southern group of stations.

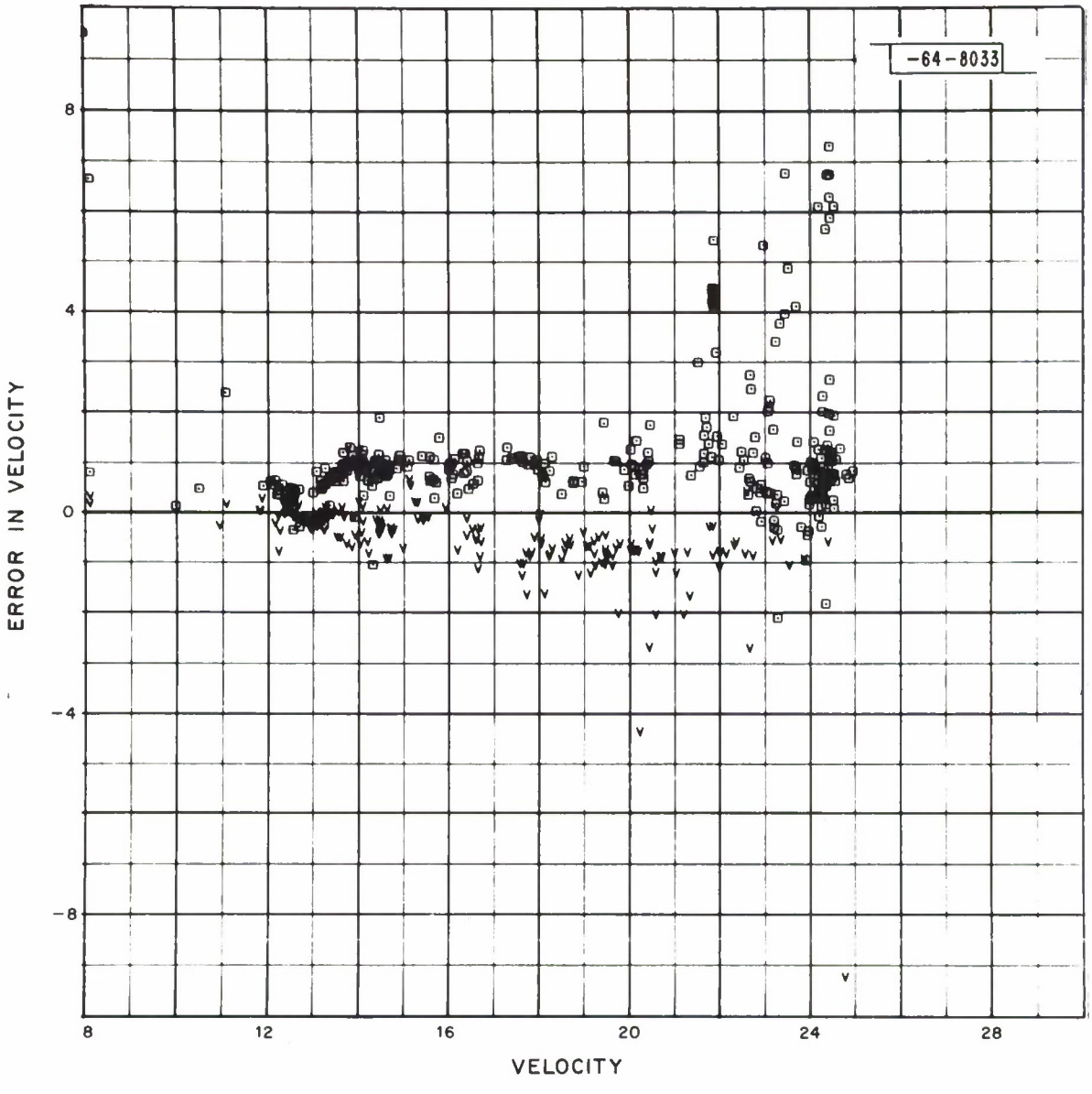

Fig. 57. Deviations in $dT/d\Delta$ of southern group from J-B $dT/d\Delta$.

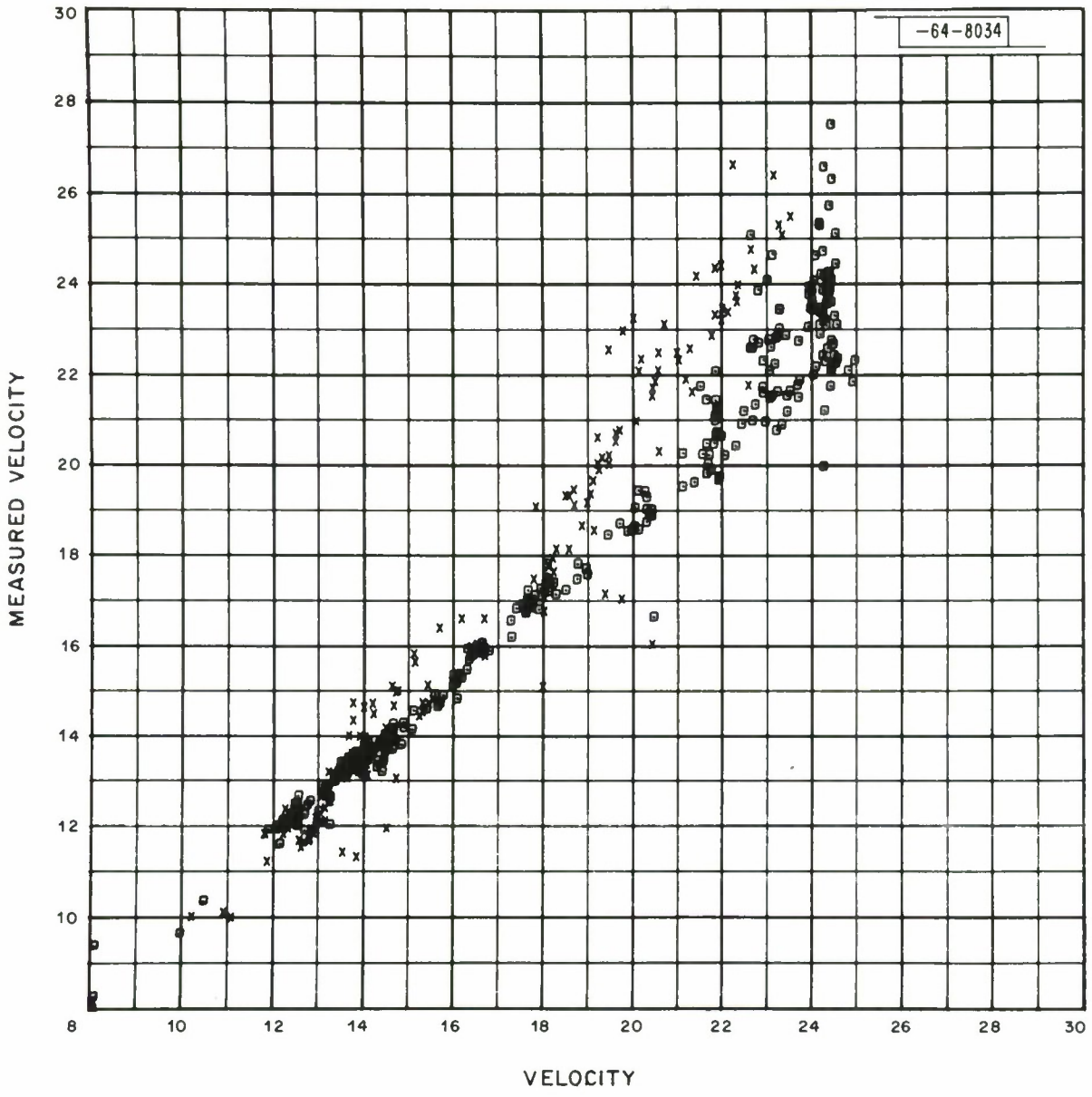

Fig. 58. Measured dT/dΔ using northern group of stations.

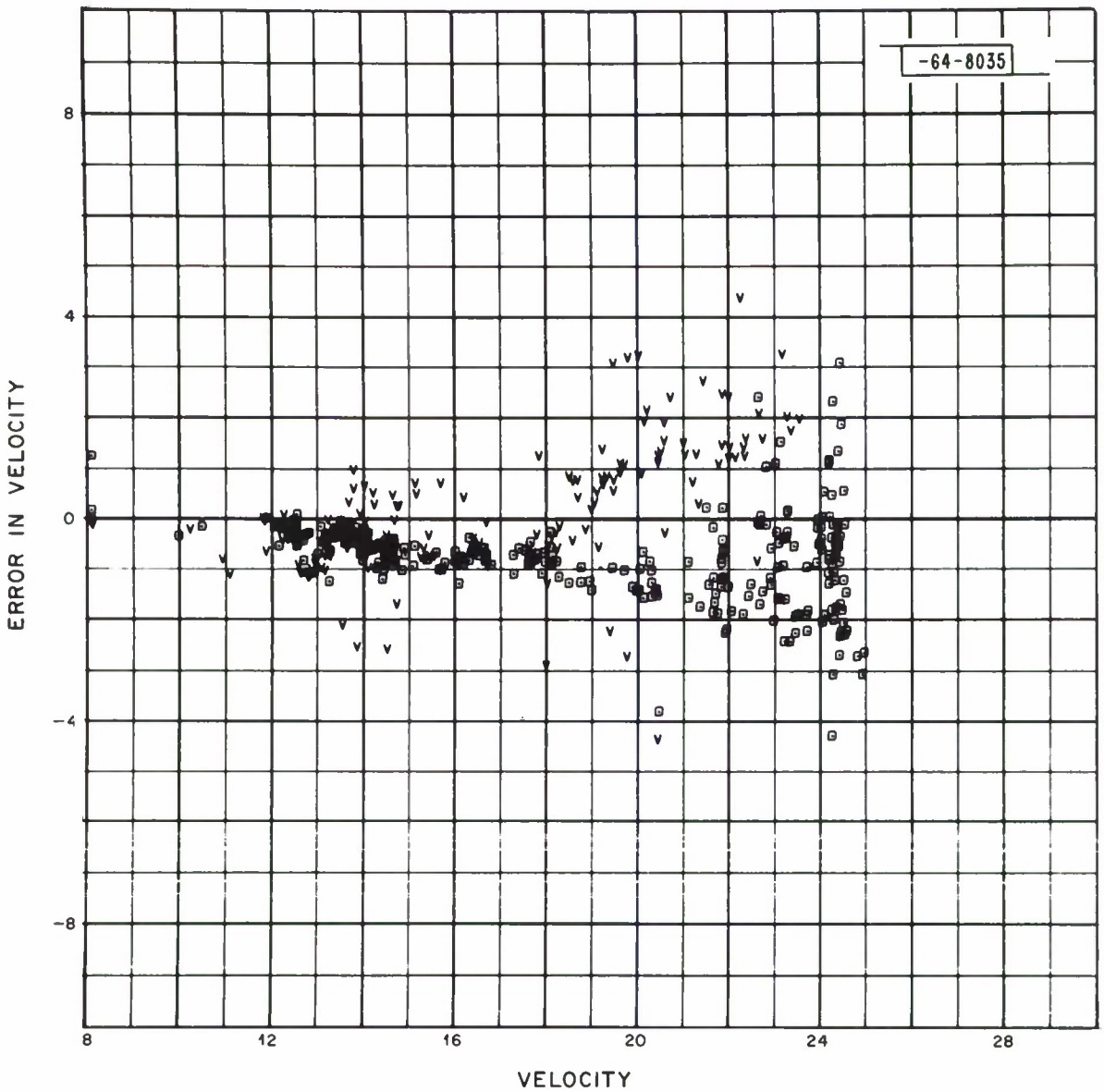

Fig. 59. Deviations in $dT/d\Delta$ of northern group from J-B $dT/d\Delta$.

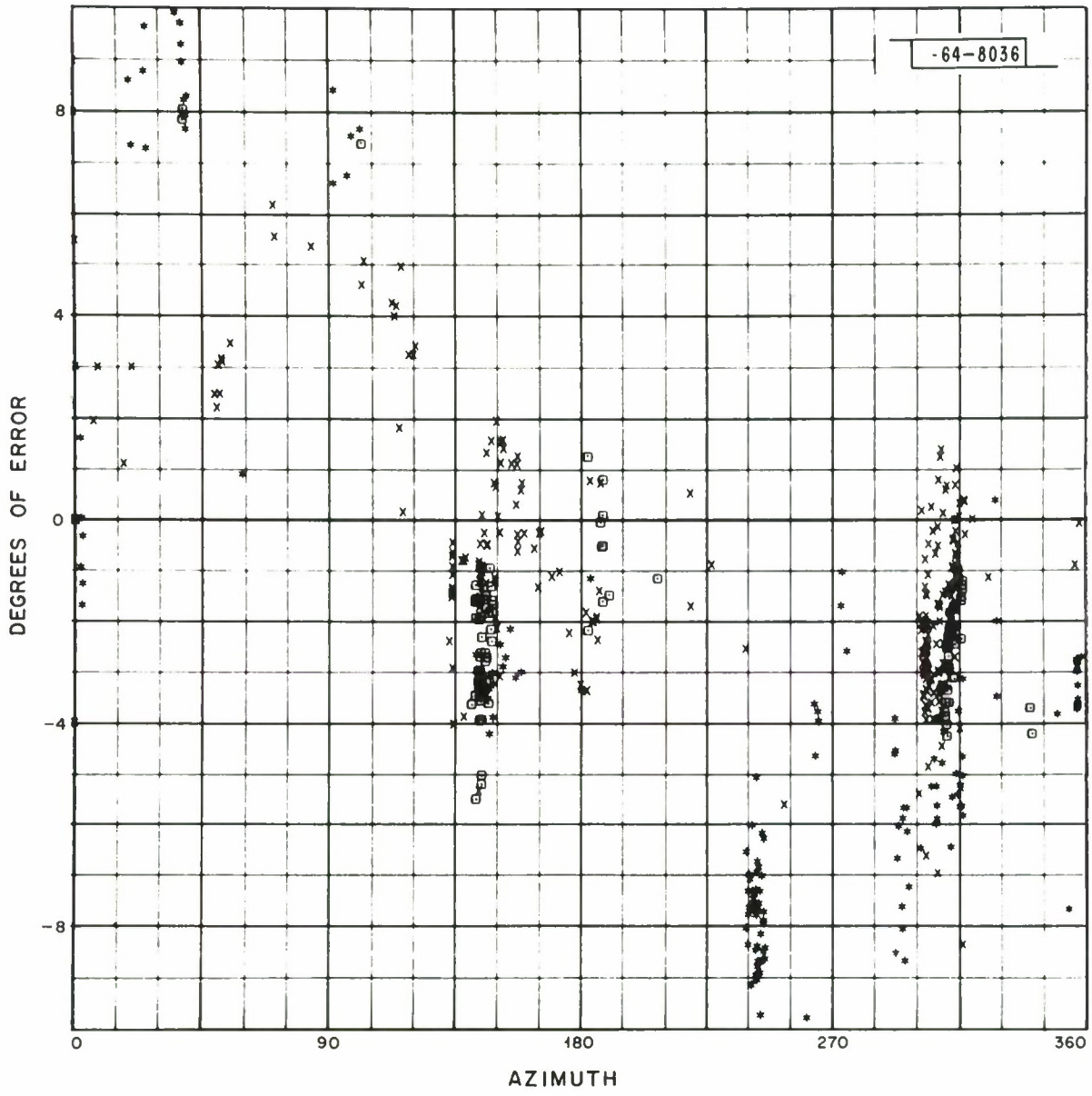

Fig. 60. Azimuth errors produced by southern group of stations.

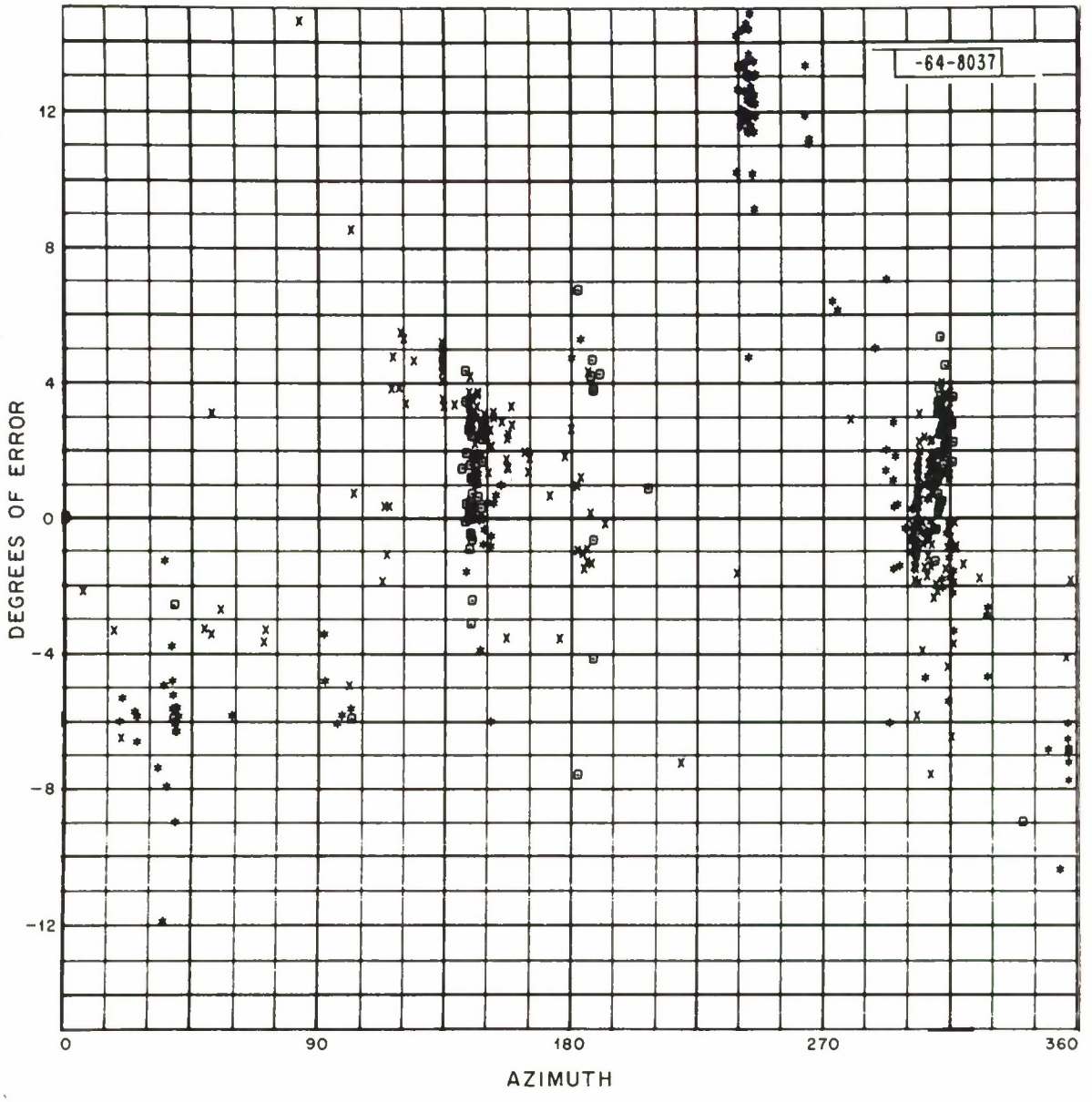

Fig. 61. Azimuth errors produced by northern group of stations.